EXECUTIVE SUMMARY

TO

PARTICULATE AND GAS PHASE MUTAGENS

IN AMBIENT AND SIMULATED ATMOSPHERES

Final Report
Contract Number A3-049-32
California Air Resources Board

Principal Investigator

James N. Pitts, Jr.

Co-Investigator

Arthur M. Winer

Program Manager

Janet A. Sweetman

Research Staff

Barbara Zielinska
William P. Harger
Roger Atkinson
Heinz W. Biermann
Timothy J. Wallington
Margaret C. Dodd
Travis M. Dinoff
Victoria Mejia
Philip C. Pelzel

LIBRARY
CALIFORNIA AIR RESOURCES BOA
P. O. Box 2815
Sacramento, CA 95812

Statewide Air Pollution Research Center
University of California
Riverside, California 92521

December 1984

EXECUTIVE SUMMARY

A. Introduction and Statement of the Problem

It is now well recognized that respirable sub-micron particles collected from ambient air contain organic compounds which exhibit strong, direct acting, mutagenic activity in the Ames Salmonella typhimurium bacterial reversion assay. However, polycyclic aromatic hydrocarbons (PAH) are not directly mutagenic, requiring microsomal activation, and it has been postulated that this observed direct mutagenicity of ambient particulate organic matter (POM) may be due, at least in part, to the presence of mono- and dinitroarenes. While certain of these nitroarenes are emitted in combustion derived POM, few data are available on their quantification in collected ambient POM. Furthermore, it is not known whether other PAH derivatives contribute in any significant manner to the observed mutagenic burden, or whether transformations of emitted PAH to nitroarenes and other PAH derivatives occur during transport through the atmosphere or on collection.

Clearly, more data are needed concerning the chemical composition and associated mutagenic activity of ambient POM, collected on several substrates and under conditions where a knowledge of the gaseous co-pollutants, and their concurrent concentrations, is available. Such information is essential for the generation of reliable risk assessments concerning the possible health impacts of respirable mutagenic particles (a) emitted directly to the atmosphere (e.g., diesel soot), (b) formed in atmospheric processes, (c) or both.

B. Objectives

The overall objectives of this program were to:

- Investigate (using the Ames test) the mutagenic activity of POM collected concurrently at a mid-basin site (El Monte) and a downwind receptor site (Riverside) in the CSCAB.
- Compare different, and widely used, filter types [glass fiber (GF) and Teflon impregnated glass fiber (TIGF) filters] in terms of their influence on the mutagenicity of collected POM.
- Determine gaseous co-pollutant concentrations simultaneously with POM collections by both conventional analyzers, and with a unique, long

pathlength spectroscopic technique [UV/visible differential optical absorption spectroscopy (DOAS)] and, utilizing factor analyses, investigate correlations of POM mutagenic activities with these co-pollutant concentrations and other variables.

- Investigate possible transformation reactions of adsorbed PAH under well-defined ambient air conditions, including the use of both active and passive filter exposure techniques.

- Develop appropriate analytical methods for identification and quantification of mono- and dinitroarenes and determine their concentrations in our ambient POM samples.

- Calculate nighttime N_2O_5 levels from the available NO_3 and NO_2 concentration data at a variety of locations in southern California and Europe and estimate whether or not nitration of adsorbed PAH by N_2O_5 during nighttime hours could be a significant pathway to the formation of direct acting mutagens. An additional objective was to gain further information concerning the possible importance of N_2O_5 in nighttime atmospheric chemistry, including its role in forming nitric acid, a major component of acid rain and fogs.

- Test the validity of a homogeneous gas phase mechanism, proposed by Stockwell and Calvert (1983), to explain the ambient levels of HONO we have previously observed in the South Coast Air Basin by the DOAS technique.

- Determine spectroscopically whether nitrous acid, a gas phase mutagen and (by reaction with amines) a precursor to nitrosamines, can be formed in indoor environments from the reaction of NO_2 and H_2O vapor.

C. Methods of Approach

To achieve the objectives outlined above, we conducted extensive field studies in September 1983 and September 1984. In the September 1983 investigation, we measured concurrently the mutagenicity of ambient POM collected on TIGF and GF filters in El Monte and Riverside. As noted earlier, at Riverside, in addition to conventional gaseous pollutant analyses, our unique long optical path DOAS system was utilized to measure gas phase concentrations of the nitrate radical (NO_3), formaldehyde (HCHO) and nitrous acid (HONO).

In the September 1984 study, selected PAH adsorbed on TIGF and GF filters were exposed to the ambient atmosphere for four 6-hour time periods each day for five successive 24-hr days. Gaseous co-pollutants, including the NO_3 radical, HCHO and HONO (as well as O_3, NO_2 and SO_2), were measured concurrently utilizing our DOAS system. In addition, samples of ambient POM were collected with our SAPRC mega-sampler for nitroarene analysis.

Finally, a DOAS system was developed that incorporates a multipass optical system and this new configuration was employed to identify HONO and to measure its rate of formation from NO_2 in an indoor environment.

D. Summary of Results and Conclusions

- Depending upon the time period of collection, the ratios of mutagen densities (rev m^{-3}) for POM simultaneously collected on GF and TIGF filters ranged from a factor of 5 greater than unity (generally during periods of high O_3 and PAN) to nearly a factor of 4 less than unity (generally during the 0600-1200 hr time period associated with morning traffic peaks). The observation that the GF filter extracts generally had lower mutagenic activities, except during periods of high ozone concentration, suggests that there is an artifact effect during POM collection associated with one or both of these two types of filters. The mutagen density to CO ratios during these times gave further indication of a filter artifact on the GF filters. These observations have important implications to the CARB, and other regulatory agencies, concerning the choice of filter for collection of ambient POM.

- The observed mutagen densities (TA98, -S9) of TIGF filter extracts varied from 22 to 240 rev m^{-3} for Riverside and from 40 to 260 rev m^{-3} for El Monte. These values are higher than those generally reported in the literature for other air basins but are similar to values we have previously reported for locations in the South Coast Air Basin.

- Decreased responses relative to TA98 were seen on the nitroreductase deficient strains TA98NR and TA98/1,8-DNP_6, suggesting the presence of nitroarenes in the POM collected from ambient air in both El Monte and Riverside.

- Factor analyses for the mutagenicity of POM collected on TIGF filters and the gaseous co-pollutant data showed that in Riverside most of

the observed variation in mutagen density with time appeared to be due to a factor which included mobile source emissions.

- In our September 1984 field study, exposures of four representative PAH (pyrene, fluoranthene, benzo(a)pyrene and perylene) to ambient air led to low recoveries of benzo(a)pyrene for the 1200-1800 hr time period; this is probably the result of its reaction with ozone. Product(s) formed from pyrene and benzo(a)pyrene during their exposure to high O_3 concentrations (1200-1800 hr) are highly mutagenic without microsomal activation (i.e., -S9). The direct mutagenic activity of the extracts from pyrene-coated TIGF filters exposed in the passive mode (1200-1800 hr) was found to be in the polar fraction.

- For the first time 2-nitrofluoranthene and 2-nitropyrene (strong direct mutagens) were detected and quantified in ambient POM collected in Southern California. The presence of these specific nitro-PAH in ambient POM provides strong evidence for the transformation of PAH to mutagenic nitroarenes during transport through the atmosphere. Thus neither of these 2-NO_2 isomers are found in directly emitted diesel soot, wood smoke, etc. In addition, highly mutagenic and carcinogenic (in animals) dinitropyrene isomers were shown to be present in ambient POM collected during peak morning traffic hours. 1-Nitropyrene, an animal carcinogen, was also identified in all of the ambient POM samples analyzed. These results support the view that reliable assessments of the health impacts of POM cannot be based solely on testing of directly emitted material but should also take into account the possibility of transformations of PAH adsorbed on particulate matter during transport through the atmosphere.

- Nighttime N_2O_5 levels were calculated from simultaneous DOAS measurements of NO_2 and NO_3 radicals available for a variety of California and European atmospheres. Estimated N_2O_5 concentrations exceeded 1 ppb ~30% of the nights and reached levels as high as ~15 ppb. Combining our laboratory exposure data for the rate of the reaction between gaseous N_2O_5 and adsorbed pyrene and our calculated nighttime N_2O_5 levels, we can estimate that up to ~5% nitration of pyrene may occur during a single night (although this value rests on several major assumptions). These calculated N_2O_5 levels also have implications for its importance as a nighttime source of nitric acid, a major constituent of acid deposition.

- From an analysis of the loss rates of N_2O_5 and/or NO_3 radicals, we obtained an upper limit rate constant for the homogeneous reaction of N_2O_5 with water vapor of ~1 x 10^{-21} cm^3 $molecule^{-1}$ sec^{-1}, in good agreement with our recent laboratory measurements.

- Using long path DOAS spectroscopy, atmospheric concentrations of gaseous HONO and the NO_3 radical were measured simultaneously for the first time. Time-concentration profiles for HONO and NO_3 radicals, and upper limits for HCHO concentrations, obtained at Riverside were used to examine selected aspects of nighttime atmospheric chemistry. Our data do not support a homogeneous gas phase mechanism, proposed recently by Stockwell and Calvert, for HONO formation initiated by the reaction of the NO_3 radical with HCHO. In particular, the maximum HONO concentrations predicted from the Stockwell and Calvert mechanism and our NO_3 radical and HCHO data were at least a factor of 10 lower than the actual HONO concentrations we observed by the DOAS technique. This finding is consistent with our earlier suggestions that the nighttime HONO concentrations we have observed at several locations in the California South Coast Air Basin arise predominately from heterogeneous reactions of NO_2 with water, direct emissions from automobile exhaust, or a combination of both (as well as other possible heterogeneous processes involving surface phenomena).

- Nitrous acid was unequivocally identified and measured spectroscopically for the first time in an indoor environment by a modified DOAS system. Over an NO_2 concentration range from 5 to 11.5 ppm, an average HONO formation rate of 0.25 ppb min^{-1} per ppm of NO_2 was observed. Allowing for higher ventilation rates in a more typical home environment, for a more realistic concentration of NO_2 of 1 ppm, a steady state concentration of ~15 ppb of HONO can be estimated. Although this must be viewed as a rough estimate, a steady state concentration of ~15 ppb is about 2-4 times higher than the HONO levels we have previously measured in polluted ambient air at several sites in the South Coast Air Basin. Since HONO is a known gas phase mutagen, and an <u>in vitro</u> precursor to nitrosamines, our finding would appear to have potential health effects implications.

E. <u>Recommendations for Future Research</u>

- An attempt should be made to identify N_2O_5 in ambient air by FT-IR spectroscopy, concurrently with DOAS measurements of NO_3 and NO_2. Thus

our calculations show that for ~30% of nights for which data are available, N_2O_5 concentrations exceeded 1 ppb, with calculated levels as high as ~10-15 ppb being attained on two occasions. Since the detection limit for the measurement of N_2O_5 using long pathlength Fourier transform infrared absorption spectroscopy is ~5 ppb at 1 km pathlength, the unambiguous detection of N_2O_5 is possible.

- Since we have shown in an earlier SAPRC/ARB program that a large portion of the mutagenicity of extracts of ambient POM is contained in the polar fractions, and little is known about the identities of these polar mutagens, attempts should be made to identify the compound(s) responsible for the mutagenicity observed during exposure of adsorbed pyrene, benzo-(a)pyrene and perylene during periods of high ozone.

- The role of HNO_3 in nitroarene formation during POM collection on filters should be clarified. Since it is likely that HNO_3 present in ambient air is removed by TIGF filters and/or collected ambient POM, further experimental studies should be carried out to investigate the role of HNO_3 in the formation of nitroarenes during POM collection. One method of approach is via the use of deuterated PAH-doped ambient POM, which avoids the use of a prefilter to remove ambient POM.

- Much further experimental work is necessary to elucidate the mechanism of formation of 2-nitrofluoranthene and 2-nitropyrene from their respective parent PAH. Since 1-NO_2-PY is an animal carcinogen and 2-NO_2-PY and 2-NO_2-FL are at least as strong direct mutagens as 1-NO_2-PY, we believe that animal tests to assess the carcinogenicity of 2-NO_2-PY and 2-NO_2-FL are also desirable.

- An attempt should be made to estimate the degree of PAH volatilization from filters during POM collection through the use of, for example, polyurethane foam plugs beneath the filters to trap the volatilized PAH.

50272-101

REPORT DOCUMENTATION PAGE	1. REPORT NO. ARB/R-85/260	2.	3. Recipient's Accession No. PB86 116191/AS

4. Title and Subtitle
PARTICULATE AND GAS PHASE MUTAGENS IN AMBIENT AND SIMULATED ATMOSPHERES

5. Report Date
December 1984

6.

7. Author(s) J.N. Pitts, A.M. Winer, J.A. Sweetman, B. Zielinska, W. Harger, R. Atkinson, H. Biermann, T. Wallington

8. Performing Organization Rept. No.

9. Performing Organization Name and Address
Statewide Air Pollution Research Center
University of California, Riverside
Riverside, CA 92521

10. Project/Task/Work Unit No.

11. Contract(C) or Grant(G) No.
(C) A3-049-32
(G)

12. Sponsoring Organization Name and Address
Air Resources Board
State of California
P.O. Box 2815
Sacramento, CA 95812

13. Type of Report & Period Covered
Final

14.

15. Supplementary Notes
Executive Summary available from the California Air Resources Board.

16. Abstract (Limit: 200 words)

Ambient POM samples were collected concurrently at two sites in California's South Coast Air Basin (El Monte and Riverside), and analyzed for both chemical composition and mutagenic activity with the Ames Salmonella typhimurium bacterial assay. 2-Nitrofluoranthene and 2-nitropyrene were detected and quantified in ambient POM. The transformation of selected polycyclic aromatic hydrocarbons (PAH) adsorbed on glass fiber (GF) and Teflon-impregnated glass fiber (TIGF) filters were also investigated under ambient conditions. Simultaneously, the ambient concentrations of a wide range of gaseous co-pollutants, which may participate in the atmospheric transformation and formation of ambient mutagens were characterized. UV/visible differential optical absorption spectroscopy (DOAS) was used to determine the ambient concentrations of HONO, NO_3 radicals, HCHO, NO_2 and SO_2. Nighttime concentrations of dinitrogen pentoxide (N_2O_5) were calculated. The formation of nitrous acid (HONO) from the hydrolysis of NO_2 was studied in an indoor environment, using a DOAS system especially modified and developed.

17. Document Analysis a. Descriptors

Mutagens
Ames Test
Nitroarenes
Polysyclic Aromatic Hydrocarbons
Nitrous Acid
Nitrate Radical
Oxides of Nitrogen
Sulfur Dioxide

b. Identifiers/Open-Ended Terms

Polluted Atmospheres
Atmospheric Chemistry
Gas Phase Reactions

c. COSATI Field/Group

18. Availability Statement	19. Security Class (This Report)	21. No. of Pages
Release Unlimited. Available from National Technical Information Service 5285 Port Royal Rd. Springfield, VA 22161	20. Security Class (This Page)	22. Price A12/$22.95

(See ANSI-Z39.18) See Instructions on Reverse OPTIONAL FORM 272 (4-77) (Formerly NTIS-35)

PARTICULATE AND GAS PHASE MUTAGENS IN AMBIENT AND SIMULATED ATMOSPHERES

Final Report
Contract Number A3-049-32
California Air Resources Board

Principal Investigator

James N. Pitts, Jr.

Co-Investigator

Arthur M. Winer

Program Manager

Janet A. Sweetman

Research Staff

Barbara Zielinska
William P. Harger
Roger Atkinson
Heinz W. Biermann
Timothy J. Wallington
Margaret C. Dodd
Travis M. Dinoff
Victoria Mejia
Philip C. Pelzel

Statewide Air Pollution Research Center
University of California
Riverside, California 92521

December 1984

ABSTRACT

In order to carry out meaningful risk assessments for respirable mutagenic particulate organic matter (POM), from which cost-effective control strategies can be developed, critical information is needed concerning the chemical structures of the mutagenic compounds, their concentrations in ambient POM and their pathways for formation and destruction.

In this study we carried out investigations designed to generate data addressing all three of these questions. Specifically, we collected ambient POM samples concurrently at two sites in California's South Coast Air Basin (El Monte and Riverside) and analyzed them for both chemical composition and mutagenic activity with the Ames Salmonella typhimurium bacterial assay. We also investigated the transformations of selected polycyclic aromatic hydrocarbons (PAH) adsorbed on glass fiber (GF) and Teflon-impregnated glass fiber (TIGF) filters under ambient conditions. Simultaneously, we characterized the ambient concentrations of a wide range of gaseous co-pollutants, which may participate in the atmospheric transformations and formation of ambient mutagens. In these latter measurements we employed UV/visible differential optical absorption spectroscopy (DOAS) to determine the ambient concentrations of HONO, NO_3 radicals, HCHO, NO_2 and SO_2.

From simultaneous NO_3 radical and NO_2 nighttime ambient concentrations we have calculated the corresponding nighttime concentrations of dinitrogen pentoxide (N_2O_5) and we report here implications of these predicted N_2O_5 concentrations for the nighttime nitration of adsorbed, and possibly gas phase, PAH. These results also are highly relevant to the nighttime formation of nitric acid in acid rain and fogs.

Finally, we studied the formation of nitrous acid (HONO) from the hydrolysis of NO_2 in an indoor environment using a DOAS system especially modified and developed for this purpose. HONO is a gas phase mutagen and, by reaction with amines, a precursor to carcinogenic nitrosamines.

The following include our major findings:

- The ratios of mutagen densities for POM simultaneously collected on GF and TIGF filters were observed to vary from a low of 0.27 to a high of 4.95. The higher values occurred during periods of elevated O_3 and PAN concentrations, suggesting there may be an artifact effect during particulate collection associated with one or both of these two types of filters. While analysis of

the mutagen density/CO ratios suggests that a filter artifact is associated with the GF filters, we cannot rule out possible artifacts occurring on the TIGF filters. However, at the present time we prefer TIGF as the filter of choice based on its more inert properties.

- Mutagenic products were formed during exposure to ambient air of pyrene, perylene and benzo(a)pyrene, adsorbed on TIGF and GF filters. Higher mutagenicities were observed during a period of high O_3 concentration (1200-1800 hr).

- For the first time 2-nitrofluoranthene and 2-nitropyrene were detected and quantified in ambient POM collected in Southern California. The presence of these nitro-PAH in ambient POM provides evidence for the transformation of certain PAH to mutagenic nitroarenes during transport through the atmosphere. Strongly mutagenic and carcinogenic (in animals) dinitropyrene isomers were also found in ambient POM collected during peak morning traffic hours. 1-Nitropyrene, an animal carcinogen, was also identified in all ambient POM samples analyzed. Both 2-nitropyrene and 2-nitrofluoranthene are strong direct mutagens in the Ames assay (as is 1-nitropyrene) but their possible carcinogenicities are not yet known.

- Nighttime N_2O_5 concentrations were estimated for ambient atmospheres in California and in Europe, and were often found to exceed 1 ppb with calculated concentrations as high as 15-20 ppb. These predicted levels suggest that N_2O_5 may be important as an atmospheric constituent, both in nitration reactions of PAH and in the nighttime formation of nitric acid, a major component of acidic deposition.

- From an analysis of the NO_3 radical, NO_2, HCHO and HONO data obtained during the 1983 field study, we showed that the homogeneous gas phase mechanism proposed by Stockwell and Calvert for HONO formation (initiated by the reaction of the NO_3 radical with formaldehyde) is, at most, of minor importance.

- We demonstrated for the first time that significant amounts of HONO can be formed from NO_2 in an indoor environment.

These results have important consequences for our current understanding of PAH transformations and particulate mutagenicity in California's atmosphere, as well as of the formation of nitric acid in acidic rain and fogs. They also illustrate the need for further studies concerning the role of ozone and gaseous nitrogenous pollutants not only in the formation of atmospheric mutagens, but also acid deposition. Finally, they constitute relevant input into risk assessment evaluations being developed for both of these major atmospheric phenomena.

TABLE OF CONTENTS

	Page
Abstract	iii
Acknowledgments	ix
List of Figures	xi
List of Tables	xvii
Glossary of Terms, Abbreviations and Symbols	xxi
I. PROJECT SUMMARY	I-1
A. Introduction and Statement of the Problem	I-1
B. Objectives	I-1
C. Methods of Approach	I-2
D. Summary of Results and Conclusions	I-3
E. Recommendations for Future Research	I-5
II. MUTAGENICITY OF AMBIENT PARTICULATES AT CENTRAL AND DOWNWIND RECEPTOR SITES IN THE CSCAB: SEPTEMBER 1983 FIELD STUDY	II-1
A. Introduction	II-1
B. Background	II-1
C. Experimental	II-2
1. Gas Phase Analyses During Collection Period	II-3
2. Collection of Particulate Matter	II-3
3. Mutagenicity Bioassay Procedures	II-5
4. Data Manipulation	II-6
5. Air Mass Trajectories	II-6
D. Results and Discussion	II-7
E. Conclusions	II-43
III. INVESTIGATION OF PAH TRANSFORMATIONS UNDER AMBIENT ATMOSPHERIC CONDITIONS: SEPTEMBER 1984 FIELD STUDY	III-1
A. Introduction	III-1

TABLE OF CONTENTS (continued)

	Page
B. Experimental	III-1
1. Gas Phase Analyses During Collection Period	III-1
2. Exposures of PAH-Coated Filters	III-2
3. Filter Extractions and Sample Analysis	III-3
C. Results and Discussion	III-4
1. Gaseous Species	III-4
2. Active and Passive PAH Exposures	III-4
D. Conclusions	III-17
IV. INVESTIGATION OF MUTAGENICITY AND NITROARENE LEVELS IN AMBIENT PARTICULATE	IV-1
A. Introduction	IV-1
B. Experimental	IV-2
1. Mega-Sampler Ambient POM Collection	IV-2
2. Synthesis of Nitroarene Standards	IV-3
3. Experimental Procedure for Determination of Selected Nitroarene Concentrations in Ambient POM	IV-4
C. Results	IV-9
1. Mutagenicity of Ambient POM Extracts	IV-9
2. Nitroarene Identification and Quantification	IV-14
D. Discussion	IV-22
E. Conclusions	IV-26
V. CALCULATIONS OF NIGHTTIME N_2O_5 CONCENTRATIONS AND IMPLICATIONS FOR PAH TRANSFORMATIONS	V-1
A. Introduction	V-1
B. Ambient Atmospheric Data	V-2
C. The Magnitude of N_2O_5 and/or NO_3 Radical Loss Processes	V-11
D. Reaction of N_2O_5 with PAH as a Source of Nitroarenes	V-20
E. Conclusions	V-22

TABLE OF CONTENTS (continued)

		Page
VI.	MEASUREMENT OF GASEOUS POLLUTANTS BY LONGPATH DIFFERENTIAL OPTICAL ABSORPTION SPECTROSCOPY: IMPLICATIONS FOR NIGHTTIME ATMOSPHERIC CHEMISTRY	VI-1
	A. Introduction	VI-1
	B. Experimental	VI-2
	C. Results	VI-6
	D. Discussion	VI-16
	E. Conclusions	VI-18
VII.	IDENTIFICATION AND MEASUREMENT OF NITROUS ACID (A GAS PHASE MUTAGEN) IN AN INDOOR ENVIRONMENT	VII-1
	A. Introduction	VII-1
	B. Experimental	VII-2
	C. Results and Discussion	VII-5
	D. Conclusions	VII-8
VIII.	REFERENCES	VIII-1
IX.	APPENDICES	IX-1
	A. September 1983 Field Study	
	1. Twenty-Four Hour Air Mass Trajectories	
	2. Correlation Coefficients for El Monte Data	
	3. Correlation Coefficients for Riverside Data	
	B. DOAS Measurements During the September 1984 Field Study	
	C. Ambient Air Data For the September 1984 Field Study	
	D. Electron Impact Mass Spectra of a Series of Standard Nitroarenes	

ACKNOWLEDGMENTS

We express our appreciation to Drs. John R. Holmes and Jack K. Suder of the California Air Resources Board staff for their valuable technical and administrative advice.

We thank Professor Bruce N. Ames for the Salmonella strain TA98, Professor Herbert S. Rosenkranz for Salmonella strains TA98NR and TA98/1,8-DNP_6, and Dr. Dennis Schuetzle of Ford Motor Co., MI, for the generous gift of 2-nitropyrene. We also thank Mr. Robert Giauque at the Lawrence Berkeley Laboratory for elemental analyses and Dr. James Huntzicker of the Oregon Graduate Center for the carbon analyses. We appreciate the excellent assistance of Ms. Minn Poe and Ms. Verpi Lindfors in providing statistical analyses and computer plots of the data, and thank statistician Mr. Ted Younglove for many valuable discussions concerning the statistical analyses. The contributions of Mr. Dennis Fitz and Dr. Hanns Paur to our September 1983 field study were appreciated. We also thank Mr. Chuck Daly, Dr. Hélène Mac Leod and Ms. Becky Ohta for their contributions to our September 1984 field study. In addition, we wish to acknowledge the participation of Drs. Bruce Appel and Yosh Tokima of the Air Industrial Hygiene Laboratory during the 1984 study. The assistance of Mr. Mike Kienitz and Mr. Erv Mateer of our technical staff is also gratefully acknowledged, as is the work of our laboratory technicians Mr. Greg Butters, Ms. Stacy Trouard, Ms. Tricia McElroy and Ms. Becky Ohta. We also wish to thank Ms. Chris LaClaire, Ms. Mae Minnich, Ms. Neva Friesen, Mr. Joe Kriz and Mr. Chuck Daly for their valuable assistance in preparing this report.

This report was submitted in partial fulfillment of Contract No. A3-049-32 "Particulate and Gas Phase Mutagens in Ambient and Simulated Atmospheres," by the Statewide Air Pollution Research Center, University of California, Riverside, under the sponsorship of the California Air Resources Board. Work was completed as of November 30, 1984.

The statements and conclusions in this report are those of the contractor and not necessarily those of the California Air Resources Board. The mention of commercial products, their source or their use in connection with material reported herein is not to be construed as either an actual or implied endorsement of such products.

LIST OF FIGURES

Figure Number	Title	Page
II-1	Ozone Concentrations for El Monte (X) and Riverside (□) for September 12, 1983	II-8
II-2	Ozone Concentrations for El Monte (X) and Riverside (□) for September 13, 1983	II-9
II-3	Ozone Concentrations for El Monte (X) and Riverside (□) for September 14, 1983	II-10
II-4	Ozone Concentrations for El Monte (X) and Riverside (□) for September 15, 1983	II-11
II-5	Ozone Concentrations for El Monte (X) and Riverside (□) for September 16, 1983	II-12
II-6	Ozone Concentrations for El Monte (X) and Riverside (□) for September 17, 1983	II-13
II-7	Carbon Monoxide (Solid Line), Nitric Oxide (Δ) and Nitrogen Dioxide (□)* Concentrations at El Monte for September 12, 1983 *NO_2 is Uncorrected for PAN Positive Interference	II-14
II-8	Carbon Monoxide (Solid Line), Nitric Oxide (Δ) and Nitrogen Dioxide (□)* Concentrations at El Monte for September 13, 1983 *NO_2 is Uncorrected for PAN Positive Interference	II-15
II-9	Carbon Monoxide (Solid Line), Nitric Oxide (Δ) and Nitrogen Dioxide (□)* Concentrations at El Monte for September 14, 1983 *NO_2 is Uncorrected for PAN Positive Interference	II-16
II-10	Carbon Monoxide (Solid Line), Nitric Oxide (Δ) and Nitrogen Dioxide (□)* Concentrations at El Monte for September 15, 1983 *NO_2 is Uncorrected for PAN Positive Interference	II-17
II-11	Carbon Monoxide (Solid Line), Nitric Oxide (Δ) and Nitrogen Dioxide (□)* Concentrations at El Monte for September 16, 1983 *NO_2 is Uncorrected for PAN Positive Interference	II-18
II-12	Carbon Monoxide (Solid Line), Nitric Oxide (Δ) and Nitrogen Dioxide (□)* Concentrations at El Monte for September 17, 1983 *NO_2 is Uncorrected for PAN Positive Interference	II-19

LIST OF FIGURES (continued)

Figure Number	Title	Page
II-13	Carbon Monoxide (Solid Line), Nitric Oxide (Δ) and Nitrogen Dioxide (□)* Concentrations at Riverside for September 12, 1983 *NO_2 is Uncorrected for PAN Positive Interference	II-20
II-14	Carbon Monoxide (Solid Line), Nitric Oxide (Δ) and Nitrogen Dioxide (□) Concentrations at Riverside for September 13, 1983	II-21
II-15	Carbon Monoxide (Solid Line), Nitric Oxide (Δ) and Nitrogen Dioxide (□) Concentrations at Riverside for September 14, 1983	II-22
II-16	Carbon Monoxide (Solid Line), Nitric Oxide (Δ) and Nitrogen Dioxide (□) Concentrations at Riverside for September 15, 1983	II-23
II-17	Carbon Monoxide (Solid Line), Nitric Oxide (Δ) and Nitrogen Dioxide (□) Concentrations at Riverside for September 16, 1983	II-24
II-18	Carbon Monoxide (Solid Line), Nitric Oxide (Δ) and Nitrogen Dioxide (□) Concentrations at Riverside for September 17, 1983	II-25
III-1	Carbon Monoxide Concentration at U.C. Riverside for 1200 PDT September 18 to 1200 PDT September 19, 1984	III-5
III-2	Nitric Oxide Concentration at U.C. Riverside for 1200 PDT September 18 to 1200 PDT September 19, 1984	III-6
III-3	Nitrogen Dioxide Concentration at U.C. Riverside for 1200 PDT September 18 to 1200 PDT September 19, 1984 (Chemiluminescence Detection Uncorrected for Interferences)	III-7
III-4	Ozone Concentration at U.C. Riverside for 1200 PDT September 18 to 1200 PDT September 19, 1984	III-8
III-5	Peroxyacetyl Nitrate Concentration at U.C. Riverside for 1200 PDT September 18 to 1200 PDT September 19, 1984	III-9
III-6	Nitrous Acid Concentration at U.C. Riverside for 1200 PDT September 18 to 1200 PDT September 19, 1984, as Measured by Differential Optical Absorption Spectroscopy	III-10

LIST OF FIGURES (continued)

Figure Number	Title	Page
III-7	Nitrate Radical Concentration (Measured by DOAS) and Dinitrogen Pentoxide (N_2O_5) Concentration (Calculated) at U.C. Riverside for 1200 PDT September 18 to 1200 PDT September 19, 1984	III-11
III-8	Temperatures Measured at U.C. Riverside for 1200 PDT September 18 to 1200 PDT September 19, 1984	III-12
IV-1	MID Traces Showing Resolution of Nitrofluoranthene and Nitropyrene Isomers on 60-m DB-5 Capillary Column. The Isomers in Order of Elution are: 1-Nitrofluoranthene (1-NF), 7-Nitrofluoranthene (7-NF), 2-Nitrofluoranthene (2-NF), 3-Nitrofluoranthene (3-NF), 8-Nitrofluoranthene (8-NF), 1-Nitropyrene (1-NP) and 2-Nitropyrene (2-NP). All ions shown to same scale. Column Conditions: 50 to 200 C at 20 C min^{-1}, then increased at 6 C min^{-1}	IV-5
IV-2	Outline of Chemical Analysis for Nitro-PAH	IV-6
IV-3	HPLC Trace (254 nm) and Gradient Program for Separation of Ambient Sample	IV-8
IV-4	MID Traces of Deuterated Mononitro-PAH used to Spike Ambient Samples Prior to the Separation Procedure. Samples were Spiked with 8.5 µg 3- and 8-Nitrofluoranthene-d_9 and 10 µg 1-Nitropyrene-d_9. Note the Lack of Interfering Ion Peaks at 247($[M]^+$) and 217($[M-NO]^+$) [the Scale to Which these Ions are Plotted is 100X More Sensitive than for the Deuterated Ions]. GC Conditions: 60-m DB-5 Column, 50 to 200 C at 20 C min^{-1}, then increased at 6 C min^{-1}	IV-10
IV-5	Nitro-PAH Standard Used for Quantification. Standard Contained 3-Nitrofluoranthene, 3-Nitrofluoranthene-d_9, 8-Nitrofluoranthene-d_9, 1-Nitropyrene, 1-Nitropyrene-d_9 and 2-Nitropyrene. Note that the Retention Times of the Deuterated Species is Slightly Lower than the Corresponding Non-Deuterated Isomer. GC Conditions as Given in Figure IV-4	IV-11
IV-6	MID Traces of Deuterated Dinitropyrene Isomers. The Isomers in Order of Elution are: 1,3-Dinitropyrene-d_8, 1,6-Dinitropyrene-d_8; 1,8-Dinitropyrene-d_8. Samples were Spiked with 20 µg of this Mixture. GC Conditions: 60-m DB-5 Column, 50 to 200 C at 20 C min^{-1} then increased at 8 C min^{-1}. Ions m/e 292 and m/e 200 Integrated 10X Other Ions	IV-12

LIST OF FIGURES (continued)

Figure Number	Title	Page
IV-7	MID Traces of CH_2Cl_2 Extract from Ambient POM, 1200-1800 hr September 18, 1984 Collection Period. HPLC Fraction Containing Mononitro-isomers is Shown. GC Conditions as Given in Figure IV-4	IV-15
IV-8	MID Traces of POM Extract Shown in Figure IV-7. Ten Times Longer Integration Times were used for m/e 247 and 217 than for m/e 256	IV-16
IV-9	MID Traces of CH_2Cl_2 Extract from Ambient POM, 1800-2400 hr September 18, 1984 Collection Period. HPLC Fraction Containing Mononitro-isomers is Shown. GC Conditions as Given in Figure IV-4	IV-17
IV-10	MID Traces of CH_2Cl_2 Extract from Ambient POM, 0000-0600 hr September 19, 1984 Collection Period. HPLC Fraction Containing Mononitro-isomers is Shown. GC Conditions as Given in Figure IV-4	IV-18
IV-11	MID Traces of CH_2Cl_2 Extract from Ambient POM, 0600-1200 hr September 19, 1984 Collection Period. HPLC Fraction Containing Mononitro-isomers is Shown. GC Conditions as Given in Figure IV-4	IV-19
IV-12	MID Traces of CH_2Cl_2 Extract from Ambient POM, 0600-1200 hr September 19, 1984 Collection Period. Two HPLC Fractions Containing di-NO_2-PY Isomers are Shown. GC Conditions as Given in Figure IV-6	IV-21
V-1	Time-Concentation Profiles Observed for NO_3 Radicals by DOAS Spectroscopy at (a) Riverside, CA During Evening of September 12, 1979 (Platt et al. 1980a) and (b) Death Valley, CA on night of May 3-4, 1982 (Platt et al. 1984). The Experimental Data are Denoted by the Crosses (Figure V-1a) and Horizontal Bars (Figure V-1b)	V-12
V-2	Experimental Data (Solid Horizontal Bars) for NO_3 Radicals at Edwards AFB on Night of May 23-24, 1982 (Platt et al. 1984), Together with Calculated Profiles from Equation (V) for Various Values of k_7 (the Rate Constant for Reaction of N_2O_5 with Water Vapor) or $k_5[X]$ (the NO_3 Radical Decay Rate): A, $k_7 = 1.1 \times 10^{-21}$ cm^3 $molecule^{-1}$ sec^{-1} of $k_5[X] = 1.2 \times 10^{-4}$ sec^{-1}; B, $k_7 = 2.8 \times 10^{-21}$ cm^3 $molecule^{-1}$ sec^{-1} or $k_5[X] = 3.0 \times 10^{-4}$ sec^{-1}; C, $k_7 = 5.6 \times 10^{-21}$ cm^3 $molecule^{-1}$ sec^{-1} or $k_5[X] = 6.1 \times 10^{-4}$ sec^{-1}. The Observed Photodissociation of NO_3 Radicals Around Sunrise is Shown by the Dashed Line	V-13

LIST OF FIGURES (continued)

Figure Number	Title	Page
V-3	NO_2 Time-Concentration Profiles Measured by DOAS (---) and by a Chemiluminescence Analyzer, Uncorrected for Interferences, (——) on September 18, 1984	V-18
V-4	Plot of the Rate Constant k_7 Against Temperature	V-19
V-5	Percent of 1-Nitropyrene Formed from Passive Exposures of Pyrene in the Dark to Various Gaseous Nitrogenous Species at Initial Concentrations as Follows: ◊ - Exposure to N_2O_5 (1.5 ppm), NO_2 (5 ppm), HNO_3 (~0.1 ppm) and the NO_3 Radical (~0.0005 ppm); ● - Exposure to N_2O_5 (1.5 ppm), NO_2 (~0.3 ppm), HNO_3 (~0.1 ppm) and the NO_3 Radical (~0.01 ppm)	V-21
VI-1	Long Pathlength Differential Optical Absorption Spectrometer	VI-3
VI-2	The "Slotted Disk" Rapid Scanning Device Located in the Focal Plane of the Differential Optical Absorption Spectrometer (from Platt and Perner 1983)	VI-5
VI-3	Experimental Time-Concentration Profiles for O_3, NO, NO_2, the NO_3 Radical and HONO for 1600 hr, September 15, 1983 Through 1200 hr, September 16, 1983. --- Calculated HONO Concentrations Based Upon Reactions (1-4) of Text, Using the $NO_2 + NO_3 \rightleftarrows N_2O_5$ Equilibrium Constant of Malko and Troe (1982) to Derive our Experimental Rate Constant for Reaction (1)	VI-14
VI-4	Experimental Time-Concentration Profiles for O_3, NO, NO_2, the NO_3 Radical and HONO for 1600 hr, September 16, 1983 Through 1200 hr, September 17, 1983. --- Calculated HONO Concentrations Based Upon Reactions (1-4) of Text, Using the $NO_2 + NO_3 \rightleftarrows N_2O_5$ Equilibrium Constant of Malko and Troe (1982) to Derive our Experimental Rate Constant for Reaction (1)	VI-15
VII-1	Experimental Arrangement of the Differential Optical Absorption Spectrometer (DOAS) Within the Mobile Laboratory	VII-3
VII-2	DOAS Spectra Showing Generation of Nitrous Acid for Mobile Laboratory Filled with 11.5 ppm of NO_2 in Air	VII-6

LIST OF FIGURES (continued)

Figure Number	Title	Page
VII-3	HONO Concentrations Plotted as a Function of Time for Mobile Laboratory Filled with 11.5 ppm of NO_2	VII-6
VII-4	Initial HONO Formation Rate, d[HONO]/dt Versus $[NO_2]$ for Several Experimental Systems. (▲ This Work; T = 301 ± 6 K, RH = 45 ± 15%, X SAPRC 5800-Liter Evacuable Chamber; T = 301 ± 4 K, RH ≈ 50%: ● SAPRC 4300-Liter All Teflon Chamber; T = 297 K, RH ≈ 50%: ■ NIES 6065-Liter Evacuable Chamber; T = 303 K, RH ≈ 50%. The Dashed Line is the Best Fit Line with Unit Slope through the Data for the SAPRC 5800-Liter Evacuable Chamber	VII-7

LIST OF TABLES

Table Number	Title	Page
II-1	Instrumentation for Measurement of Gaseous Pollutants During September 1983 Field Study	II-3
II-2	Sampling Schedule in September 1983 Field Study	II-4
II-3	Mutagenicity of El Monte Ambient Particulate Matter (TIGF Filters) Collected Over the Following Time Intervals: 1 = 0600-1000 hr, 2 = 1000-1500 hr, 3 = 1500-2100 hr, 4 = 2100-0600 hr	II-26
II-4	Mutagenicity of Riverside Ambient Particulate Matter (TIGF Filters) Collected Over the Following Time Intervals: 1 = 0600-1000 hr, 2 = 1000-1500 hr, 3 = 1500-2100 hr, 4 = 2100-0600 hr	II-27
II-5	Mutagen Densities Obtained at El Monte on September 12-15, 1983 for Particles Collected on EPM 2000 GF and TX40HI20WW TIGF Filters	II-29
II-6	Mutagen Densities Obtained at Riverside on September 12-15, 1983 for Particles Collected on EPM 2000 GF and TX40HI20WW TIGF Filters	II-30
II-7	Values for Standard Mutagens (rev μg^{-1}) [-S9] 2-Nitrofluorene (2-NF) and Quercetin (Q) Included in Mutagenicity Tests Reported in Tables II-3 to II-6	II-30
II-8	Particulate Carbon, Lead and Bromine Values and Gaseous Co-pollutants at El Monte Averaged Over the Following Time Intervals: 1 = 0600-1000 hr, 2 = 1000-1500 hr, 3 = 1500-2100 hr, 4 = 2100-0600 hr, which Corresponded to the Particulate Sampling Intervals	II-31
II-9	Particulate Carbon, Lead and Bromine Values and Gaseous Co-pollutants at Riverside Averaged Over the Following Time Intervals: 1 = 0600-1000 hr, 2 = 1000-1500 hr, 3 = 1500-2100 hr, 4 = 2100-0600 hr, which Corresponded to the Particulate Sampling Intervals	II-32
II-10	Elements Determined by X-Ray Fluorescence Analyses of Particulate Collected on Nuclepore Filters in El Monte. Time Interval: 1 = 0600-1000 hr, 2 = 1000-1500 hr, 3 = 1500-2100 hr, 4 = 2100-0600 hr. Units: $\mu g\ m^{-3}$	II-33
II-11	Elements Determined by X-Ray Fluorescence Analyses of Particulate Collected on Nuclepore Filters in Riverside. Time Interval: 1 = 0600-1000 hr, 2 = 1000-1500 hr, 3 = 1500-2100 hr, 4 = 2100-0600 hr. Units: µg m-3	II-34

LIST OF TABLES (continued)

Table Number	Title	Page
II-12	Ratios of Mutagen Densities for Two Filter Types, Mutagen Density to CO Ratios, and Ozone and PAN Concentrations for September 12-15, 1983 in El Monte	II-36
II-13	Ratios of Mutagen Densities for Two Filter Types, Mutagen Densities to CO Ratios, and Ozone and PAN Concentrations for September 12-15, 1983 in Riverside	II-37
II-14	Definition of Variables Used in Factor Analyses and Regressions	II-39
II-15	Principal Component Factors for El Monte	II-41
II-16	Regression of Factors for El Monte	II-41
II-17	Principal Component Factors for Riverside	II-42
II-18	Regression of Factors for Riverside	II-42
II-19	Regression of Original Data for El Monte with Mutagenicity Parameters	II-44
II-20	Regression of Original Data for Riverside with Mutagenicity Parameters	II-44
III-1	Instrumentation for Measurement of Gaseous Pollutants During September 1984 Field Study	III-2
III-2	Dominant Pollutants Expected During the Exposure Periods	III-3
III-3	PAH Recovered (HPLC Analyses) from 1200 hr September 18 to 1200 hr September 19. Active Exposures on TIGF and GF Filters	III-14
III-4	PAH Recovered (HPLC Analyses) from 1200 hr September 18 to 1200 hr September 19. Passive Exposures on TIGF and GF Filters	III-14
III-5	Mutagenic Activity for Active Exposures - Spot Test Results (Total Revertants per Filter)	III-15
III-6	TA98 Activity for Passive Exposures - Spot Test Results (Total Revertants per Filter)	III-16

LIST OF TABLES (continued)

Table Number	Title	Page
IV-1	Mutagen Density [rev m^{-3}, Strain TA98 (-S9)] of CH_2Cl_2 and CH_3CN Extracts from Ambient POM Collected on Different Filter Substrates from 1200 hr September 18 to 1200 hr September 19, 1984 and Particulate and Extract Weights (mg)	IV-13
IV-2	Concentration of Nitro-PAH in Ambient POM	IV-22
V-1	Reported Ambient Atmospheric NO_3 Radical Concentration Data, Other Relevant Parameters, and Estimates of the Rate Constant k_7 and the NO_3 Radical Decay Rate $k_5[X]$	V-4
VI-1	Observed Concentrations of NO_2 and HONO on September 12-14, 1983	VI-7
VI-2	Observed Concentrations of NO_2, HONO, NO_3 Radicals and SO_2 on September 15, 1983	VI-11
VI-3	Observed Concentrations of NO_2, HONO, NO_3 Radicals and SO_2 on September 16, 1983	VI-12
VII-1	Experimental Conditions and Corresponding Rates of HONO Formation	VII-7

GLOSSARY OF TERMS, ABBREVIATIONS AND SYMBOLS

BaP: Benzo(a)pyrene

C: Degrees Centigrade

CARB: California Air Resources Board

Di-NO_2-PY: Dinitropyrene(s)

Di-NO_2-PY-d_8: Deuterated dinitropyrene(s)

DOAS: Differential optical absorption spectroscopy

^oF: Degrees Fahrenheit

FL: Fluoranthene

FT-IR: Fourier-transform infrared absorption spectroscopy

GC: Gas chromatograph

GC-MS: Gas chromatography-mass spectrometry

GF filters: Glass fiber filters

Hi-Vol: High volume sampler

HPLC: High performance liquid chromatography

hr: Hour

K: Degrees Kelvin

K_i: Reaction rate constant

$K_{i,j}$: Equilibrium constant for the reaction system i, j

Lo-Vol: Low volume sampler

m: Meter

MID: Multiple ion detection technique, used together with GC-MS

mℓ: Milliliter

mm: Millimeter

Nitroarenes: Nitrated polycyclic aromatic hydrocarbons (PAH)

nm: Nanometer

NO_2-FL: Nitrofluoranthene

NO_2-FL-d_9: Deuterated nitrofluoranthene

NO_2-PAH: Nitrated PAH

NO_2-PY: Nitropyrene

1-NO_2-PY-d_9: Deuterated 1-nitropyrene

Open Column Chromatography: Liquid chromatography technique, used for compound separation or purification

PAH: Polycyclic aromatic hydrocarbons

PAN: Peroxyacetyl nitrate

PDT: Pacific daylight time

PER: Perylene

POM: Particulate organic matter

ppb: Part per billion

ppt: Part per trillion

PY: Pyrene

SAPRC: Statewide Air Pollution Research Center

SCFM: Standard cubic feet per minute

Semi-prep column: Semi preparative column used for compound separation or purification by HPLC method

TIGF filters: Teflon impregnated glass fiber filters

µg: Microgram

µm: Micrometer

I. PROJECT SUMMARY

A. Introduction and Statement of the Problem

It is now well recognized that respirable sub-micron particles collected from ambient air contain organic compounds which exhibit strong, direct acting, mutagenic activity in the Ames Salmonella typhimurium bacterial reversion assay. However, polycyclic aromatic hydrocarbons (PAH) are not directly mutagenic, requiring microsomal activation, and it has been postulated that this observed direct mutagenicity of ambient particulate organic matter (POM) may be due, at least in part, to the presence of mono- and dinitroarenes. While certain of these nitroarenes are emitted in combustion derived POM, few data are available on their quantification in collected ambient POM. Furthermore, it is not known whether other PAH derivatives contribute in any significant manner to the observed mutagenic burden, or whether transformations of emitted PAH to nitroarenes and other PAH derivatives occur during transport through the atmosphere or on collection.

Clearly, more data are needed concerning the chemical composition and associated mutagenic activity of ambient POM, collected on several substrates and under conditions where a knowledge of the gaseous co-pollutants, and their concurrent concentrations, is available. Such information is essential for the generation of reliable risk assessments concerning the possible health impacts of respirable mutagenic particles (a) emitted directly to the atmosphere (e.g., diesel soot), (b) formed in atmospheric processes, (c) or both.

B. Objectives

The overall objectives of this program were to:

- Investigate (using the Ames test) the mutagenic activity of POM collected concurrently at a mid-basin site (El Monte) and a downwind receptor site (Riverside) in the CSCAB.
- Compare different, and widely used, filter types [glass fiber (GF) and Teflon impregnated glass fiber (TIGF) filters] in terms of their influence on the mutagenicity of collected POM.
- Determine gaseous co-pollutant concentrations simultaneously with POM collections by both conventional analyzers, and with a unique, long

pathlength spectroscopic technique [UV/visible differential optical absorption spectroscopy (DOAS)] and, utilizing factor analyses, investigate correlations of POM mutagenic activities with these co-pollutant concentrations and other variables.

- Investigate possible transformation reactions of adsorbed PAH under well-defined ambient air conditions, including the use of both active and passive filter exposure techniques.
- Develop appropriate analytical methods for identification and quantification of mono- and dinitroarenes and determine their concentrations in our ambient POM samples.
- Calculate nighttime N_2O_5 levels from the available NO_3 and NO_2 concentration data at a variety of locations in southern California and Europe and estimate whether or not nitration of adsorbed PAH by N_2O_5 during nighttime hours could be a significant pathway to the formation of direct acting mutagens. An additional objective was to gain further information concerning the possible importance of N_2O_5 in nighttime atmospheric chemistry, including its role in forming nitric acid, a major component of acid rain and fogs.
- Test the validity of a homogeneous gas phase mechanism, proposed by Stockwell and Calvert (1983), to explain the ambient levels of HONO we have previously observed in the South Coast Air Basin by the DOAS technique.
- Determine spectroscopically whether nitrous acid, a gas phase mutagen and (by reaction with amines) a precursor to nitrosamines, can be formed in indoor environments from the reaction of NO_2 and H_2O vapor.

C. Methods of Approach

To achieve the objectives outlined above, we conducted extensive field studies in September 1983 and September 1984. In the September 1983 investigation, we measured concurrently the mutagenicity of ambient POM collected on TIGF and GF filters in El Monte and Riverside. As noted earlier, at Riverside, in addition to conventional gaseous pollutant analyses, our unique long optical path DOAS system was utilized to measure gas phase concentrations of the nitrate radical (NO_3), formaldehyde (HCHO) and nitrous acid (HONO).

In the September 1984 study, selected PAH adsorbed on TIGF and GF filters were exposed to the ambient atmosphere for four 6-hour time periods each day for five successive 24-hr days. Gaseous co-pollutants, including the NO_3 radical, HCHO and HONO (as well as O_3, NO_2 and SO_2), were measured concurrently utilizing our DOAS system. In addition, samples of ambient POM were collected with our SAPRC mega-sampler for nitroarene analysis.

Finally, a DOAS system was developed that incorporates a multipass optical system and this new configuration was employed to identify HONO and to measure its rate of formation from NO_2 in an indoor environment.

D. Summary of Results and Conclusions

- Depending upon the time period of collection, the ratios of mutagen densities (rev m^{-3}) for POM simultaneously collected on GF and TIGF filters ranged from a factor of 5 greater than unity (generally during periods of high O_3 and PAN) to nearly a factor of 4 less than unity (generally during the 0600-1200 hr time period associated with morning traffic peaks). The observation that the GF filter extracts generally had lower mutagenic activities, except during periods of high ozone concentration, suggests that there is an artifact effect during POM collection associated with one or both of these two types of filters. The mutagen density to CO ratios during these times gave further indication of a filter artifact on the GF filters. These observations have important implications to the CARB, and other regulatory agencies, concerning the choice of filter for collection of ambient POM.

- The observed mutagen densities (TA98, -S9) of TIGF filter extracts varied from 22 to 240 rev m^{-3} for Riverside and from 40 to 260 rev m^{-3} for El Monte. These values are higher than those generally reported in the literature for other air basins but are similar to values we have previously reported for locations in the South Coast Air Basin.

- Decreased responses relative to TA98 were seen on the nitroreductase deficient strains TA98NR and TA98/1,8-DNP_6, suggesting the presence of nitroarenes in the POM collected from ambient air in both El Monte and Riverside.

- Factor analyses for the mutagenicity of POM collected on TIGF filters and the gaseous co-pollutant data showed that in Riverside most of

the observed variation in mutagen density with time appeared to be due to a factor which included mobile source emissions.

- In our September 1984 field study, exposures of four representative PAH (pyrene, fluoranthene, benzo(a)pyrene and perylene) to ambient air led to low recoveries of benzo(a)pyrene for the 1200-1800 hr time period; this is probably the result of its reaction with ozone. Product(s) formed from pyrene and benzo(a)pyrene during their exposure to high O_3 concentrations (1200-1800 hr) are highly mutagenic without microsomal activation (i.e., -S9). The direct mutagenic activity of the extracts from pyrene-coated TIGF filters exposed in the passive mode (1200-1800 hr) was found to be in the polar fraction.

- For the first time 2-nitrofluoranthene and 2-nitropyrene (strong direct mutagens) were detected and quantified in ambient POM collected in Southern California. The presence of these specific nitro-PAH in ambient POM provides strong evidence for the transformation of PAH to mutagenic nitroarenes during transport through the atmosphere. Thus neither of these 2-NO_2 isomers are found in directly emitted diesel soot, wood smoke, etc. In addition, highly mutagenic and carcinogenic (in animals) dinitropyrene isomers were shown to be present in ambient POM collected during peak morning traffic hours. 1-Nitropyrene, an animal carcinogen, was also identified in all of the ambient POM samples analyzed. These results support the view that reliable assessments of the health impacts of POM cannot be based solely on testing of directly emitted material but should also take into account the possibility of transformations of PAH adsorbed on particulate matter during transport through the atmosphere.

- Nighttime N_2O_5 levels were calculated from simultaneous DOAS measurements of NO_2 and NO_3 radicals available for a variety of California and European atmospheres. Estimated N_2O_5 concentrations exceeded 1 ppb ~30% of the nights and reached levels as high as ~15 ppb. Combining our laboratory exposure data for the rate of the reaction between gaseous N_2O_5 and adsorbed pyrene and our calculated nighttime N_2O_5 levels, we can estimate that up to ~5% nitration of pyrene may occur during a single night (although this value rests on several major assumptions). These calculated N_2O_5 levels also have implications for its importance as a nighttime source of nitric acid, a major constituent of acid deposition.

- From an analysis of the loss rates of N_2O_5 and/or NO_3 radicals, we obtained an upper limit rate constant for the homogeneous reaction of N_2O_5 with water vapor of ~1 x 10^{-21} cm^3 $molecule^{-1}$ sec^{-1}, in good agreement with our recent laboratory measurements.

- Using long path DOAS spectroscopy, atmospheric concentrations of gaseous HONO and the NO_3 radical were measured simultaneously for the first time. Time-concentration profiles for HONO and NO_3 radicals, and upper limits for HCHO concentrations, obtained at Riverside were used to examine selected aspects of nighttime atmospheric chemistry. Our data do not support a homogeneous gas phase mechanism, proposed recently by Stockwell and Calvert, for HONO formation initiated by the reaction of the NO_3 radical with HCHO. In particular, the maximum HONO concentrations predicted from the Stockwell and Calvert mechanism and our NO_3 radical and HCHO data were at least a factor of 10 lower than the actual HONO concentrations we observed by the DOAS technique. This finding is consistent with our earlier suggestions that the nighttime HONO concentrations we have observed at several locations in the California South Coast Air Basin arise predominately from heterogeneous reactions of NO_2 with water, direct emissions from automobile exhaust, or a combination of both (as well as other possible heterogeneous processes involving surface phenomena).

- Nitrous acid was unequivocally identified and measured spectroscopically for the first time in an indoor environment by a modified DOAS system. Over an NO_2 concentration range from 5 to 11.5 ppm, an average HONO formation rate of 0.25 ppb min^{-1} per ppm of NO_2 was observed. Allowing for higher ventilation rates in a more typical home environment, for a more realistic concentration of NO_2 of 1 ppm, a steady state concentration of ~15 ppb of HONO can be estimated. Although this must be viewed as a rough estimate, a steady state concentration of ~15 ppb is about 2-4 times higher than the HONO levels we have previously measured in polluted ambient air at several sites in the South Coast Air Basin. Since HONO is a known gas phase mutagen, and an *in vitro* precursor to nitrosamines, our finding would appear to have potential health effects implications.

E. Recommendations for Future Research

- An attempt should be made to identify N_2O_5 in ambient air by FT-IR spectroscopy, concurrently with DOAS measurements of NO_3 and NO_2. Thus

our calculations show that for ~30% of nights for which data are available, N_2O_5 concentrations exceeded 1 ppb, with calculated levels as high as ~10-15 ppb being attained on two occasions. Since the detection limit for the measurement of N_2O_5 using long pathlength Fourier transform infrared absorption spectroscopy is ~5 ppb at 1 km pathlength, the unambiguous detection of N_2O_5 is possible.

- Since we have shown in an earlier SAPRC/ARB program that a large portion of the mutagenicity of extracts of ambient POM is contained in the polar fractions, and little is known about the identities of these polar mutagens, attempts should be made to identify the compound(s) responsible for the mutagenicity observed during exposure of adsorbed pyrene, benzo-(a)pyrene and perylene during periods of high ozone.

- The role of HNO_3 in nitroarene formation during POM collection on filters should be clarified. Since it is likely that HNO_3 present in ambient air is removed by TIGF filters and/or collected ambient POM, further experimental studies should be carried out to investigate the role of HNO_3 in the formation of nitroarenes during POM collection. One method of approach is via the use of deuterated PAH-doped ambient POM, which avoids the use of a prefilter to remove ambient POM.

- Much further experimental work is necessary to elucidate the mechanism of formation of 2-nitrofluoranthene and 2-nitropyrene from their respective parent PAH. Since 1-NO_2-PY is an animal carcinogen and 2-NO_2-PY and 2-NO_2-FL are at least as strong direct mutagens as 1-NO_2-PY, we believe that animal tests to assess the carcinogenicity of 2-NO_2-PY and 2-NO_2-FL are also desirable.

- An attempt should be made to estimate the degree of PAH volatilization from filters during POM collection through the use of, for example, polyurethane foam plugs beneath the filters to trap the volatilized PAH.

II. MUTAGENICITY OF AMBIENT PARTICULATES AT CENTRAL AND DOWNWIND RECEPTOR SITES IN THE CSCAB: SEPTEMBER 1983 FIELD STUDY

A. Introduction

With past research support, to a major extent from the CARB, we have shown that extracts of respirable ambient POM in the CSCAB are mutagenic (Pitts et al. 1977, 1982b,c, 1984e, Pitts 1980, 1981, 1983). In addition, this activity predominates in respirable sub-micron particles (Pitts et al. 1978c, Talcott and Harger 1980, Löfroth 1981). Extracts of POM from both diesel exhaust and gasoline engine exhaust are also directly mutagenic (Huisingh et al. 1978, Löfroth 1981, Lewtas 1982, Pierson et al. 1983). Moreover, the direct activity towards Salmonella typhimurium of motor vehicle POM emissions, both from gasoline and diesel engines, correlates with mammalian cell mutagenesis and skin tumor initiation assays (Lewtas 1983).

The potential health hazard of nitroarenes, which are major contributors to the direct mutagenic activity of organic extracts of POM, collected from light duty motor vehicles (LDMV) with either diesel or spark ignition engines, has been discussed recently by Rosenkranz (1984). He placed special emphasis on diesel soot because of its much higher emission rate relative to that of particles from gasoline-fueled engines.

Questions regarding the mutagenic activity of POM samples collected during smog episodes in the CSCAB, and how chemical transformations of this POM (due to interactions with gaseous copollutants) might affect this activity, led us to collect respirable POM simultaneously at a central and a downwind receptor site in the CSCAB.

B. Background

The formation of directly mutagenic nitro-derivatives from PAH such as benzo(a)pyrene (BaP), perylene (PER) and pyrene (PY), coated on glass fiber filters and exposed in simulated atmospheres to flows of air containing NO_2 and traces of nitric acid was first established in these laboratories (Pitts et al. 1978a, Pitts 1979). We also isolated and identified a strong direct mutagen [benzo(a)pyrene-4,5-oxide] from the reaction of ozone with adsorbed BaP in a similar "active" exposure system (Pitts et al. 1980).

In agreement with our product studies, Brorström et al. (1983) observed enhanced mutagenicity in ambient POM samples collected after the addition of 1 ppm NO_2 (however, without precautions to remove traces of nitric acid) to the ambient air being sampled. However, Fitz et al. (1984) observed no changes in mutagenic activity for ambient POM re-exposed to pollutant gases for approximately eight hours (although it should be noted that these workers used a pre-filter which may have removed HNO_3, as well as ambient POM).

Furthermore, in accordance with our earlier predictions (Pitts et al. 1978a), the filter media, e.g., GF or TIGF filters, can affect the degradation of PAH collected on the filter and the associated mutagenic activities (the so-called "filter artifact") [Lee et al. 1980]. For example, Daisey and co-workers (1983) found differences between mutagenic activities of samples collected on TIGF and GF filters with higher mutagenicity (TA98, -S9) in the polar extracts of the GF filters. In contrast, Alfheim and Lindskog (1984) observed higher activity (TA98, +S9) in samples from TIGF filters compared to those from GF filters. In the earlier study by Fitz et al. (1984) concerning the mutagenicity of POM simultaneously collected on TIGF, GF and other filter media over eight-hour intervals, no significant differences in the mutagenic activity among the POM samples collected on different media were reported.

Clearly, the results described above contain significant contradictions, especially when comparing results predicted from laboratory studies with those obtained from ambient exposures. Thus, to add to the data base concerning sampling artifacts which may affect the mutagenic activity of ambient POM we utilized a novel sampling protocol and two filter types (TIGF and GF) in the field study described in the following sections. Additionally, various gaseous nitrogenous and oxidant pollutants were quantitatively determined.

C. Experimental

This study took place from 1500 PDT on September 12, 1983 to 1500 PDT on September 17, 1983. The ARB Haagen-Smit Laboratory in El Monte (located ~12 miles from the downtown area of Los Angeles) served as the mid-basin monitoring site, and the UC campus at Riverside (40 miles east of Los Angeles) served as the downwind smog receptor site. First stage

ozone alert levels were reached in Riverside each day during the collection period. The maximum ozone concentration during the sampling period was 290 ppb at Riverside on September 14.

1. Gas Phase Analyses During Collection Period

The array of instruments used for measuring gaseous pollutant concentrations is given in Table II-1. With the exception of the PAN gas chromatographic data, the output of each instrument was fed into a data acquisition system based on an Apple II micro-computer. Data were averaged over 10-min intervals and stored on a floppy disk. A hard copy of the data was also printed simultaneously. A multipoint recorder was utilized as a backup to the computer system. The data stored on disk were later processed using the main computing facilities at SAPRC.

2. Collection of Particulate Matter

The daily schedule which was employed for collection of particulate matter is shown in Table II-2. It was based on the findings

Table II-1. Instrumentation for Measurement of Gaseous Pollutants During September 1983 Field Study

Parameter	Site	Instrument	Principle of Operation
O_3	El Monte	Dasibi Model 1003AH Ozone Analyzer	UV Absorption
	Riverside	Monitor Labs Model 8410 Ozone Analyzer	Chemiluminescence
NO, NO_x	El Monte	Columbia S.I. Model 1600	O_3 Chemiluminescence
	Riverside	Columbia S.I. Model 1600	O_3 Chemiluminescence
CO	El Monte	Dasibi Model 3003	IR Gas Filter Correlation
	Riverside	Dasibi Model 3003	IR Gas Filter Correlation
PAN	El Monte	Varian Model 600	GC/ECD
	Riverside	Varian Model 600	GC/ECD

Table II-2. Sampling Schedule in September 1983 Field Study

Time Interval, PDT	Reason for Interval
0600-1000	Maximum emission of primary pollutants in El Monte and Riverside and period of peak mutagenicities of POM
1000-1500	Local photochemical formation of O_3 and other secondary pollutants in El Monte and Riverside
1500-2100	Influx of "aged" air mass containing O_3 and other secondary pollutants into Riverside
2100-0600	Night sample of primary pollutants in El Monte and Riverside

of our CARB-funded September 1980 time-resolved studies of the diurnal variations in particulate mutagenicities and gaseous co-pollutant concentrations. Conclusions drawn from these studies regarding sampling procedures were also used in deciding upon the schedule shown in Table II-2.

Particulate matter for chemical analyses was collected at El Monte with the SAPRC-designed and constructed ultra-high volume "mega-sampler" (Fitz et al. 1983). This device has an inlet with a 50% cut-point of 20 μm, limiting the particulate collection to the respirable range. The total flow was 640 scfm through four 16-in x 20-in filters. The same face velocity as a standard Hi-vol sampler was maintained while the capacity was 16 times larger than that of a standard Hi-vol sampler (640 cfm versus 40 cfm).

At Riverside particulate matter for chemical analyses was collected using 12 standard Hi-vol samplers. At both sites, TIGF filters (Pallflex TX40HI20) were used. These were pre-washed with dichloromethane and methanol before use.

Three additional Hi-vol samplers with 10 μm size selective inlets were operated at each sample site. Two of these samplers at each site used TIGF filters. For September 12 through September 14 (11 sampling intervals), the third Hi-vol at each site was used to sample particulate

on Whatman EPM 2000 glass microfiber (GF) filters. These were used as received, without pre-washing. These EPM 2000 GF filters were chosen for comparison with the TIGF filters since they are the EPA standard filter for total solid particulate collection.

All filters were equilibrated at 50% relative humidity and 70°F and weighed before and after use. Following sampling, they were immediately sealed in aluminum foil, sealed in plastic bags and stored at -10 C prior to weighing and extraction. The filters were sequentially Soxhlet extracted with dichloromethane followed by acetonitrile. The combined extracts were assayed with Ames Salmonella strains TA98, TA98NR and TA98/1,8-DNP_6. The two TIGF filters at each site were combined for analysis.

Two Lo-vol samplers were also operated at each site. One was equipped with a Nuclepore polycarbonate filter for determination of lead, bromine and several other elements, the other with a pre-fired quartz (Pallflex 2500 QAO) filter for total and elemental carbon analyses. The carbon analyses were contracted to Dr. J. Huntzicker at the Oregon Graduate Research Center and were analyzed by a thermal-optical method (Huntzicker et al. 1982). The X-ray fluorescence analyses of lead, bromine and other elements were carried out by Mr. R. Giauque at the Lawrence Berkeley Laboratories.

3. Mutagenicity Bioassay Procedures

The Ames assay (Ames et al. 1975) was carried out in our microbiological facility using our modified procedure developed with earlier CARB and DOE support (Belser et al. 1981, Pitts 1981). Ames Salmonella typhimurium strain TA98 and its nitroreductase-deficient counterparts, TA98NR and TA98/1,8-DNP_6, were used in these assays.

Strain TA98 was used because it has been found to be the most sensitive strain to airborne frameshift mutagens. Strain TA98NR is an isolate of TA98 deficient in the "classical" bacterial nitroreductase, which catalyzes the bioactivation of most mononitroarenes to their ultimate mutagenic species. Thus, a lower response on this strain relative to that on TA98 indicates the probable presence of mononitroarenes in the sample. Strain TA98/1,8-DNP_6, which possesses a functional nitroreductase, is deficient in a second enzyme which activates the potent mutagens 1,8-dinitropyrene and 1,3-dinitropyrene, and consequently is less sensitive to

the mutagen action of these compounds. Thus a lower response on TA98/1,8-DNP_6, relative to those of TA98NR and TA98, may indicate the presence of dinitropyrenes in the sample (Rosenkranz et al. 1981, 1982, Rosenkranz and Mermelstein 1983).

Cultures were grown for 16 hr in L-broth and diluted with sterile medium until the optical density at 550 nm reached a previously determined value corresponding to a concentration of 10^9 cells $m\ell^{-1}$. In each test, the strains were checked for the following genetic markers: (1) ampicillin sensitivity, (2) ultraviolet sensitivity, (3) crystal violet sensitivity, (4) standard spontaneous reversion and (5) mutagenic response to the standard mutagens 2-nitrofluorene, quercetin and for strain TA98/1,8-DNP_6, 1,8-dinitropyrene.

After dilution, the cultures were kept at ice temperature to ensure that the culture density remained the same. Exact titers were determined by dilution and plating on histidine-supplemented minimal medium. After a 63-hr incubation period, the colonies on the plates were counted with a New Brunswick Scientific Biotran II automatic colony counter directly interfaced via a New Brunswick Scientific Omni-Interface to an Apple II microcomputer for data logging and reduction.

Each sample was tested for at least six different concentrations in a range which bracketed the linear region of the dose-response curve; three replicates were run at each concentration and the averages of the three responses were used to determine the dose-response curve. The mutagenic potency (specific activity in revertants μg^{-1} of sample) was defined as the slope of the line determined by a least-squares regression in the region of linear response.

4. Data Manipulation

The 10-min. average gaseous pollutant concentrations stored on floppy disks during the study period were used to generate average concentration values for the intervals listed in Table II-2. These averaged values, together with the particulate species measured, could then be used as a data set.

5. Air Mass Trajectories

In order to determine the origins of the air masses sampled in Riverside and El Monte and to determine if the air masses in El Monte later reached Riverside, twenty-four hour air mass trajectories were

generated backward from Riverside and El Monte, and forward from El Monte. Four starting times were used each day of the study, approximately in the middle of the particulate collection intervals. The trajectories were calculated using wind direction and velocity data from monitoring stations throughout the SCAB. Each trajectory was calculated by moving backwards in hourly intervals from the chronological termination point (Riverside and El Monte) or forwards in hourly intervals from the starting point (El Monte).

At each point on the trajectory (x_y, y_t, t), the wind speed and direction data for the previous hour at the three closest monitoring stations were used to calculate a vector with the closer stations receiving a proportionately higher mathematical weighting. The new coordinates for t_{t-1}, y_{t-1} were then calculated from this vector. This process was repeated for the next previous, or following, hour using another set of coordinates. Vectors were plotted for twenty-four hours or until no station was deemed close or a mountain range or ocean was reached.

D. Results and Discussion

Figures II-1 through Figures II-6 show the daily ozone profiles (with data points every 10 minutes) at El Monte and Riverside for each day of the study. In general, as would be expected, the ozone maxima occurred later in the day at Riverside than at El Monte.

Figures II-7 through II-12 show the CO, NO and NO_2 profiles observed at El Monte. These pollutants are largely attributed to vehicle traffic in the CSCAB and evidence of morning "traffic peaks" is clear from the data of September 13, 14 and 15. The lack of a significant morning commuter traffic peak in the data of September 16, as well as the lack of evening commuter peaks each day, shows the influence of meteorology. (September 17 was a Saturday and hence a commuting traffic peak was not expected.) As seen from Figures II-13 through II-18, in which the CO, NO and NO_2 data are plotted for Riverside, the morning commuter traffic had somewhat less influence on the air quality data in Riverside.

Table II-3 gives the particulate and extract weights and the mutagenicity values determined for POM collected on TIGF filters (TX40H120WW) at El Monte. Table II-4 gives the corresponding data for Riverside. The mutagenic activity is expressed as the number of revertants per microgram

(Text continues on pg. II-28)

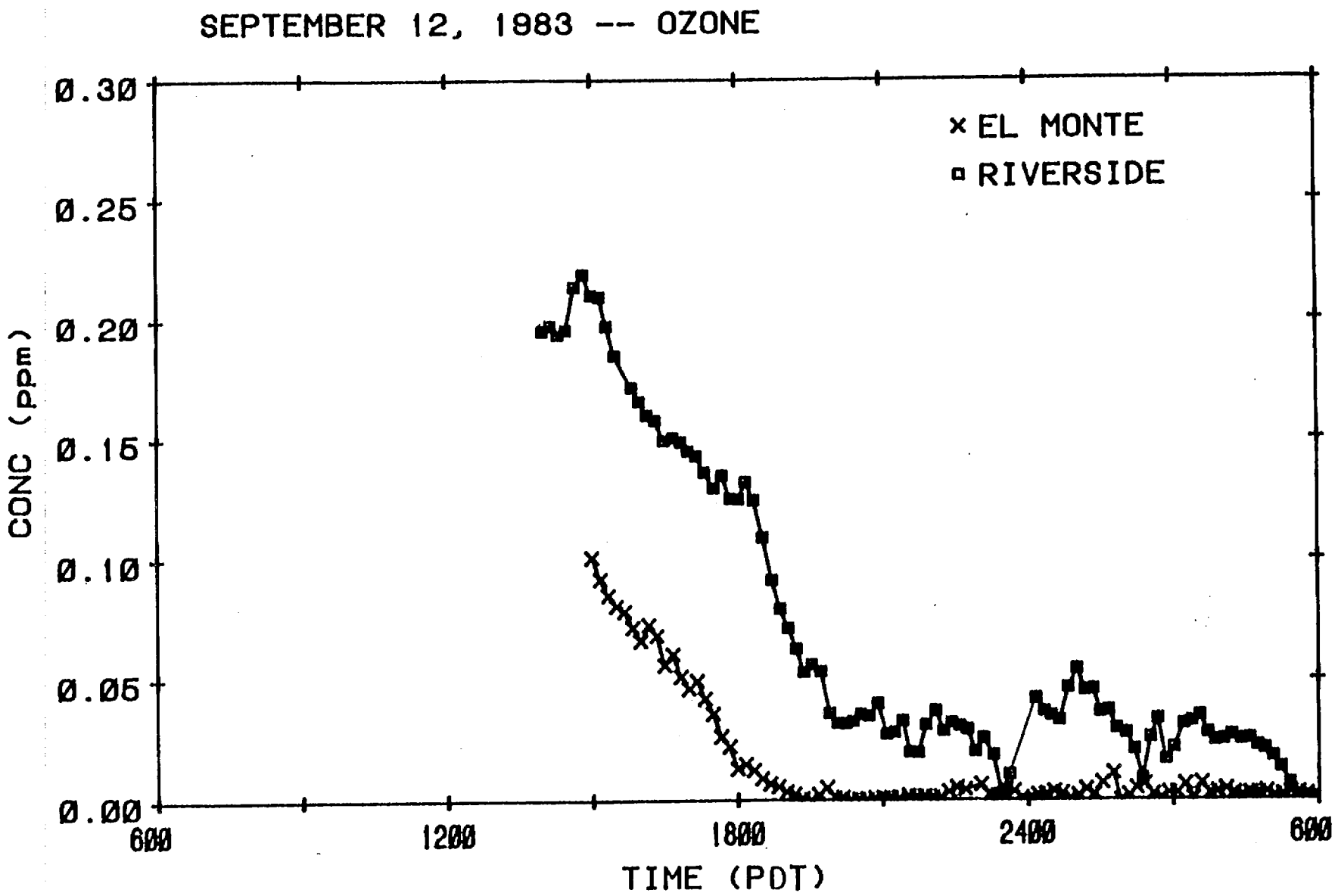

Figure II-1. Ozone concentrations for El Monte (X) and Riverside (□) for September 12, 1983.

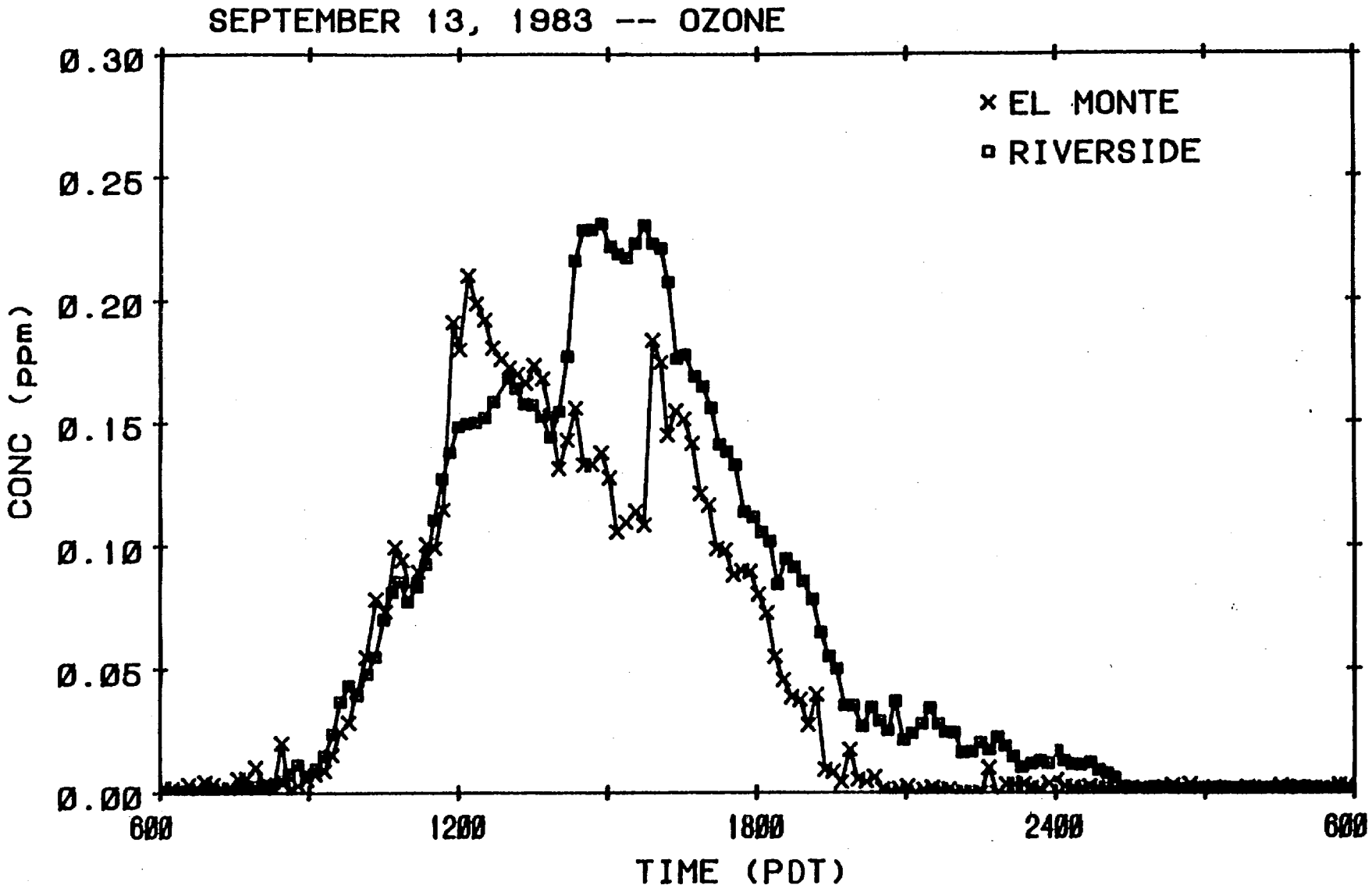

Figure II-2. Ozone concentrations for El Monte (X) and Riverside (□) for September 13, 1983.

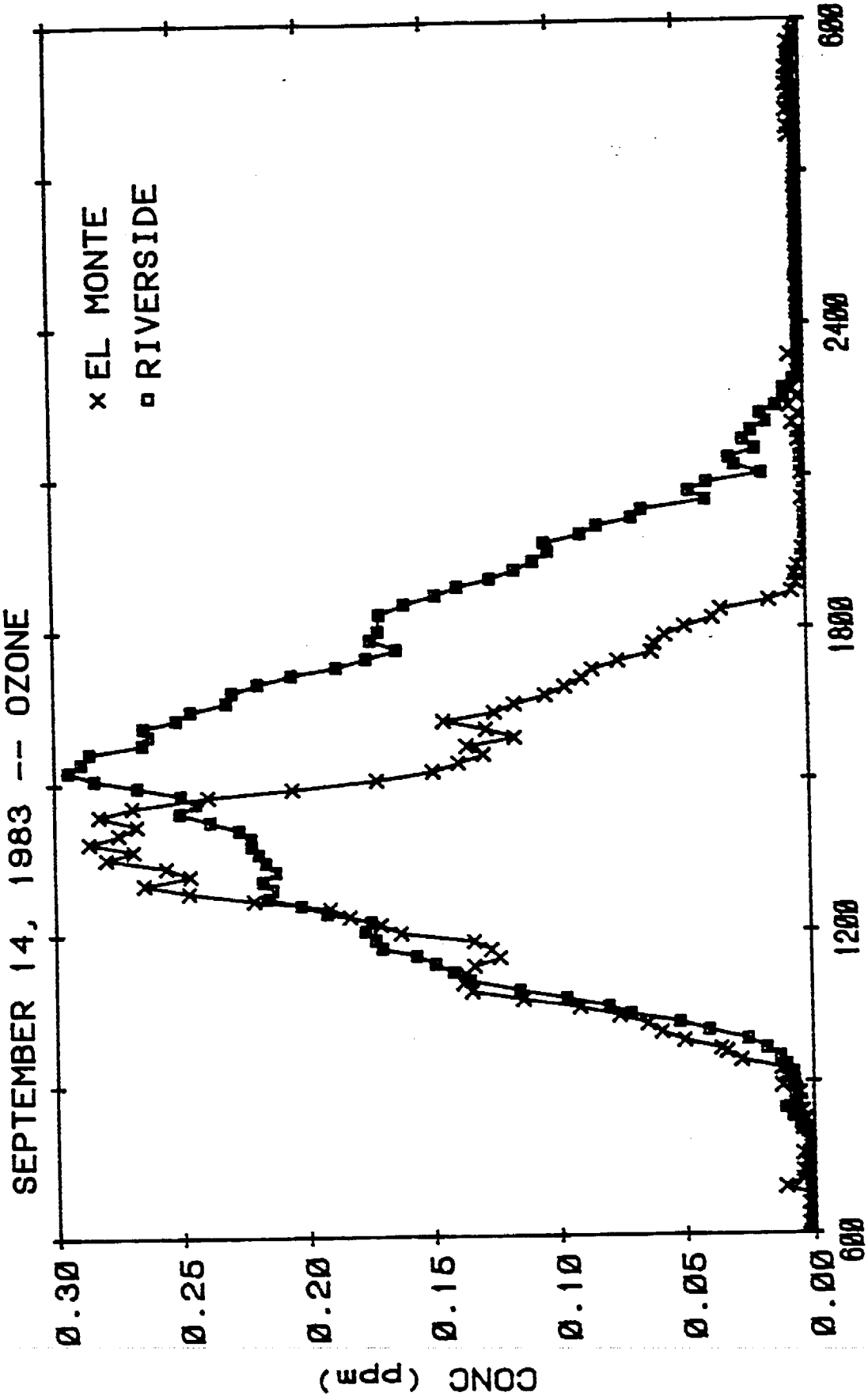

Figure II-3. Ozone concentrations for El Monte (X) and Riverside (□) for September 14, 1983.

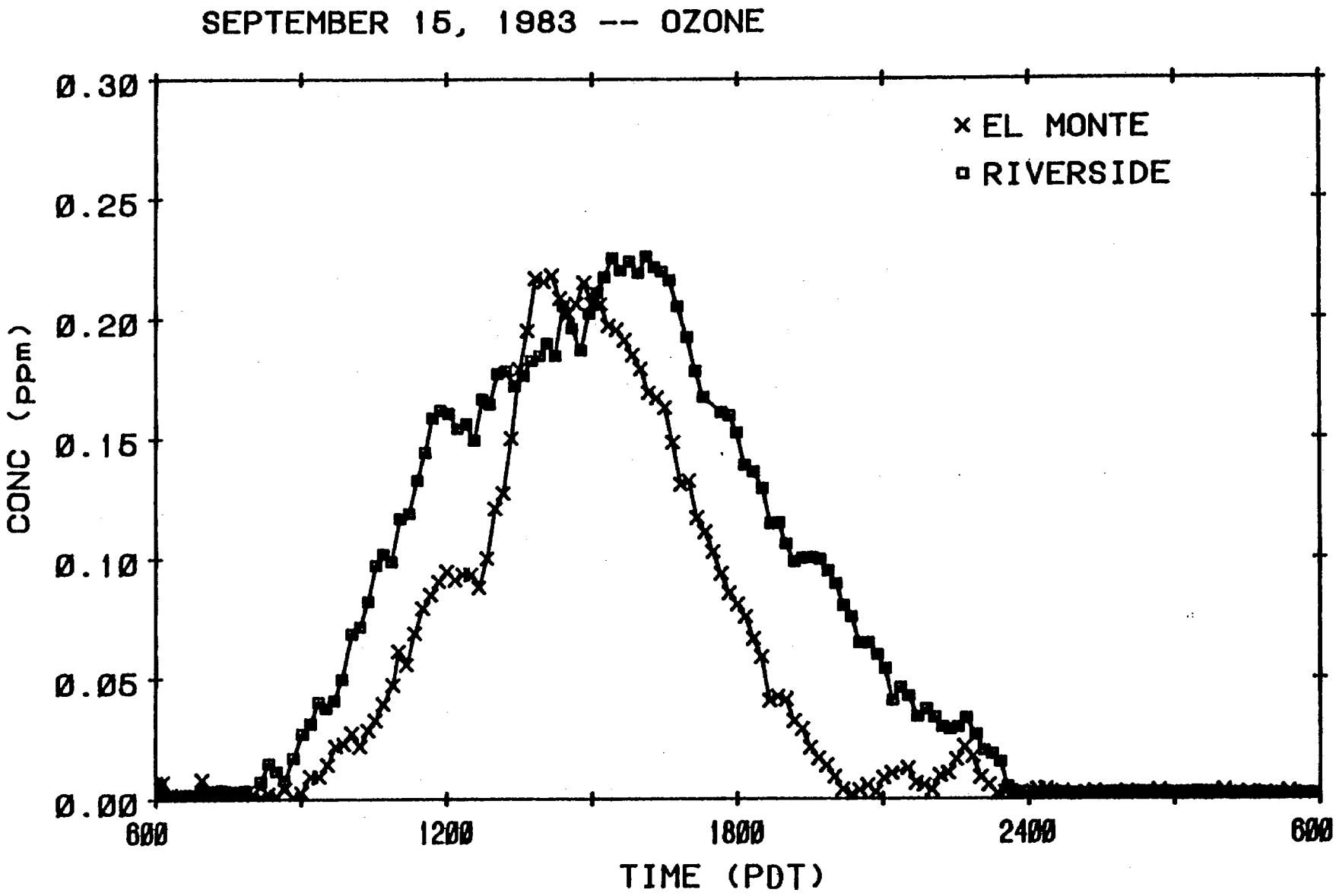

Figure II-4. Ozone concentrations for El Monte (X) and Riverside (□) for September 15, 1983.

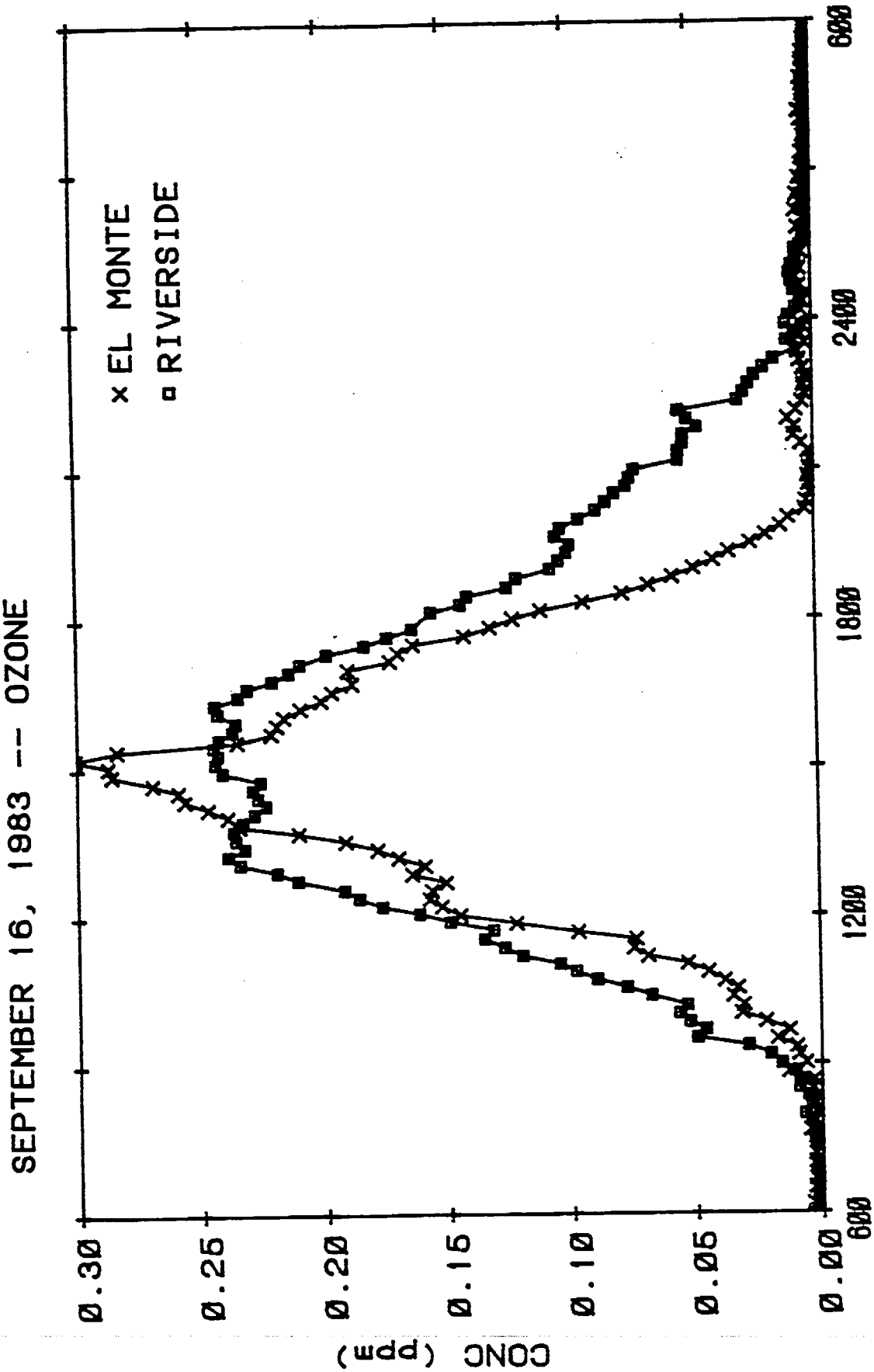

Figure II-5. Ozone concentrations for El Monte (X) and Riverside (□) for September 16, 1983.

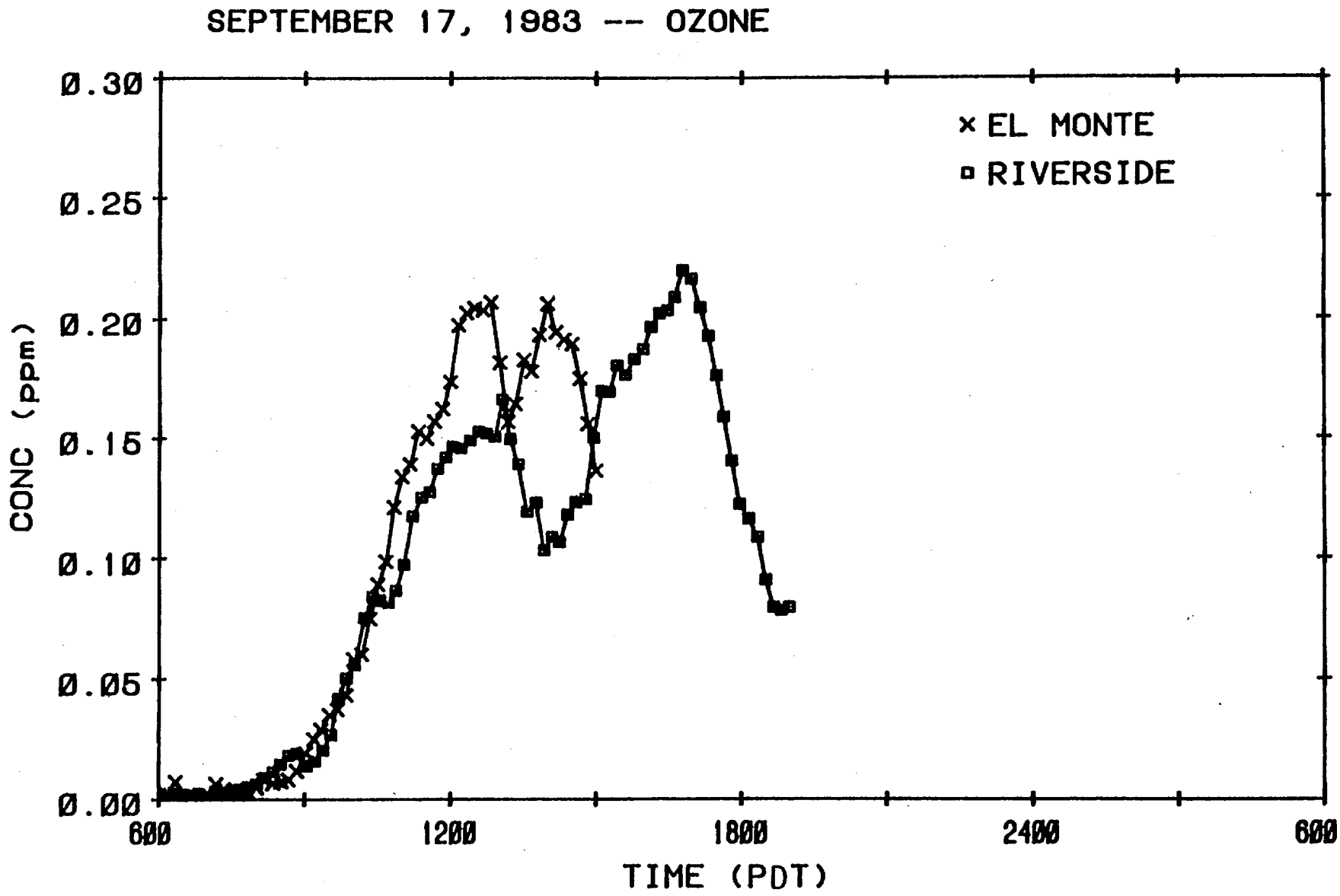

Figure II-6. Ozone concentrations for El Monte (X) and Riverside (□) for September 17, 1983.

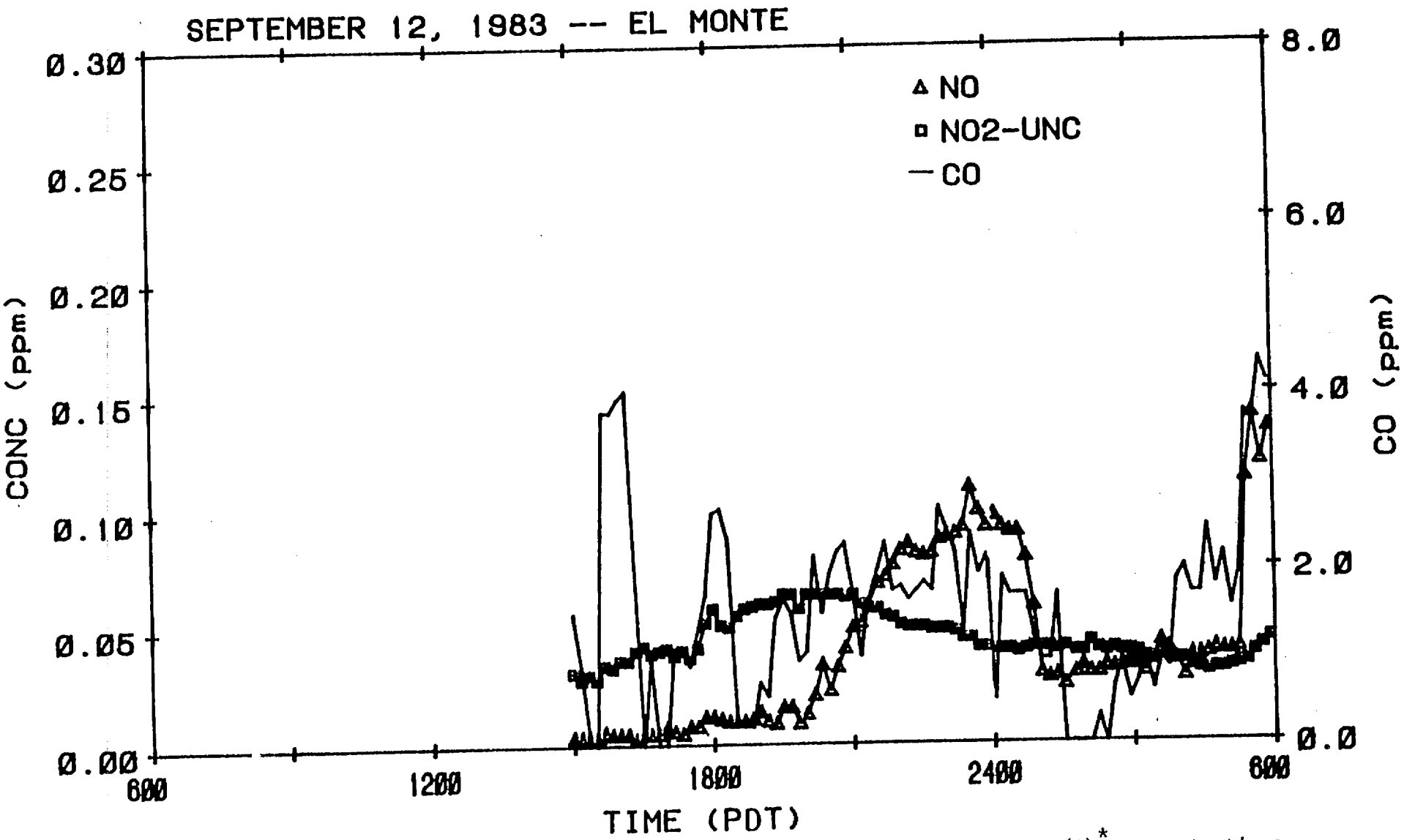

Figure II-7. Carbon monoxide (solid line), nitric oxide (Δ) and nitrogen dioxide (□)* concentrations at El Monte for September 12, 1983.
*NO_2 is uncorrected for PAN positive interference.

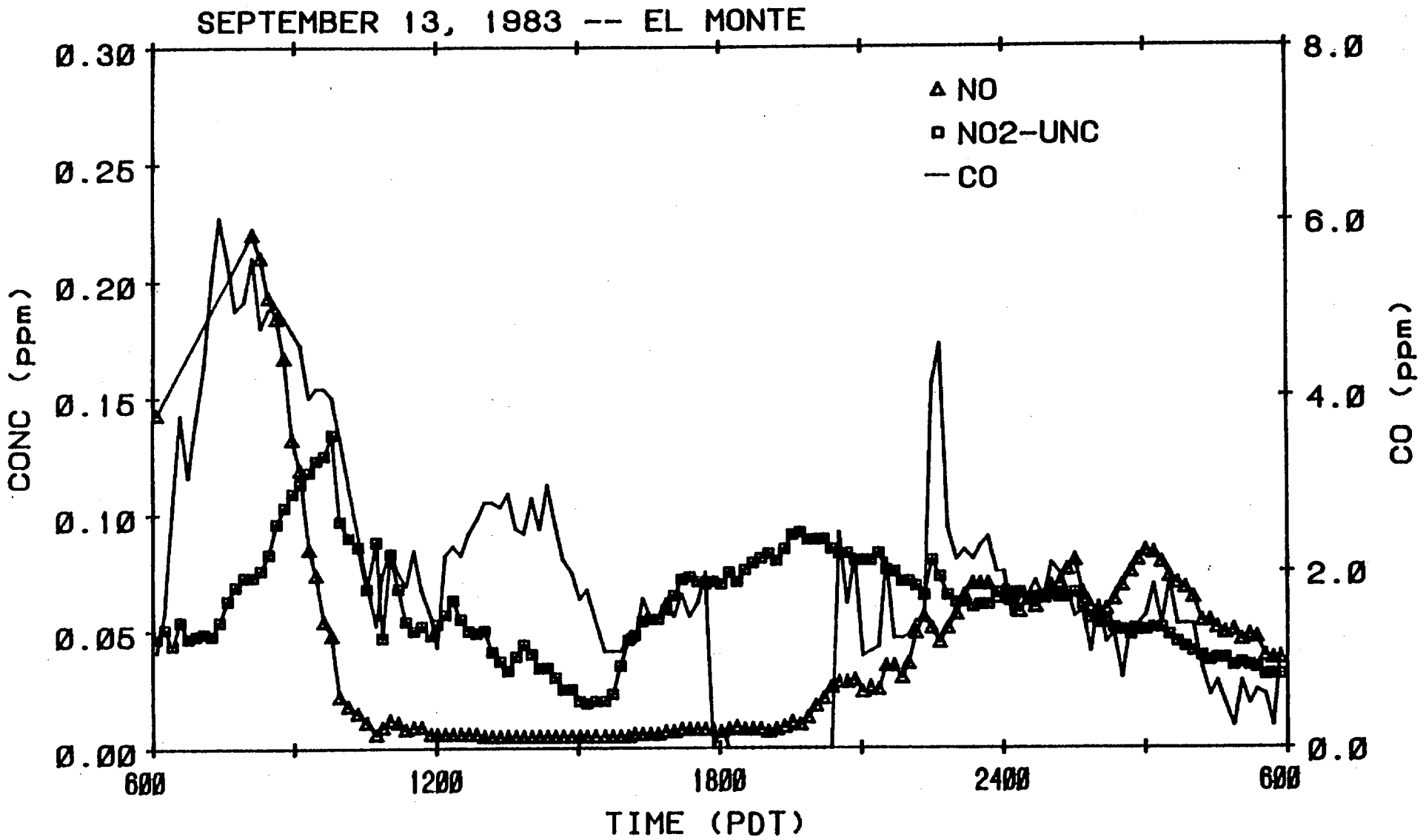

Figure II-8. Carbon monoxide (solid line), nitric oxide (Δ) and nitrogen dioxide (□)* concentrations at El Monte for September 13, 1983.
*NO_2 is uncorrected for PAN positive interference.

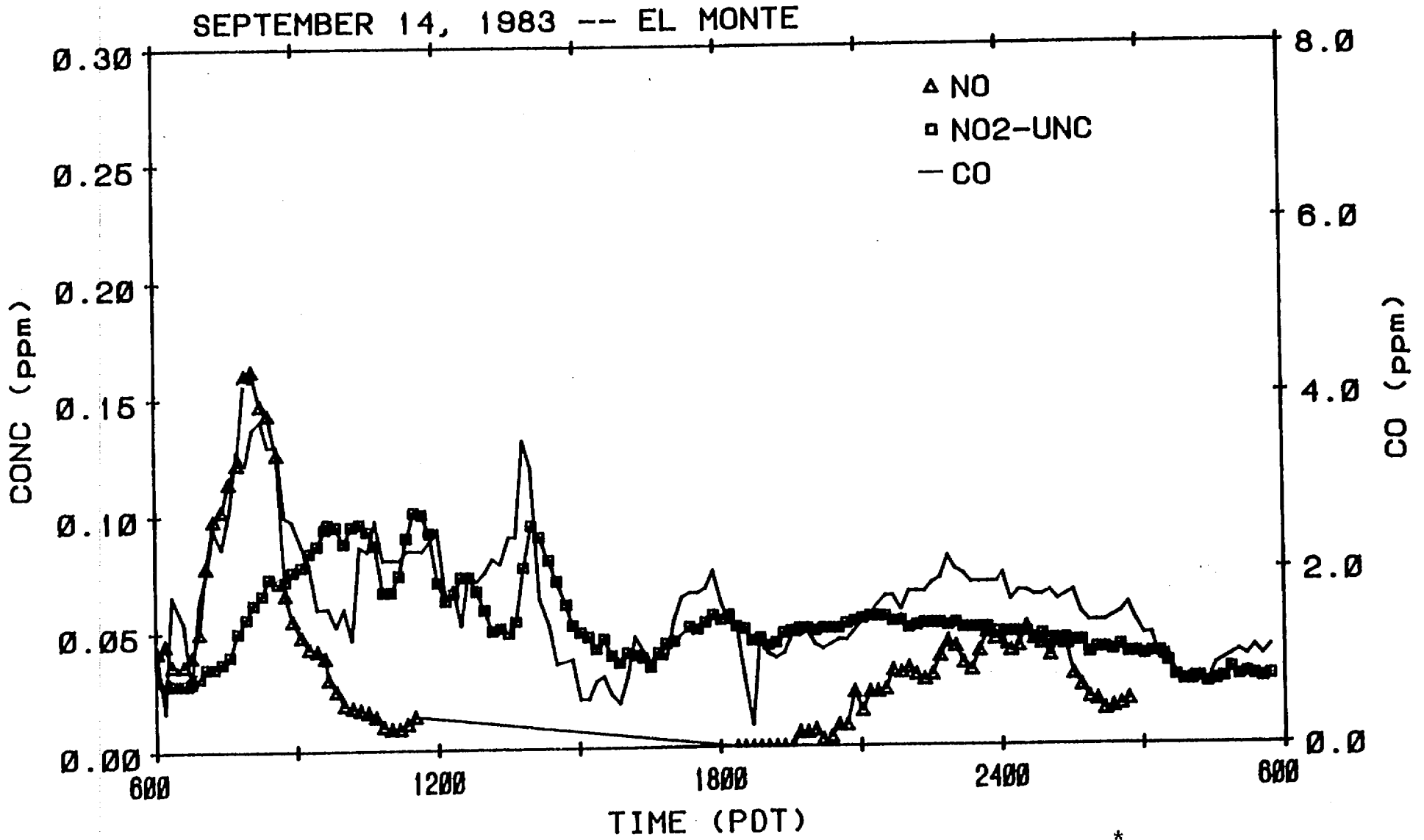

Figure II-9. Carbon monoxide (solid line), nitric oxide (Δ) and nitrogen dioxide (□)* concentrations at El Monte for September 14, 1983.
*NO_2 is uncorrected for PAN positive interference.

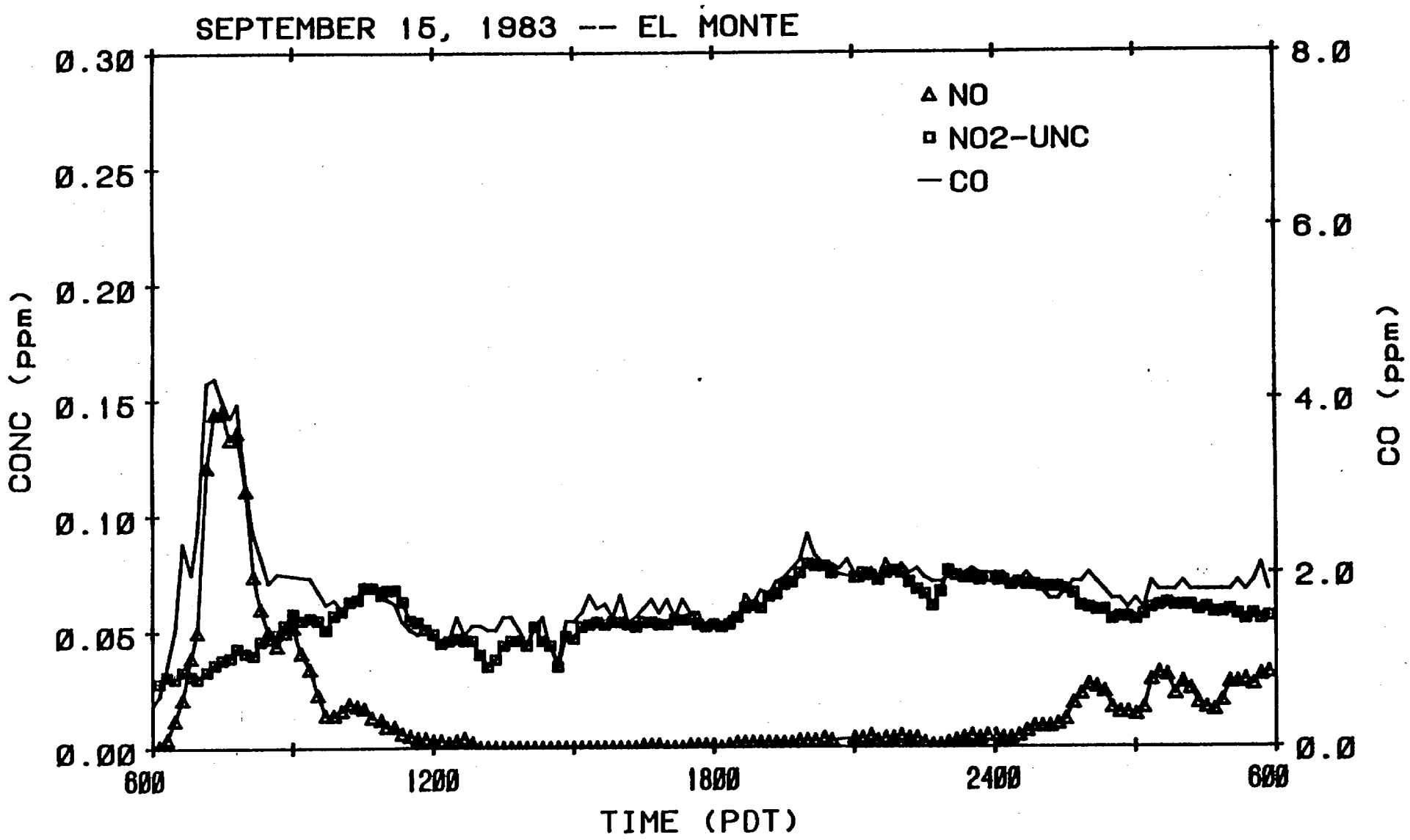

Figure II-10. Carbon monoxide (solid line), nitric oxide (Δ) and nitrogen dioxide (□)* concentrations at El Monte for September 15, 1983.
*NO_2 is uncorrected for PAN positive interference.

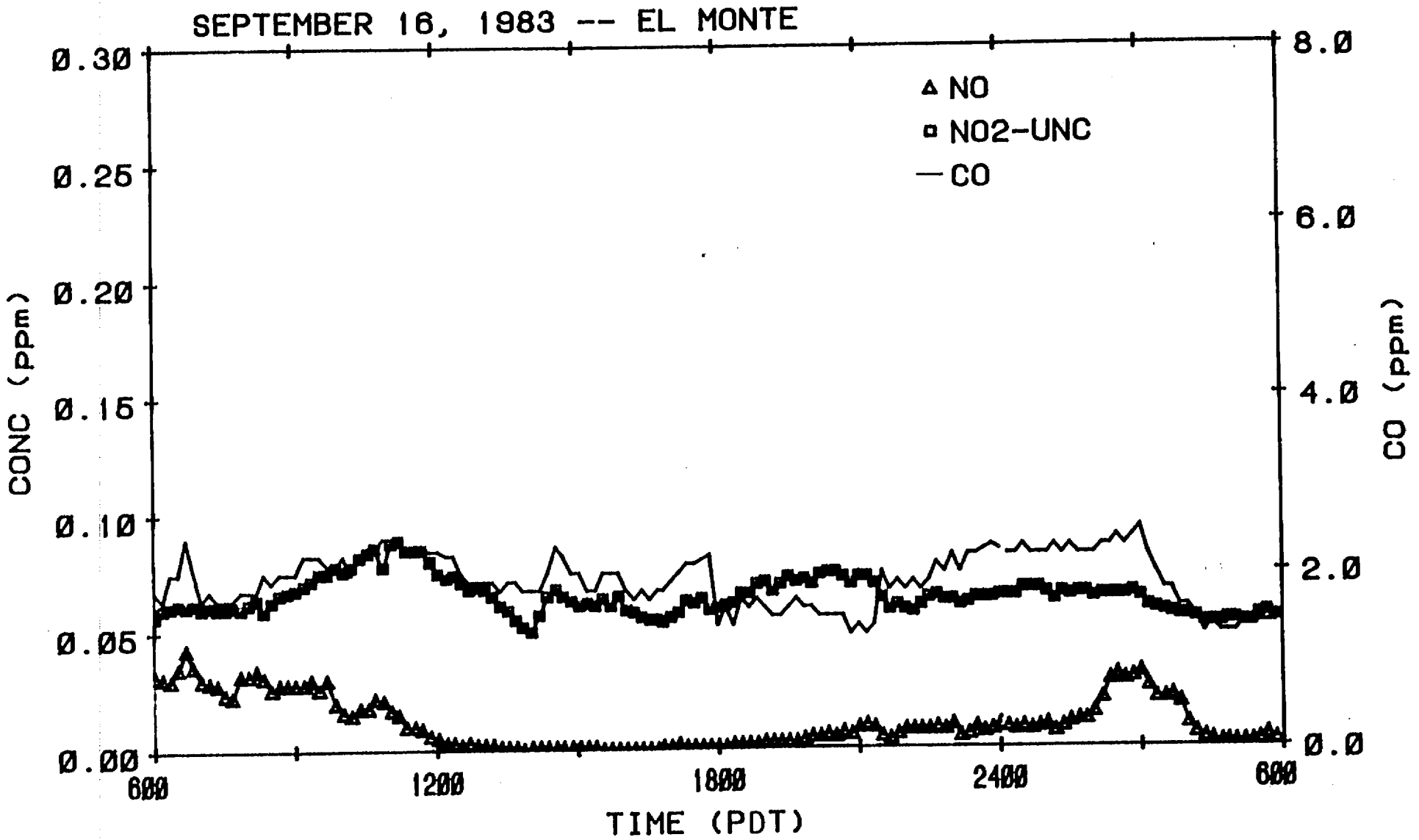

Figure II-11. Carbon monoxide (solid line), nitric oxide (Δ) and nitrogen dioxide (□)* concentrations at El Monte for September 16, 1983.

*NO_2 is uncorrected for PAN positive interference

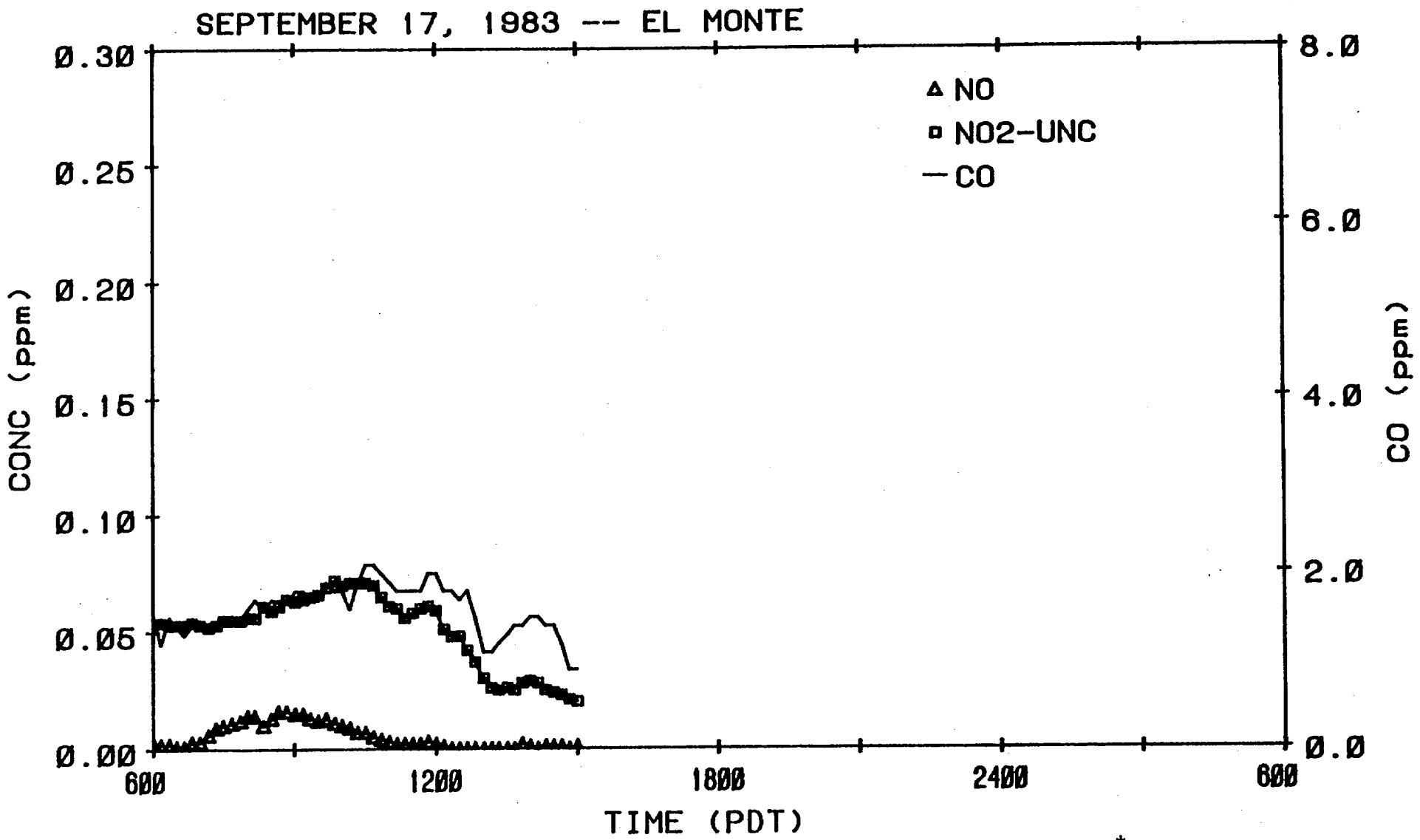

Figure II-12. Carbon monoxide (solid line), nitric oxide (Δ) and nitrogen dioxide (□)* concentrations at El Monte for September 17, 1983.
*NO_2 is uncorrected for PAN positive interference.

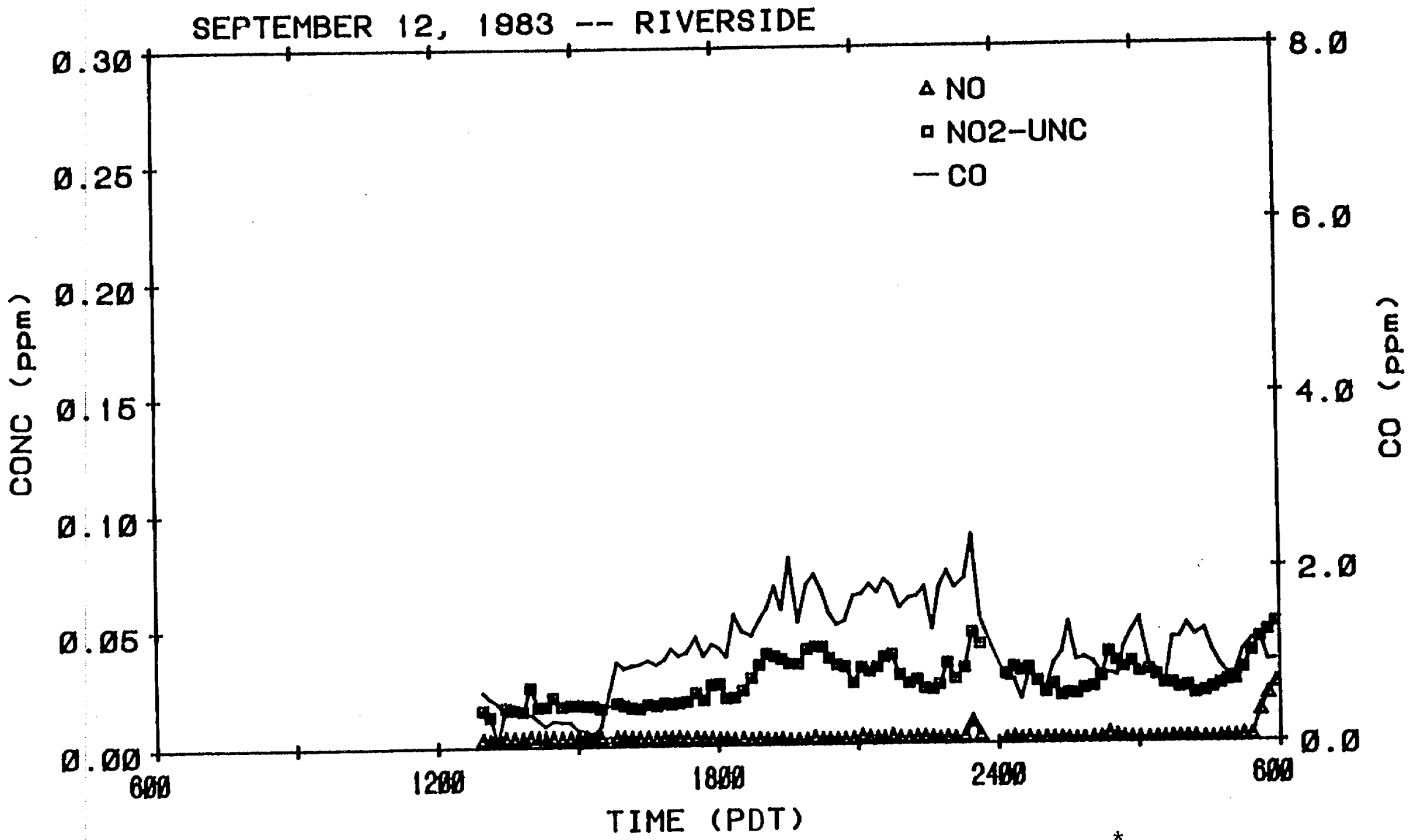

Figure II-13. Carbon monoxide (solid line), nitric oxide (Δ) and nitrogen dioxide (□)* concentrations at Riverside for September 12, 1983.
*NO_2 is uncorrected for PAN positive interference.

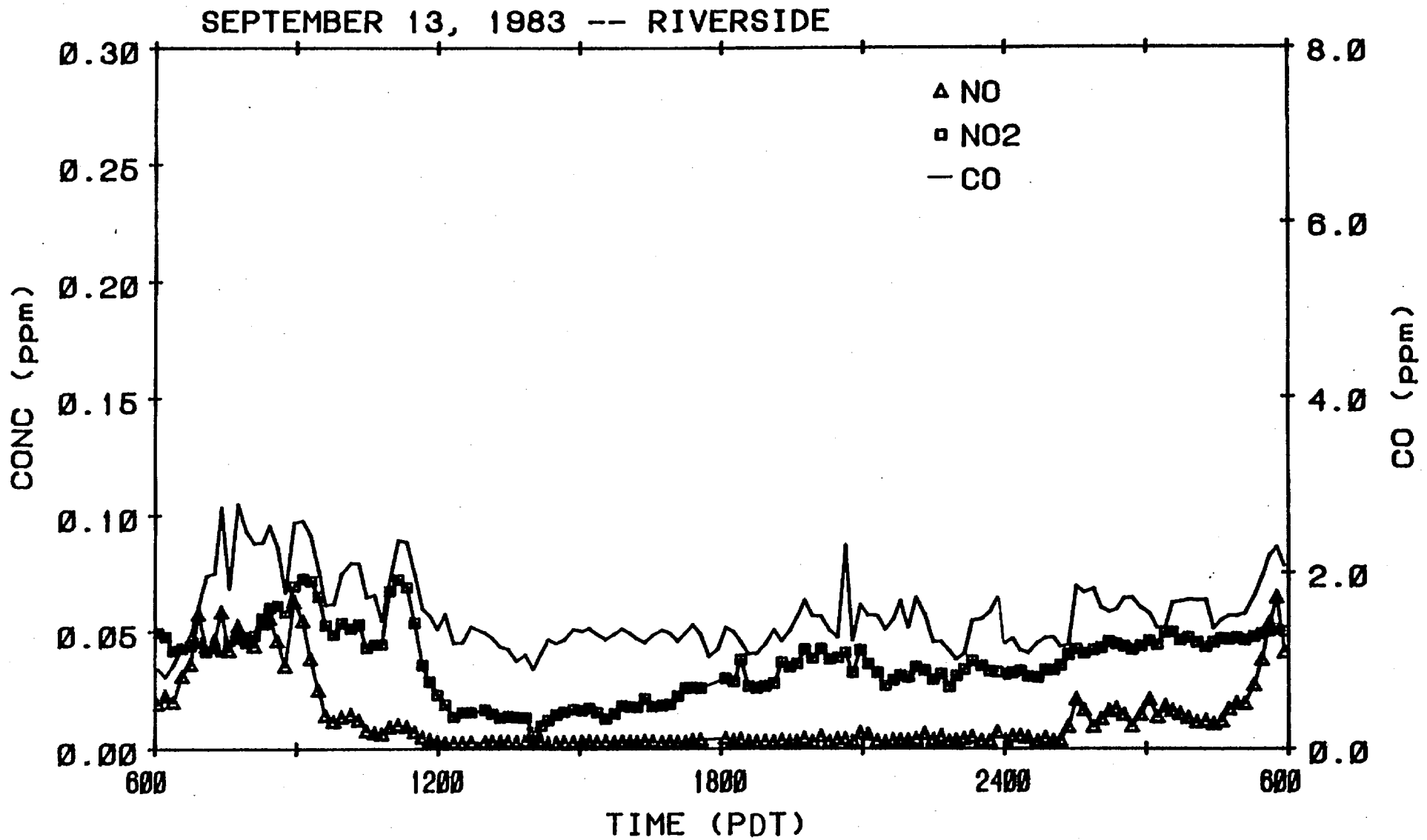

Figure II-14. Carbon monoxide (solid line), nitric oxide (Δ) and nitrogen dioxide (□) concentrations at Riverside for September 13, 1983.

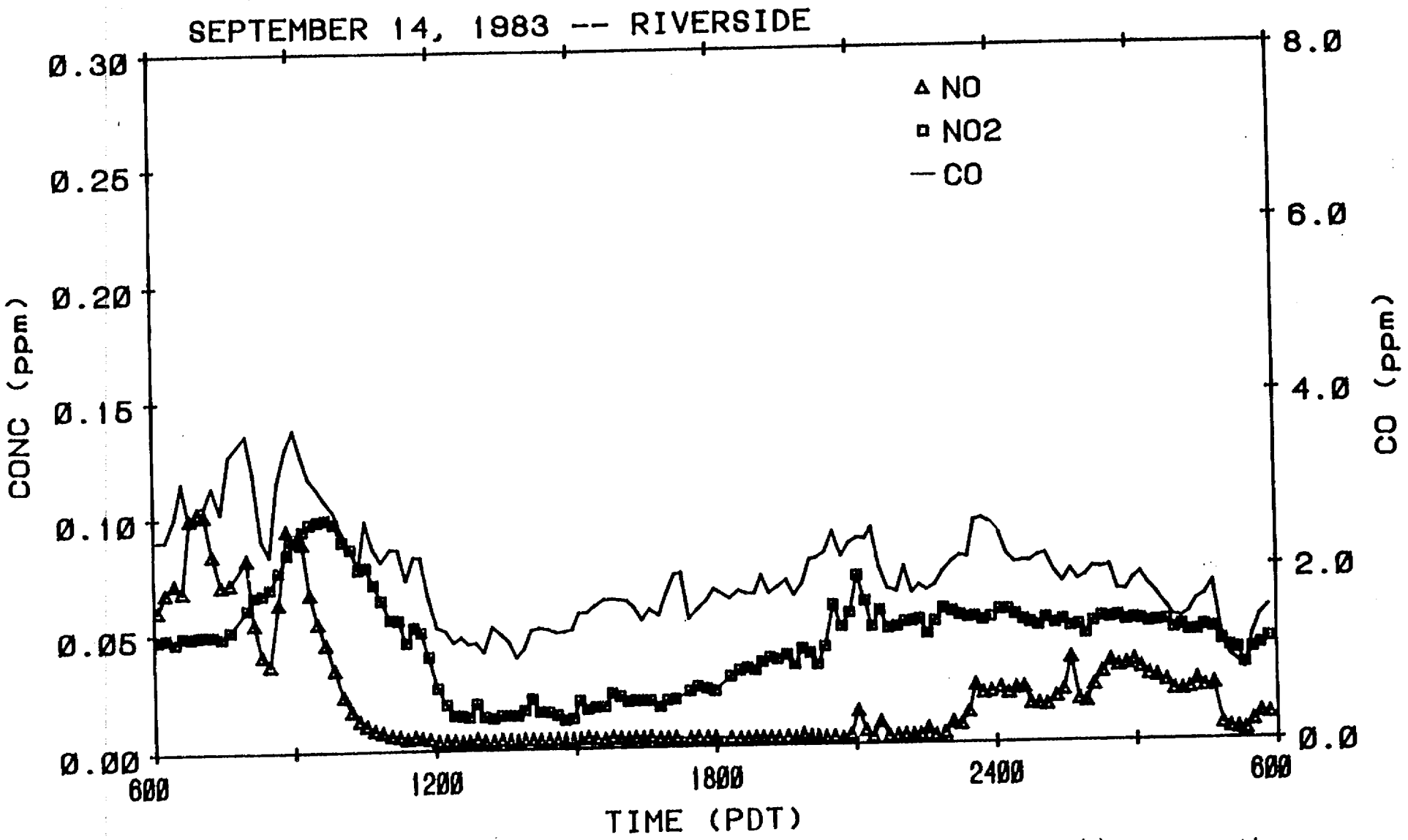

Figure II-15. Carbon monoxide (solid line), nitric oxide (Δ) and nitrogen dioxide (□) concentrations at Riverside for September 14, 1983.

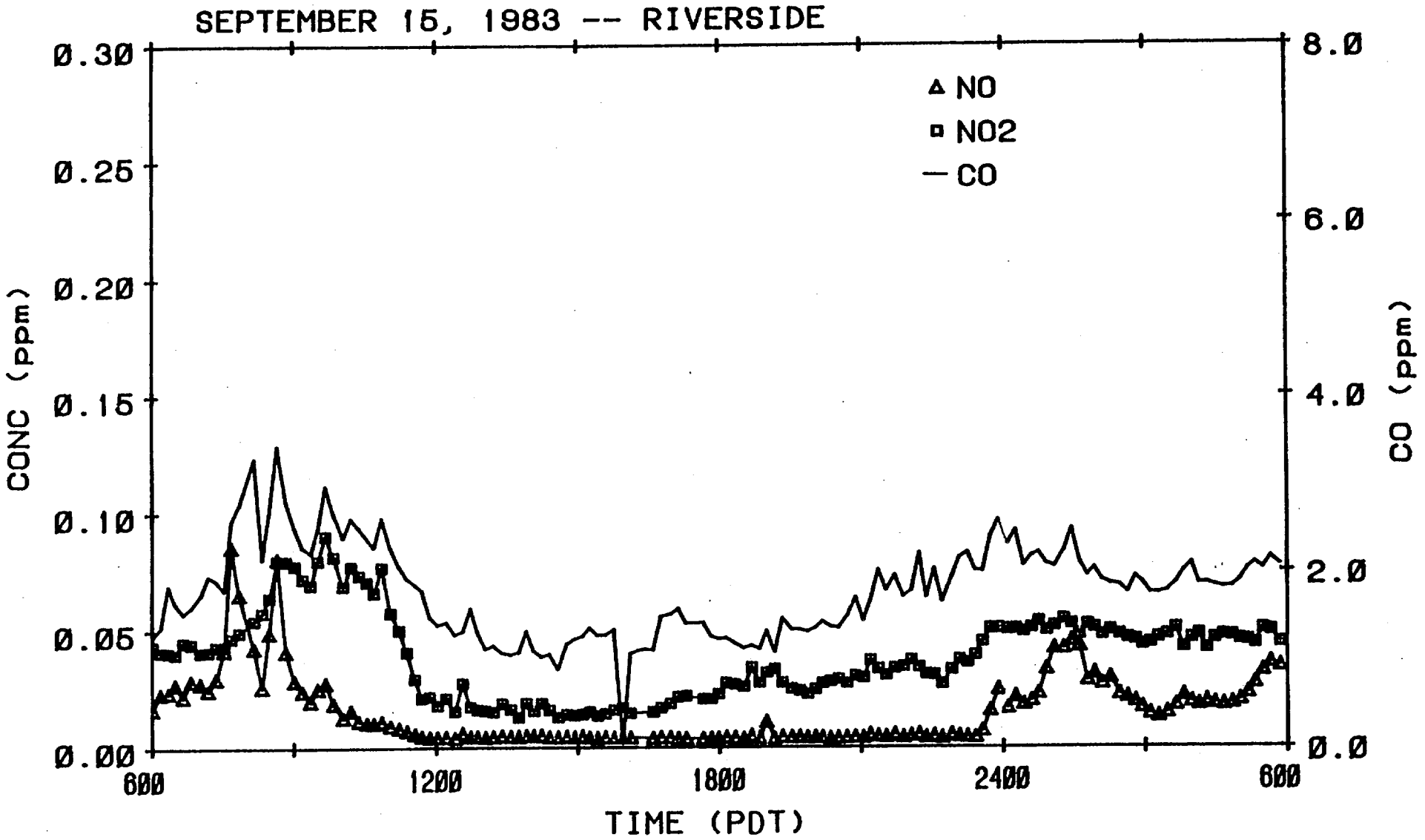

Figure II-16. Carbon monoxide (solid line), nitric oxide (Δ) and nitrogen dioxide (□) concentrations at Riverside for September 15, 1983.

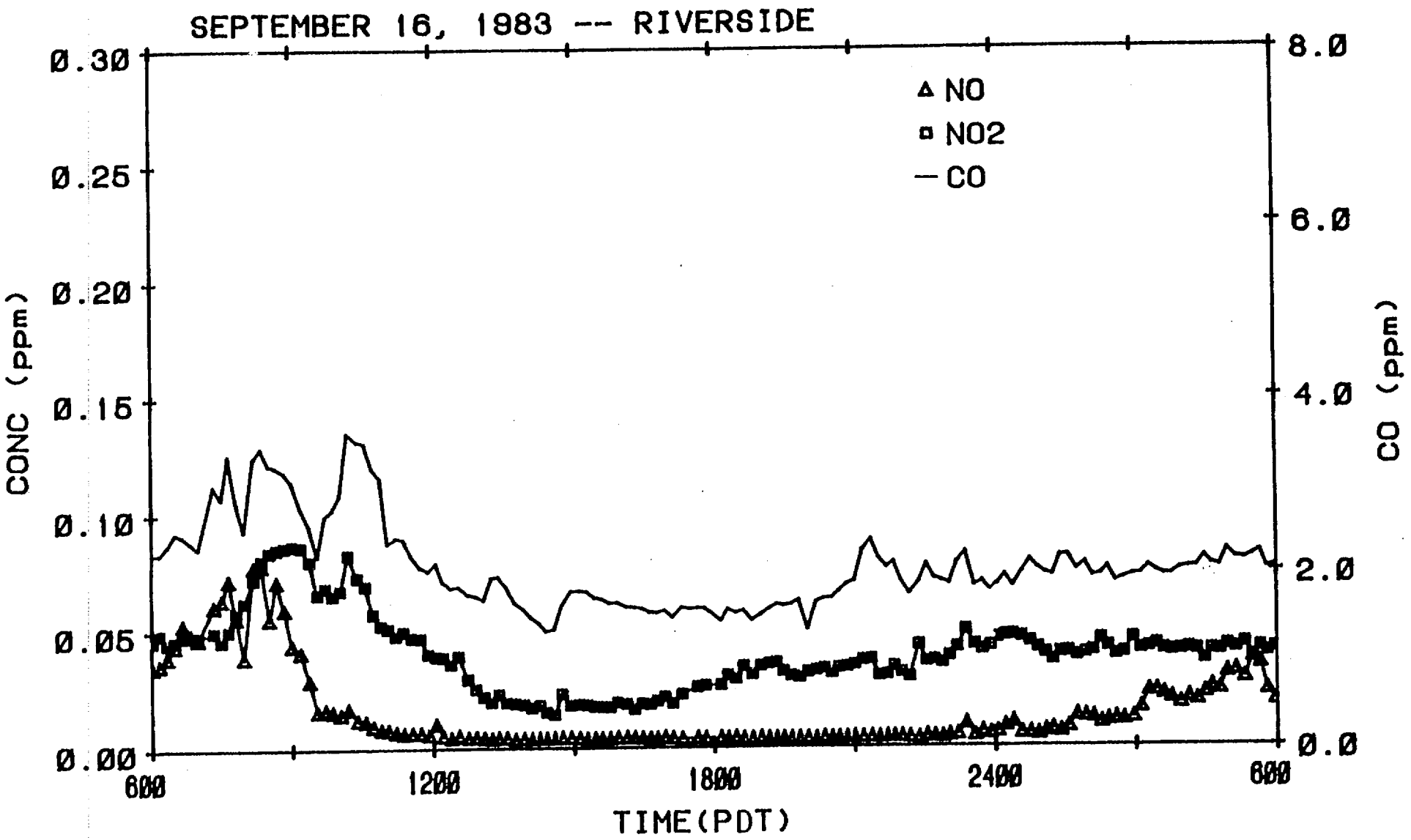

Figure II-17. Carbon monoxide (solid line), nitric oxide (Δ) and nitrogen dioxide (□) concentrations at Riverside for September 16, 1983.

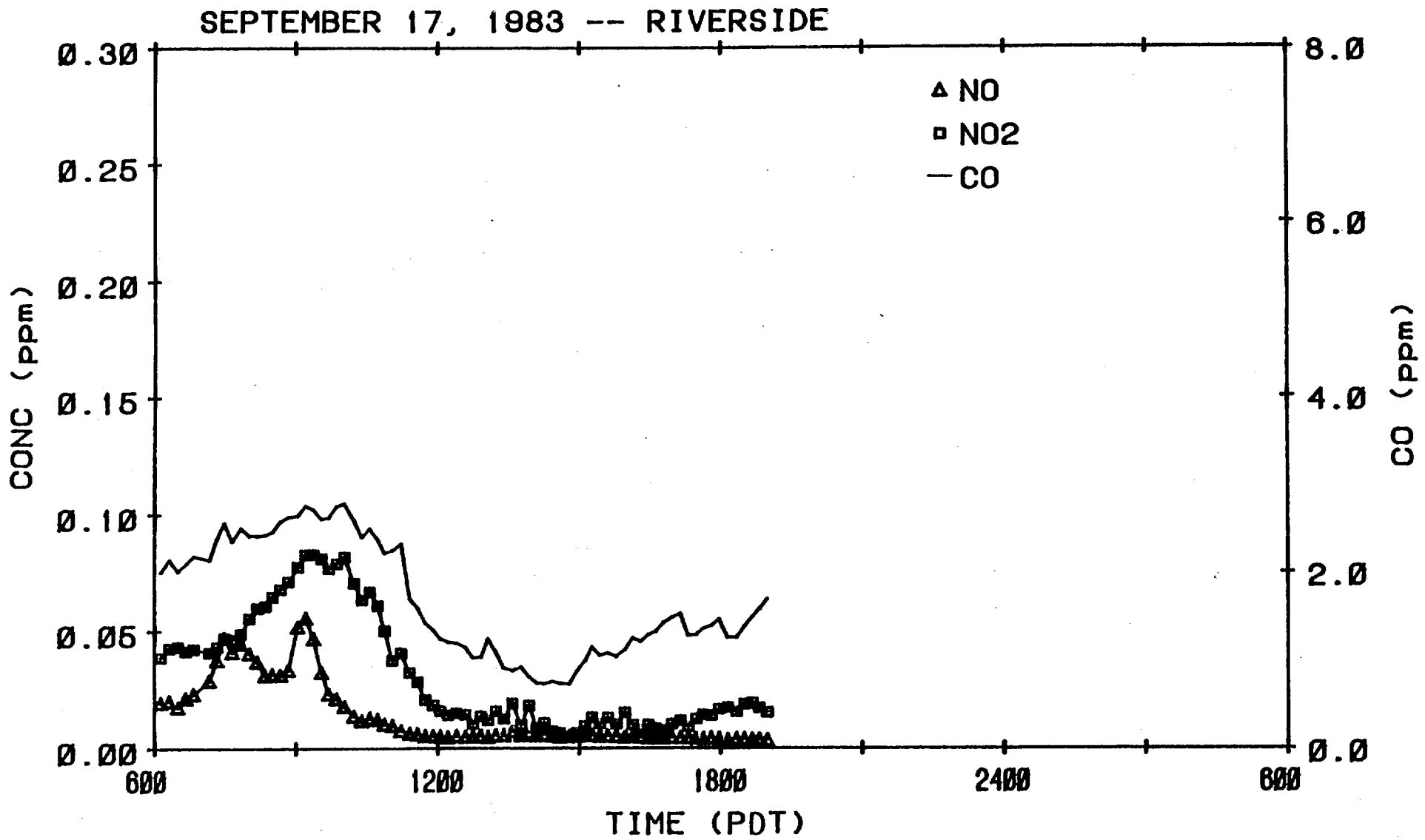

Figure II-18. Carbon monoxide (solid line), nitric oxide (Δ) and nitrogen dioxide (□) concentrations at Riverside for September 17, 1983.

Table II-3. Mutagenicity of El Monte Ambient Particulate Matter (TIGF Filters) Collected Over the Following Time Intervals: 1 = 0600-1000 hr, 2 = 1000-1500 hr, 3 = 1500-2100 hr, 4 = 2100-0600 hr

Date	Time Interval	Net Weight Particulates (g)	Net Weight Extract (g)	Percent Extractable	TA98 Activity (rev μg^{-1})	TA98 Mutagen Density (rev m^{-3})	TA98 Mutagen Loading (rev mg^{-1})	TA98NR Activity (rev μg^{-1})	TA98NR Mutagen Density (rev m^{-3})	TA98NR Mutagen Loading (rev mg^{-1})	TA98/ 1,8-DNP_6 Activity (rev μg^{-1})	TA98/ 1,8-DNP_6 Mutagen Density (rev m^{-3})	TA98/ 1,8-DNP_6 Mutagen Loading (rev mg^{-1})
9-12-83	3	0.0448	0.0135	30.2	3.1	57	920	1.5	27	440	0.41	7.6	120
9-12-83 / 9-13-83	4	0.0575	0.0256	45.2	1.8	40	830	1.2	27	550	0.65	14	290
9-13-83	1	0.0633	0.0196	30.9	3.8	140	1200	1.7	62	510	0.48	18	150
9-13-83	2	0.0620	0.0177	28.5	2.2	58	610	0.78	21	220	0.20	5.3	56
9-13-83	3	0.0740	0.0237	32.0	2.4	72	770	1.3	39	420	0.35	10	110
9-13-83 / 9-14-83	4	0.0757	0.0266	35.1	4.0	88	1400	2.6	57	910	0.88	19	310
9-14-83	1	0.0428	0.0164	38.2	4.4	140	1700	2.7	83	1000	0.85	26	330
9-14-83	2	0.0924	0.0308	33.4	1.6	76	540	0.68	32	230	0.18	8.4	60
9-14-83	3	0.0540	0.0169	31.3	2.4	51	750	1.5	31	460	0.40	9.2	140
9-14-83 / 9-15-83	4	0.0688	0.0273	39.7	2.7	60	1100	1.8	40	700	0.81	18	320
9-15-83	1	0.0432	0.0177	40.1	5.2	170	2100	3.5	120	1400	0.91	31	370
9-15-83	2	0.0635	0.0203	31.9	1.7	51	530	0.81	25	260	0.19	5.7	60
9-15-83	3	0.0907	0.0298	32.8	2.7	100	880	1.6	60	530	0.43	16	140
9-15-83 / 9-16-83	4	0.1427	0.0600	42.1	2.5	130	1100	1.8	91	770	0.52	26	220
9-16-83	1	0.0713	0.0267	37.5	5.1	260	1900	3.3	170	1300	0.64	32	240
9-16-83	2	0.0562	0.0181	32.2	2.6	140	830	1.1	58	350	0.22	12	70
9-16-83	3	0.1078	0.0343	30.1	2.6	110	810	1.5	63	470	0.32	14	100
9-16-83 / 9-17-83	4	0.1228	0.0490	39.9	3.1	130	1200	2.2	91	880	0.49	20	190
9-17-83	1	0.0628	0.0230	36.6	2.1	130	750	1.2	54	450	0.37	16	130
9-17-83	2	0.0801	0.0259	32.3	1.2	45	370	0.68	27	220	0.15	5.9	50

Table II-4. Mutagenicity of Riverside Ambient Particulate Matter (TIGF Filters) Collected Over the Following Time Intervals: 1 = 0600-1000 hr, 2 = 1000-1500 hr, 3 = 1500-2100 hr, 4 = 2100-0600 hr

Date	Time Interval	Net Weight Particulates (g)	Net Weight Extract (g)	Percent Extractable	TA98 Activity (rev μg^{-1})	TA98 Mutagen Density (rev m^{-3})	TA98 Mutagen Loading (rev mg^{-1})	TA98NR Activity (rev μg^{-1})	TA98NR Mutagen Density (rev m^{-3})	TA98NR Mutagen Loading (rev mg^{-1})	TA98/ 1,8-DNP_6 Activity (rev μg^{-1})	TA98/ 1,8-DNP_6 Mutagen Density (rev m^{-3})	TA98/ 1,8-DNP_6 Mutagen Loading (rev mg^{-1})
9-12-83	3	0.0865	0.0209	24.2	2.4	63	570	1.3	35	320	0.37	9.9	89
9-12-83/9-13-83	4	0.1055	0.0361	34.2	3.9	120	1300	2.0	61	670	0.55	17	190
9-13-83	1	0.0611	0.0194	31.8	4.3	160	1400	2.7	100	860	0.74	28	240
9-13-83	2	0.0785	0.0097	12.4	1.4	22	180	0.48	7.3	59	0.16	2.5	20
9-13-83	3	0.0746	0.0192	25.7	1.8	43	460	0.83	20	210	0.25	6.1	64
9-13-83/9-14-83	4	0.0928	0.0325	35.0	4.0	110	1400	2.1	56	720	0.60	16	210
9-14-83	1	0.0658	0.0233	35.5	5.2	240	1800	3.0	140	1100	0.91	41	320
9-14-83	2	0.0766	0.0275	35.9	1.7	71	600	0.80	34	290	0.25	10	88
9-14-83	3	0.1238	0.1925	155.0[a]	ND	97	620	ND	46	300	ND	12	76
9-14-83/9-15-83	4	0.1007	0.0396	39.4	3.6	120	1400	1.7	56	670	0.55	18	220
9-15-83	1	0.0775	0.0288	37.1	2.3	130	860	1.1	63	420	0.30	17	110
9-15-83	2	0.0868	0.0313	36.1	1.6	77	580	0.84	40	300	0.21	10	76
9-15-83	3	0.0984	0.0385	39.1	1.4	66	530	0.62	30	240	0.18	8.6	68
9-15-83/9-16-83	4	0.1137	0.0497	43.7	2.3	96	1000	1.2	51	540	0.39	16	170
9-16-83	1	0.0749	0.0280	37.4	3.2	170	1200	2.2	120	810	0.49	27	190
9-16-83	2	0.1598	0.0653	40.9	1.3	130	520	0.60	60	250	0.17	17	70
9-16-83	3	0.1211	0.0242	20.0	1.1	33	210	0.61	19	120	0.12	3.7	24
9-16-83/9-17-83	4	0.1495	0.0697	46.6	2.0	120	950	1.1	61	490	0.25	15	120
9-17-83	1	0.0725	0.0342	47.2	2.3	150	1100	1.3	82	600	0.38	25	180
9-17-83	2	0.0586	0.0188	32.1	1.3	37	420	0.71	20	230	0.17	4.9	55

[a]Contamination with hydrocarbon.

ND = Not determined.

of extract weight (rev μg^{-1}). The mutagen density is expressed as the number of revertants per cubic meter of air sampled, and the mutagen loading is given as the number of revertants per milligram of particulate collected. The mutagen densities obtained using the EPM 2000 GF filters are given in Tables II-5 and II-6 along with, for comparison, the corresponding values obtained on TIGF filters for El Monte and Riverside, respectively. The samples were tested for mutagenic activity in five groups and Table II-7 gives the standard mutagen values for each group. It can be seen from Table II-7 that, within the typical ranges of variation in the Ames test, the reproducibility of the standard mutagen values was good, allowing direct comparisons to be made among the mutagen density data in Tables II-3 through II-6.

Table II-8 gives the carbon, lead and bromine data obtained for El Monte, while Table II-9 gives the corresponding data for Riverside. In addition, Tables II-8 and II-9 contain the gaseous co-pollutant concentrations averaged over the time intervals used for particulate collection. Tables II-10 and II-11 give the additional elements determined by X-ray fluorescence.

Air mass trajectories were calculated for each day of the study and are presented in Appendix IX.A.1. It can be seen from these trajectories that a pattern of on-shore air flow persisted throughout this study with some increases in wind speed through the course of the week.

The mutagen densities (TA98, -S9) observed for POM collected on TIGF filters ranged from 40-260 rev m^{-3} at El Monte and 22-240 rev m^{-3} at Riverside. These values are higher than those generally reported in the literature at other locations (Daisey et al. 1980, Flessel et al. 1981, 1983) but are similar to values we have previously reported for sites in Los Angeles (Pitts et al. 1982b), including one close to a major freeway (Pitts et al. 1984e,f). The response was reduced on strains TA98NR and TA98/1,8-DNP_6, indicating that nitroarenes (Rosenkranz et al. 1981, 1982, Rosenkranz and Mermelstein 1983) may have contributed to the observed mutagenic activity.

It can be seen from Tables II-5 and II-6 that the mutagen densities obtained on the GF filters were generally lower by up to a factor of 3-4 than those for the TIGF filters. The manufacturer reports that the

Table II-5. Mutagen Densities Obtained at El Monte on September 12-15, 1983 for Particles Collected on EPM 2000 GF and TX40HI20WW TIGF Filters

Date	Time Interval (hr)	Mutagen Density (rev m^{-3})					
		TA98(-S9)		TA98NR(-S9)		TA98/1,8-DNP_6(-S9)	
		TIGF	GF	TIGF	GF	TIGF	GF
9-12-83	1500-2100	57	21	27	11	7.6	2.9
9-12-83 / 9-13-83	2100-0600	40	15	27	16	14	3.5
9-13-83	0600-1000	140	64	62	31	18	9
9-13-83	1000-1500	58	35	21	14	5.3	30
9-13-83	1500-2100	72	63	39	24	10	6.8
9-13-83 / 9-14-83	2100-0600	88	69	57	39	19	13
9-14-83	0600-1000	140	42	83	19	26	5.8
9-14-83	1000-1500	76	103	32	46	8.4	15
9-14-83	1500-2100	51	36	31	17	9.2	5.8
9-14-83 / 9-15-83	2100-0600	60	50	40	29	18	14
9-15-83	0600-1000	170	77	120	43	31	13

Table II-6. Mutagen Densities Obtained at Riverside on September 12-15, 1983 for Particles Collected on EPM 2000 GF and TX40HI20WW TIGF Filters

Date	Time Interval (hr)	Mutagen Density (rev m^{-3}) TA98(-S9) TIGF	TA98(-S9) GF	TA98NR(-S9) TIGF	TA98NR(-S9) GF	TA98/1,8-DNP_6(-S9) TIGF	TA98/1,8-DNP_6(-S9) GF
9-12-83	1500-2100	63	312	35	168	9.9	25
9-12-83 / 9-13-83	2100-0600	120	62	61	34	17	11
9-13-83	0600-1000	160	43	100	18	28	5
9-13-83	1000-1500	22	66	7.3	31	2.5	8
9-13-83	1500-2100	43	188	20	8.3	6.1	13
9-13-83 / 9-14-83	2100-0600	110	68	56	29	16	12
9-14-83	0600-1000	240	96	140	43	41	12
9-14-83	1000-1500	71	64	34	33	10	9
9-14-83	1500-2100	97	110	46	59	12	16
9-14-83 / 9-15-83	2100-0600	120	81	56	40	18	15
9-15-83	0600-1000	130	94	63	49	17	14

Table II-7. Values for Standard Mutagens (rev μg^{-1}) [-S9] 2-Nitrofluorene (2-NF) and Quercetin (Q) Included in Mutagenicity Tests Reported in Tables II-3 to II-6

	TA98	TA98NR	TA98/1,8-DNP_6
2-NF	380	53	66
Q	11	15	10
2-NF	390	61	64
Q	13	13	12
2-NF	390	77	57
Q	10	11	11
2-NF	410	70	66
Q	15	16	12
2-NF	360	50	57
Q	11	16	11

Table II-8. Particulate Carbon, Lead and Bromine Values and Gaseous Co-pollutants at El Monte Averaged Over the Following Time Intervals: 1 = 0600-1000 hr, 2 = 1000-1500 hr, 3 = 1500-2100 hr, 4 = 2100-0600 hr, which Corresponded to the Particulate Sampling Intervals

Date	Time Interval	Organic Carbon ($\mu g\ m^{-3}$)	Elemental Carbon ($\mu g\ m^{-3}$)	Lead ($\mu g\ m^{-3}$)	Bromine ($\mu g\ m^{-3}$)	CO (ppm)	NO (ppm)	NO_x[a] (ppm)	PAN (ppm)	O_3 (ppm)
9-12-83	3	17.0	2.8	0.38	0.08	1.48	0.012	0.061	0.0005	0.032
9-12-83 / 9-13-83	4	10.0	2.8	0.40	0.10	1.60	0.062	0.104	0.0001	0.003
9-13-83	1	29.0	12.0	1.40	0.35	4.25	0.127	0.206	0.0002	0.009
9-13-83	2	26.0	5.8	0.46	0.09	2.26	0.007	0.059	0.0044	0.140
9-13-83	3	12.0	1.9	0.59	0.09	0.88	0.010	0.076	0.0030	0.074
9-13-83 / 9-14-83	4	5.7	1.2	0.52	0.10	1.53	0.057	0.114	0.0001	0.002
9-14-83	1	23.0	6.4	0.78	0.13	2.20	0.075	0.134	0.0001	0.012
9-14-83	2	35.0	8.1	ND	ND	2.05	0.014	0.089	0.0110	0.188
9-14-83	3	16.0	3.4	0.34	0.06	1.14	0.004	0.051	0.0013	0.059
9-14-83 / 9-15-83	4	10.0	3.2	ND	ND	1.46	0.033	0.075	0.0001	0.003
9-15-83	1	22.0	7.4	0.62	0.11	2.34	0.060	0.102	0.0001	0.005
9-15-83	2	25.0	7.3	0.53	0.10	1.45	0.005	0.056	0.0081	0.118
9-15-83	3	23.0	5.3	0.45	0.09	1.73	0.001	0.060	0.0060	0.093
9-15-83 / 9-16-83	4	18.0	5.1	ND	ND	1.89	0.014	0.079	0.0016	0.004
9-16-83	1	22.0	7.0	0.57	0.10	1.94	0.030	0.094	0.0004	0.006
9-16-83	2	36.0	8.9	0.73	0.13	2.10	0.007	0.079	0.0011	0.144
9-16-83	3	28.0	6.2	0.58	0.11	1.71	0.002	0.067	0.0087	0.118
9-16-83 / 9-17-83	4	15.0	5.0	0.45	0.07	1.92	0.011	0.073	0.0011	0.004
9-17-83	1	26.0	4.7	0.74	0.12	1.58	0.009	0.068	0.0018	0.013
9-17-83	2	30.0	5.5	0.66	0.13	1.60	0.002	0.047	0.0085	0.158

[a] NO_x uncorrected for PAN and other nitrates. ND = Not determined.

Table II-9. Particulate Carbon, Lead and Bromine Values and Gaseous Co-pollutants at Riverside Averaged Over the Following Time Intervals: 1 = 0600-1000 hr, 2 = 1000-1500 hr, 3 = 1500-2100 hr, 4 = 2100-0600 hr, which Corresponded to the Particulate Sampling Intervals

Date	Time Interval	Organic Carbon ($\mu g\ m^{-3}$)	Elemental Carbon ($\mu g\ m^{-3}$)	Lead ($\mu g\ m^{-3}$)	Bromine ($\mu g\ m^{-3}$)	CO (ppm)	NO (ppm)	NO_x[a] (ppm)	PAN (ppm)	O_3 (ppm)
9-12-83	3	21.0	3.7	0.43	0.10	1.18	0.003	0.032	0.0040	0.112
9-12-83 / 9-13-83	4	20.0	4.6	ND	0.05	1.21	0.004	0.035	0.0017	0.026
9-13-83	1	32.0	7.1	0.56	0.10	1.95	0.039	0.093	0.0021	0.009
9-13-83	2	40.0	4.4	ND	ND	1.48	0.005	0.040	0.0062	0.140
9-13-83	3	24.0	3.3	0.32	0.07	1.34	0.004	0.035	0.0043	0.120
9-13-83 / 9-14-83	4	16.0	3.5	0.31	0.04	1.52	0.013	0.054	0.0014	0.009
9-14-83	1	36.0	11.0	0.89	0.14	2.94	0.071	0.140	0.0015	0.006
9-14-83	2	39.0	4.9	0.46	0.09	1.65	0.006	0.050	0.0086	0.178
9-14-83	3	37.0	6.7	0.43	0.11	1.79	0.004	0.044	0.0104	0.170
9-14-83 / 9-15-83	4	15.0	5.1	0.44	0.06	1.84	0.017	0.069	0.0018	0.005
9-15-83	1	27.0	7.3	0.70	0.11	2.24	0.035	0.096	0.0031	0.014
9-15-83	2	32.0	3.2	ND	ND	1.57	0.007	0.048	0.0089	0.151
9-15-83	3	24.0	3.8	0.30	0.06	1.28	0.005	0.035	0.0078	0.150
9-15-83 / 9-16-83	4	17.0	5.3	0.49	0.06	1.99	0.019	0.066	0.0025	0.011
9-16-83	1	26.0	6.5	0.80	0.12	2.74	0.048	0.114	0.0024	0.012
9-16-83	2	44.0	6.0	0.59	0.11	2.13	0.007	0.056	0.0118	0.171
9-16-83	3	28.0	6.0	0.41	0.08	1.62	0.004	0.041	0.0106	0.161
9-16-83 / 9-17-83	4	18.0	4.2	0.58	0.07	2.02	0.013	0.057	0.0038	0.014
9-17-83	1	26.0	6.5	0.72	0.08	2.45	0.034	0.096	0.0031	0.013
9-17-83	2	25.0	3.0	ND	ND	1.43	0.007	0.041	0.0073	0.121

[a] NO_x uncorrected for PAN and other nitrates.

ND = Not determined.

Table II-10. Elements Determined by X-Ray Fluorescence Analyses of Particulate Collected on Nuclepore Filters in El Monte. Time Interval: 1 = 0600-1000 hr, 2 = 1000-1500 hr, 3 = 1500-2100 hr, 4 = 2100-0600 hr. Units: $\mu g\ m^{-3}$

Date	Time Interval	Al	Si	S	Cl	K	Ca	Ti	V	Fe	Ni	Cu	Zn
9-12-83	3	1.46	3.60	2.11	0.092	0.75	0.90	0.14	0.039	1.48	0.00	0.10	0.053
9-12-83 / 9-13-83	4	0.33	1.04	1.88	0.54	0.32	0.47	0.00	0.00	0.46	0.007	0.092	0.040
9-13-83	1	0.00	1.64	1.73	0.13	0.60	0.86	0.12	0.00	1.42	0.00	0.090	0.27
9-13-83	2	1.47	3.67	3.48	0.076	0.92	0.98	0.17	0.065	1.63	0.00	0.068	0.14
9-13-83	3	2.09	4.85	4.42	0.10	0.88	1.19	0.23	0.075	2.16	0.013	0.096	0.17
9-13-83 / 9-14-83	4	0.93	1.88	2.80	0.22	0.49	0.68	0.096	0.053	0.76	0.013	0.42	0.16
9-14-83	1	0.99	1.98	3.68	0.21	0.50	0.75	0.16	0.073	1.03	0.00	0.15	0.38
9-14-83	2	ND	ND	ND	ND	ND	ND	ND	ND	ND	ND	ND	ND
9-14-83	3	0.00	0.71	2.96	0.00	0.27	0.61	0.053	0.00	0.49	0.010	0.039	0.058
9-14-83 / 9-15-83	4	ND	ND	ND	ND	ND	ND	ND	ND	ND	ND	ND	ND
9-15-83	1	0.00	0.99	4.15	0.071	0.27	0.39	0.00	0.052	0.63	0.00	0.049	0.15
9-15-83	2	1.54	3.85	5.84	0.051	0.70	1.12	0.12	0.00	1.76	0.00	0.060	0.14
9-15-83	3	ND	ND	ND	ND	ND	ND	ND	ND	ND	ND	ND	ND
9-15-83 / 9-16-83	4	ND	ND	ND	ND	ND	ND	ND	ND	ND	ND	ND	ND
9-16-83	1	0.00	1.49	9.77	0.00	0.39	0.59	0.087	0.59	0.62	0.00	0.044	0.21
9-16-83	2	1.18	3.91	14.37	0.074	0.68	1.34	0.12	0.00	1.63	0.00	0.067	0.27
9-16-83	3	1.36	3.12	11.29	0.084	0.55	1.01	0.22	0.12	1.21	0.00	0.047	0.13
9-16-83 / 9-17-83	4	0.51	1.35	7.46	0.00	0.33	0.42	0.038	0.071	0.47	0.00	0.26	0.080
9-17-83	1	0.00	2.61	12.97	0.062	0.59	0.93	0.085	0.14	1.08	0.00	0.050	0.10
9-17-83	2	0.88	3.46	11.29	0.050	0.69	1.21	0.18	0.057	1.73	0.00	0.041	0.16

ND = Not determined.

Table II-11. Elements Determined by X-Ray Fluorescence Analyses of Particulate Collected on Nuclepore Filters in Riverside. Time Interval: 1 = 0600-1000 hr, 2 = 1000-1500 hr, 3 = 1500-2100 hr, 4 = 2100-0600 hr. Units: $\mu g\ m^{-3}$

Date	Time Interval	Al	Si	S	Cl	K	Ca	Ti	V	Fe	Ni	Cu	Zn
9-12-83	3	2.40	5.61	6.27	0.080	2.15	2.11	0.20	0.00	1.85	0.00	0.093	0.090
9-12-83 / 9-13-83	4	ND	ND	ND	ND	ND	ND	ND	ND	ND	ND	ND	ND
9-13-83	1	1.94	4.28	3.51	0.071	1.60	1.77	0.15	0.00	1.83	0.00	0.026	0.081
9-13-83	2	ND	ND	ND	ND	ND	ND	ND	ND	ND	ND	ND	ND
9-13-83	3	2.03	4.58	3.76	0.064	1.25	1.72	0.14	0.061	1.70	0.012	0.057	0.074
9-13-83 / 9-14-83	4	0.67	2.00	2.48	0.028	0.58	0.89	0.062	0.00	0.79	0.00	0.032	0.057
9-14-83	1	3.18	6.76	3.68	0.095	1.29	2.37	0.28	0.00	3.05	0.017	0.061	0.19
9-14-83	2	1.05	3.76	4.70	0.044	0.92	1.69	0.068	0.041	1.67	0.00	0.059	0.21
9-14-83	3	1.31	4.31	4.78	0.12	2.41	1.92	0.25	0.047	1.80	0.00	0.067	0.12
9-14-83 / 9-15-83	4	1.22	3.26	3.51	0.073	0.74	1.44	0.12	0.040	1.31	0.009	0.046	0.084
9-15-83	1	5.09	10.57	4.34	0.11	1.85	2.38	0.39	0.00	5.12	0.00	0.051	0.32
9-15-83	2	ND	ND	ND	ND	ND	ND	ND	ND	ND	ND	ND	ND
9-15-83	3	1.73	4.58	4.05	0.045	0.95	1.76	0.19	0.00	1.72	0.00	0.045	0.073
9-15-83 / 9-16-83	4	0.17	1.45	4.22	0.052	0.48	0.94	0.055	0.00	0.96	0.00	0.052	0.063
9-16-83	1	2.08	4.96	5.29	0.049	0.98	1.91	0.200	0.00	2.17	0.00	0.049	0.13
9-16-83	2	1.47	4.69	6.77	0.060	1.41	3.44	0.26	0.00	3.09	0.00	0.069	0.17
9-16-83	3	1.92	4.80	7.68	0.067	0.94	2.00	0.19	0.067	1.83	0.011	0.054	0.12
9-16-83 / 9-17-83	4	0.68	2.16	7.84	0.031	0.57	1.15	0.00	0.032	0.84	0.00	0.051	0.085
9-17-83	1	1.15	2.39	7.21	0.087	0.46	0.83	0.097	0.048	0.99	0.013	0.061	0.11
9-17-83	2	ND	ND	ND	ND	ND	ND	ND	ND	ND	ND	ND	ND

ND = Not determined.

Pallflex TX40HI20 TIGF filters used in this study are >99.7% efficient (at the face velocities employed) for dioctylphthalate particles as small as 0.035 μm in diameter. Thus, these TIGF filters are essentially 100% efficient. Since the GF filters also have essentially 100% collection efficiency (B. Appel, private communication 1984), differences in collection efficiencies cannot be the cause of the differences in measured mutagen densities. However, it has been shown that for reactive PAH, such as BaP, recoveries are higher from TIGF filters than from GF filters (Lee et al. 1980) and degradation of mutagenic species on the GF filters may contribute to the large differences in measured mutagen densities between the two filter types. Since the catalytic surfaces of TIGF filters are presumably reduced by Teflon-coating, GF filters may promote degradation or formation of mutagenic species, causing large differences between the two filter types (Lee et al. 1980).

Tables II-12 and II-13 give ratios of (mutagen density on GF filters) to (mutagen density on TIGF filters) as a function of the sampling time during this study. The average O_3 and PAN concentrations and ratios of mutagen densities to CO are also given in these tables as well as averaged values for each time interval over the three days. The observed mutagen density ratios vary by up to a factor of 18 during this field study, with the higher values (i.e., those $\gtrsim 1$) correlating with elevated O_3 and PAN levels. This suggests that there is an artifact effect during particulate collection associated with one or both of the two types of filters employed. It can be seen from the average values for each time interval that this effect is more pronounced in Riverside than in El Monte.

Since CO is an essentially unreactive combustion emission, the (mutagen density/CO) ratio should, to a first approximation, take into account variations in emission profiles and in atmospheric dispersion. As can be seen in Table II-13, the two highest values for the mutagen density/CO ratio occurred on GF filters during the 1500-2100 hr time period (Riverside, 9/12 and 9/13) and were coincident with the highest values of the (GF/TIGF) mutagen density ratios. This suggests a filter artifact on the GF filters since any atmospheric transformation increasing the mutagen density/CO ratio should increase this ratio for both filter types. However, the possibility of an artifact on the TIGF filters cannot be completely eliminated.

Table II-12. Ratios of Mutagen Densities for Two Filter Types, Mutagen Density to CO Ratios, and Ozone and PAN Concentrations for September 12-15, 1983 in El Monte

Date	Time Interval (hr)	$\left[\frac{GF}{TIGF}\right]^a$	$[O_3]_{ave}$ (ppb)	$[PAN]_{ave}$ (ppb)	$\frac{MD\ TIGF^b}{CO}$	$\frac{MD\ GF^c}{CO}$
9-12-83	1500-2100	0.37	32	0.5	39	14
9-12-83 / 9-13-83	2100-0600	0.38	3	0.1	25	9
9-13-83	0600-1000	0.46	9	0.2	33	15
9-13-83	1000-1500	0.60	140	4.4	26	15
9-13-83	1500-2100	0.88	74	3.0	82	71
9-13-83 / 9-14-83	2100-0600	0.78	2	0.1	58	45
9-14-83	0600-1000	0.30	12	0.1	64	19
9-14-83	1000-1500	1.36	188	11.0	37	50
9-14-83	1500-2100	0.71	59	1.3	45	32
9-14-83 / 9-15-83	2100-0600	0.83	3	0.1	41	34
9-15-83	0600-1000	0.45	5	0.1	73	33
Average values[d]	0600-1000	0.40	8.7	0.13	57	22
	1000-1500	0.98	160	7.7	32	33
	1500-2100	0.65	55	1.6	55	39
	2100-0600	0.66	2.7	0.1	41	29

[a]TA98 mutagen density obtained for particles collected on EPM 2000 GF filters divided by the mutagen density for particles collected on TIGF filters.
[b]Mutagen density of POM collected on TIGF filters.
[c]Mutagen density of POM collected on GF filters.
[d]Arithmetic mean of individual values for each time interval.

Regression of the mutagen density ratio (GF/TIGF) for Riverside with the co-pollutant data showed a negative correlation with NO_2 (explaining ~60% of the variance), suggesting either formation of direct mutagens on the TIGF filters due to the presence of NO_2 and associated species, or destruction of labile direct mutagens on the GF filters during collection

Table II-13. Ratios of Mutagen Densities for Two Filter Types, Mutagen Densities to CO Ratios, and Ozone and PAN Concentrations for September 12-15, 1983 in Riverside

Date	Time Interval (hr)	$\left[\frac{GF}{TIGF}\right]^a$	$[O_3]_{ave}$ (ppb)	$[PAN]_{ave}$ (ppb)	$\frac{MD\ TIGF^b}{CO}$	$\frac{MD\ GF^c}{CO}$
9-12-83	1500-2100	4.95	112	4.0	53	264
9-12-83 / 9-13-83	2100-0600	0.52	26	1.7	99	51
9-13-83	0600-1000	0.27	9	2.1	82	22
9-13-83	1000-1500	3.0	140	6.2	15	45
9-13-83	1500-2100	4.37	120	4.3	32	140
9-13-83 / 9-14-83	2100-0600	0.62	9	1.4	72	45
9-14-83	0600-1000	0.40	6	1.5	82	33
9-14-83	1000-1500	0.90	178	8.6	43	39
9-14-83	1500-2100	1.13	170	10.4	54	61
9-14-83 / 9-15-83	2100-0600	0.68	5	1.8	65	44
9-15-83	0600-1000	0.72	14	3.1	58	42
Average values[d]	0600-1000	0.46	9.7	2.2	74	32
	1000-1500	2.0	160	7.4	29	42
	1500-2100	3.5	130	6.2	46	160
	2100-0600	0.61	13	1.6	79	47

[a] TA98 mutagen density obtained for particles collected on EPM 2000 GF filters divided by the mutagen density for particles collected on TIGF filters.
[b] Mutagen density of POM collected on TIGF filters.
[c] Mutagen density of POM collected on GF filters.
[d] Arithmetic mean of individual values for each time interval.

of fresh POM which is generally most abundant during periods of high NO_2 (0600-1000 hr).

In summary, at least three processes could affect the mutagenic activity of POM collected on GF and TIGF filters and lead to the observed differences in ratios of mutagenicities obtained for the two kinds of filters (Tables II-12 and II-13). These processes are:

(1) Irreversible adsorption of the mutagenic species on the filter surface, leading to differences in extraction efficiency.

(2) Destruction of mutagenic species catalyzed by the filter surface.

(3) Transformation of nonmutagenic compounds to direct mutagens involving catalysis by the filter surface and/or surface dependent accumulation of a reactive species present in the ambient gases flowing through the filter (e.g., HNO_3).

Clearly, some or all of the processes may have been operative during our filter collections of ambient POM, but at the present time no further interpretation of our data in terms of these effects is possible.

Since we view the TIGF filter surface as more inert than the GF filter surface and furthermore our data set for mutagenicity of POM collected on TIGF and GF filters showed a demonstrable artifact on the GF filters, we chose to carry out further statistical analysis of our data from the TIGF filter POM collections. In deciding whether mutagenicity arises from primary or secondary POM or from atmospheric transformations, correlations between mutagenicity and co-measured meteorological and chemical data are useful because they can provide information regarding the relative contributions of changes in emissions source strengths, secondary pollutants, and meteorology to the variation in observed mutagenicity. Accordingly, we carried out correlations on the data from the ambient POM collections on TIGF filters at the intermediate receptor site, El Monte, and the downwind receptor site, Riverside. Correlations were made both on the original data set (see Appendices IX.A.2 and IX.A.3 for the correlation coefficients for the El Monte and Riverside data sets, respectively) and on a set of independent factors obtained by factor analysis.

The principal component model of factor analysis was employed, using the BMDP419 statistical package, in the analysis of the field measurement data because of the large number of variables measured during this study. (See Table II-14 for a list of the variables included in this analysis, and their abbreviations.) The advantage of this model is that it groups the variables into a smaller, more manageable, number of uncorrelated factors which explain a large portion of the overall variance of the original data set. Ideally, the variables in each factor have a

Table II-14. Definition of Variables Used in Factor Analyses and Regressions

Variable	Abbreviation
Nitrogenous species (NO_2, NO and PAN)	NOXUNC
Nitric oxide	NO
Nitrogen dioxide (not corrected for PAN interference)	NO2UNC
Particulate lead	PB
Particulate bromine	BR
Carbon monoxide	CO
Particulate elemental carbon	ELEMC
Particulate organic carbon	ORG C
Peroxyacetyl nitrate	PAN
Ozone	OZONE
Total solid particulate	TSP
Temperature	TDRY
Relative humidity	RELHUM
Percent extractable	PERCEX
Particulate silica	SI
Aluminum	AL
Iron	FE
Titanium	TI
Chloride	CL
Zinc	ZN
Potasium	K
Vanadium	V
Nickel	NI
Copper	CU
Sulfur	S
Calcium	CA

common origin, i.e., a common emission source or formation process. In practice, only a few of the most important factors are usually needed to explain a large part of the variance.

After principal component factors were extracted, the rotated factor scores were regressed on the mutagenicity measures. The following particulate mutagenicity measures were used:

(1) Mutagen density is the mutagenicity per volume of sampled air (reverants m^{-3}). This is the airborne mutagenicity concentration, and represents the dose of mutagens to which people are exposed.

(2) Specific activity is the mutagenicity per weight of extractable material (revertants μg^{-1}) and represents the potency of the extract.

(3) Mutagen loading is the mutagenicity per weight of collected particulate matter (revertants mg^{-1}) and represents the potency of the particulate matter.

Since mutagenicity detected on the three strains used (TA98, TA98NR, and TA98/1,8-DNP_6) was very well correlated (see Appendices IX.A.2 and IX.A.3), only TA98 mutagenicity was used as the dependent variable in the regressions. Factor analyses of the combined Riverside and El Monte data were performed, but the factor analyses for the individual Riverside and El Monte data proved to be more readily interpretable and therefore are used in the discussions which follow.

In addition to principal component factors, individual variables were also regressed on mutagenicity (using the BMDP2R statistical package) to determine which specific variables are most strongly related to mutagenic activity, independent of source. Table II-15 shows the principal components derived from data taken in El Monte, together with a suggested interpretation, where possible. Variables in each factor are listed in decreasing order of importance, with minor contributors listed in parentheses. A minus sign indicates a negative association between a variable and the others in its factor. Table II-16 shows the results of significant correlations of these factors on the mutagenicity variables: mutagen density, specific activity, and mutagen loading. Tables II-17 and II-18 show the corresponding values for Riverside.

A larger portion of the changes in mutagen density observed at Riverside during the five-day field study could be accounted for than was the case for the El Monte data. Thus, the factor analysis showed that in

Table II-15. Principal Component Factors for El Monte

Factor	Factor 1	Factor 2	Factor 3	Factor 4	Factor 5
	FE	PB	ELEMC	TSP	CL
	SI	BR	ORGC	V	(PERCEX)
	K	NOXUNC	-NI	S	
	CA	CO	-CU		
	AL	NO	TSP		
	TI	PAN	(S)		
	TDRY	NO2UNC			
	-RELHUM	ELEMC			
	OZONE				
	-PERCEX				
	PAN				
Interpretation	Soil and Secondary Pollutants	Traffic		Oil Burning	

Table II-16. Regression of Factors for El Monte

Factor	Relationship	% of Variance*
With TA98 Mutagen Density as the Dependent Variable		
1	negative	25
4	positive	23
2	positive	19
		67% Total variance
With TA98 Specific Activity as the Dependent Variable		
1	negative	29
2	positive	18
		47% Total variance
With TA98 Mutagen Loading as the Dependent Variable		
1	negative	42

*Significant at the 5% level.

Table II-17. Principal Component Factors for Riverside

Factor	Factor 1	Factor 2	Factor 3	Factor 4	Factor 5	Factor 6
	NOXUNC	SI	PAN	RELHUM	V	CU
	NO	AL	ORGC	PERCEX	NI	S
	CO	FE	TSP	-TDRY		
	NO2UNC	TI	OZONE			
	PB	CL	CA			
	ELEMC	ZN				
	BR	K				
Interpretation	Traffic	Soil	Secondary Pollutants	Temperature	Fly Ash	

Table II-18. Regression of Factors for Riverside

Factor	Relationship	% of Variance*
With TA98 Mutagen Density as the Dependent Variable		
1	positive	87
5	negative	4
		91% Total variance
With TA98 Specific Activity on the Dependent Variable		
1	positive	43
3	negative	24
6	negative	12
4	negative	7
		86% Total variance
With TA98 Mutagen Loading as the Dependent Variable		
1	positive	53
3	negative	22
6	negative	11
		86% Total variance

*Significant at the 5% level.

Riverside, ~85-90% of the variation in mutagen density was accounted for by the factor identified with mobile source emissions (Factor 1, Table II-17). In contrast, the factor analysis showed that the mutagen density of POM collected in El Monte was related to three factors. The factor attributed to soil emissions and secondary photochemical pollutants was negatively related to mutagen density and accounted for 25% of the variation. Oil burning accounted for 23% of the variation and mobile source emissions accounted for an additional 19% of the variation.

A negative association between specific activity (and mutagen loading) and factors containing PAN and ozone was seen for both El Monte and Riverside data. This may be interpreted in terms of destruction of direct mutagens by ozone or the presence of less mutagenic secondary aerosol species during high ozone periods.

Tables II-19 and II-20 contain a summary of the correlations between the individual variables and mutagenicity for El Monte and Riverside, respectively. In Riverside, NO_x alone accounted for ~85-90% of the variance in mutagen density. A negative relation between the photochemical pollutants, ozone and PAN, and specific activity was again seen for both El Monte and Riverside. While the statistical analysis discussed above offers some insights into relationships between the observed mutagenicities and the large number of chemical, meteorological and source variables, it is obvious from the factor analyses that the origin of, and influences on, the observed mutagenicities cannot be explained in a simple manner, especially in the case of the El Monte data. Much further work will be required to completely elucidate the changes in the mutagenicity of ambient POM as a function of time of day and location in the basin.

E. Conclusions

- The ratios of mutagen densities for POM simultaneously collected on GF and TIGF filters were observed to vary from a low of 0.27 to a high of 4.95 (a total range of a factor of 18). The higher values occurred during periods of elevated O_3 and PAN concentrations, suggesting there is an artifact effect during particulate collection associated with one or both of these two types of filters. While analysis of the mutagen density/CO ratios suggests that the filter artifact is associated with the GF filters, we cannot rule out an artifact effect on the TIGF filters.

Table II-19. Regression of Original Data for El Monte with Mutagenicity Parameters

Variable	Relationship	% of Variance*
TA98 Mutagen Density as the Dependent Variable		
TDRY	negative	52
TSP	positive	20
		72% Total variance
TA98 Specific Activity as the Dependent Variable		
OZONE	negative	41
ZN	positive	22
		63% Total variance
TA98 Mutagen Loading as the Dependent Variable		
TDRY	negative	53

*Significant at the 5% level.

Table II-20. Regression of Original Data for Riverside with Mutagenicity Parameters

Variable	Relationship	% of Variance*
TA98 Mutagen Density as the Dependent Variable		
NOXUNC	positive	87
TA98 Specific Activity as the Dependent Variable		
PAN	negative	60
ORGC	positive	16
		76% Total variance
TA98 Mutagen Loading as Dependent Variable		
OZONE	negative	70
NO	positive	8
		78% Total variance

*Significant at the 5% level.

However, at the present time we prefer TIGF as the filter of choice based on its more inert properties.

- The observed mutagen densities (TA98, -S9) of TIGF filter extracts varied from 22 to 240 rev m^{-3} for Riverside and from 40 to 260 rev m^{-3} for El Monte. These values are higher than those generally reported in the literature for other air basins but are similar to values we have previously reported for locations in the South Coast Air Basin.

- Decreased responses relative to TA98 were seen on the nitroreductase deficient strains TA98NR and TA98/1,8-DNP_6 suggesting the presence of nitroarenes.

- Factor analyses for the mutagenicity of POM collected on TIGF filters and the gaseous co-pollutant data showed that in Riverside, most of the observed variation in mutagen density appeared to be due to a factor which included mobile source emissions.

- Much additional work will be needed to decide the extent to which the mutagenicity of ambient POM may be altered during transport and/or during POM collection.

III. INVESTIGATION OF PAH TRANSFORMATIONS UNDER AMBIENT ATMOSPHERIC CONDITIONS: SEPTEMBER 1984 FIELD STUDY

A. Introduction

A recent review (National Research Council 1983) on polycyclic aromatic hydrocarbons and their health effects makes clear the conflicting nature of results from laboratory investigations designed to determine the atmospheric fates of these toxic pollutants. In particular, substrate effects on the reaction of adsorbed PAH seem to be important. These reports and the observation of filter artifacts influencing the mutagenicity of ambient POM collected on glass fiber (GF) filters during our September 1983 field study led us to undertake a second field study in September 1984. This study was designed to evaluate the degree of chemical transformation of selected PAH deposited on GF and TIGF filter surfaces during exposures to well-defined atmospheric pollutants under "active" and "passive" conditions.

The "active" conditions represented those occurring during filter collection of POM, when large amounts of polluted air are pulled through particulate-laden filters. In contrast "passive" exposures of PAH-coated filters to ambient air were designed to simulate conditions which occur during transport of the POM in polluted air masses. Four model PAH, pyrene (PY), fluoranthene (FL), benzo(a)pyrene (BaP) and perylene (PER) were selected for investigation on the basis of our laboratory chamber exposures (Pitts et al. 1984a,d).

B. Experimental

This study took place from 1200 PDT on September 18, 1984 to 1200 PDT on September 21, 1984 on the UC campus, Riverside. First stage ozone alert levels were reached in Riverside during the first and second day of the study. The maximum ozone concentration was ~310 ppb, attained on September 18.

1. Gas Phase Analyses During Collection Period

The array of instruments used for measuring gaseous pollutant concentrations is given in Table III-1. The ozone, NO, NO_x and CO instrument outputs were fed into a data acquisition system based on an Apple II micro-computer. Data were averaged over 10-min intervals and

Table III-1. Instrumentation for Measurement of Gaseous Pollutants During September 1984 Field Study

Parameter	Instrument	Principle of Operation
O_3	REM Model 612	Chemiluminescence
NO, NO_x	Columbia S.I. Model 1600	O_3 Chemiluminescence
CO	Dasibi Model 3003	IR Gas Filter Correlation
PAN	Varian Model 600	GC/ECD
NO_2, NO_3 HONO, HCHO	SAPRC DOAS	Differential Optical Absorption

stored on a floppy disk. A hard copy of the data was also printed simultaneously. The data stored on disk were later processed using the main computing facilities at SAPRC.

Additionally, long pathlength (1.6 km) differential optical absorption spectroscopy (DOAS) was used to monitor the atmospheric concentrations of the NO_3 radical, NO_2, HONO, and HCHO.

2. Exposures of PAH-Coated Filters

The exposures of PAH coated filters to ambient air were carried out in four 6-hr time periods, 0000-0600 hr, 0600-1200 hr, 1200-1800 hr and 1800-2400 hr. Based on ambient air monitoring data previously obtained by SAPRC researchers (Tuazon et al. 1981, Pitts et al. 1984b), these 6-hr periods were chosen to allow exposure of the collected POM to different sets of pollutant species at different times during a 24-hr period, as shown in Table III-2.

TIGF and GF filters, prewashed by sequential Soxhlet extraction with CH_2Cl_2 and CH_3OH, were coated with 5 mℓ of either PY, FL, BaP or PER solution in toluene (at a concentration of ~0.2 mg $mℓ^{-1}$) and the solvent was allowed to evaporate. The filters were wrapped in aluminum foil and stored in a freezer prior to exposure.

Table III-2. Dominant Pollutants Expected During the Exposure Periods

Sampling Period (PDT)	Dominant Pollutants
0000-0600	NO_2, HONO
0600-1200	NO_2
1200-1800	O_3, PAN, HNO_3, NO_2, HCHO, HCOOH
1800-2400	NO_3, N_2O_5, NO_2, O_3

Active Exposures. Eight TIGF and eight GF filters, two each coated with PY, PER, FL and BaP, were placed in 16 Hi-vol samplers under TIGF prefilters positioned to remove ambient POM. Six of these Hi-vol samplers were equipped with 10 μm cut-off inlets and loaded with GF and TIGF filters coated with PY, BaP and PER. Exposures were carried out in four 6-hr time periods, as described above.

Passive Exposures. Simultaneously with the active exposures described above, TIGF and GF filters coated with PAH were hung from Teflon lines and exposed to the outdoor atmosphere. Two uncoated filters (TIGF and GF), which served as control filters, were also exposed during each 6-hr period.

3. Filter Extractions and Sample Analysis

After exposures, PAH coated filters were Soxhlet extracted with the CH_3CN/MeOH (81:19 v/v) azeotrope for 16 hr. The extracts were reduced to ~5 mℓ in volume by rotary evaporation at 35 C under aspirator vacuum, and then filtered through 0.5 μm Millex-SR filter cartridges. Forty percent of the extract was transferred into a tared vial and evaporated to constant (±1%) weight at 35 C under a stream of dry nitrogen. The weighed sample was then dissolved in degassed dimethylsulfoxide (DMSO) and assayed for mutagenic activity toward Salmonella strains TA98 (passive and active exposures), TA98NR and TA98/1,8-DNP_6 (active exposures only).

The recovery of the PAH under investigation was determined by high performance liquid chromatography (HPLC) of an aliquot of the samples to which an internal standard (triphenylbenzene) had been added. A Beckman Model 334 liquid chromatograph equipped with a Vydac 201 TP5415 column (CH_3CN/H_2O, isocratic) was employed. The polar fraction of extracts from PY coated TIGF and GF filters were separated on an Ultrasphere ODS (Altex) semi-preparative column.

Identification of the main products formed during these exposures was performed by GC-MS (Finnigan Model 3200) interfaced to a Teknivent interactive data system with hard disk storage capabilities. The GC was equipped with a cool on-column injection system (J&W Associates, Inc.) and a DB-5 capillary column (0.2 mm I.D., 29 m length).

C. Results and Discussion

1. Gaseous Species

The period of time when this field study took place (September 18-21, 1984) encompassed the most severe photochemical air pollution episode in Riverside in more than a year. Figures III-1 to III-8 show the time-concentration profiles for several gas phase species and the temperature profile for the first 24 hrs of the study, the period of highest pollution. A complete set of these data for the entire study period is given in the Appendices in Section IX. Appendix B lists the DOAS measurements for the NO_3 radical, NO_2, HONO and formaldehyde. Appendix C contains plots of CO, NO, NO_2 (obtained by chemiluminescence), ozone, PAN, temperature, relative humidity and wind speed and wind direction.

From the plots of CO (Figure III-1) and NO (Figure III-2) it is evident that a local traffic peak occurred between approximately 0600-0900 hr on September 19. As would be expected an NO_2 peak occurs slightly later on September 19 (see Figure III-3). The highest ozone level reached during our study occurred on September 18. It is clear from Figure III-4 that this ozone peak occurred largely in the 1200-1800 hr exposure interval. PAN (Figure III-5) also peaked during this time interval. As anticipated, HONO peaked during the 0000-0600 hr exposure interval (see Figure III-6). Figure III-7 shows the NO_3 radical concentration measured by DOAS and the calculated N_2O_5 concentration for the evening of September 18-19. Unlike our September 1983 field study, NO_3 radicals persisted throughout the night in Riverside (see Section V for a detailed discussion of this topic). The implications for PAH recovery at the high temperatures reached (Figure III-8) are discussed below.

2. Active and Passive PAH Exposures

We chose to analyze the filters exposed from 1200 hr September 18 to 1200 hr September 19 since this 24-hr period encompassed the highest secondary pollutant levels (as evidenced by the gas phase species) during

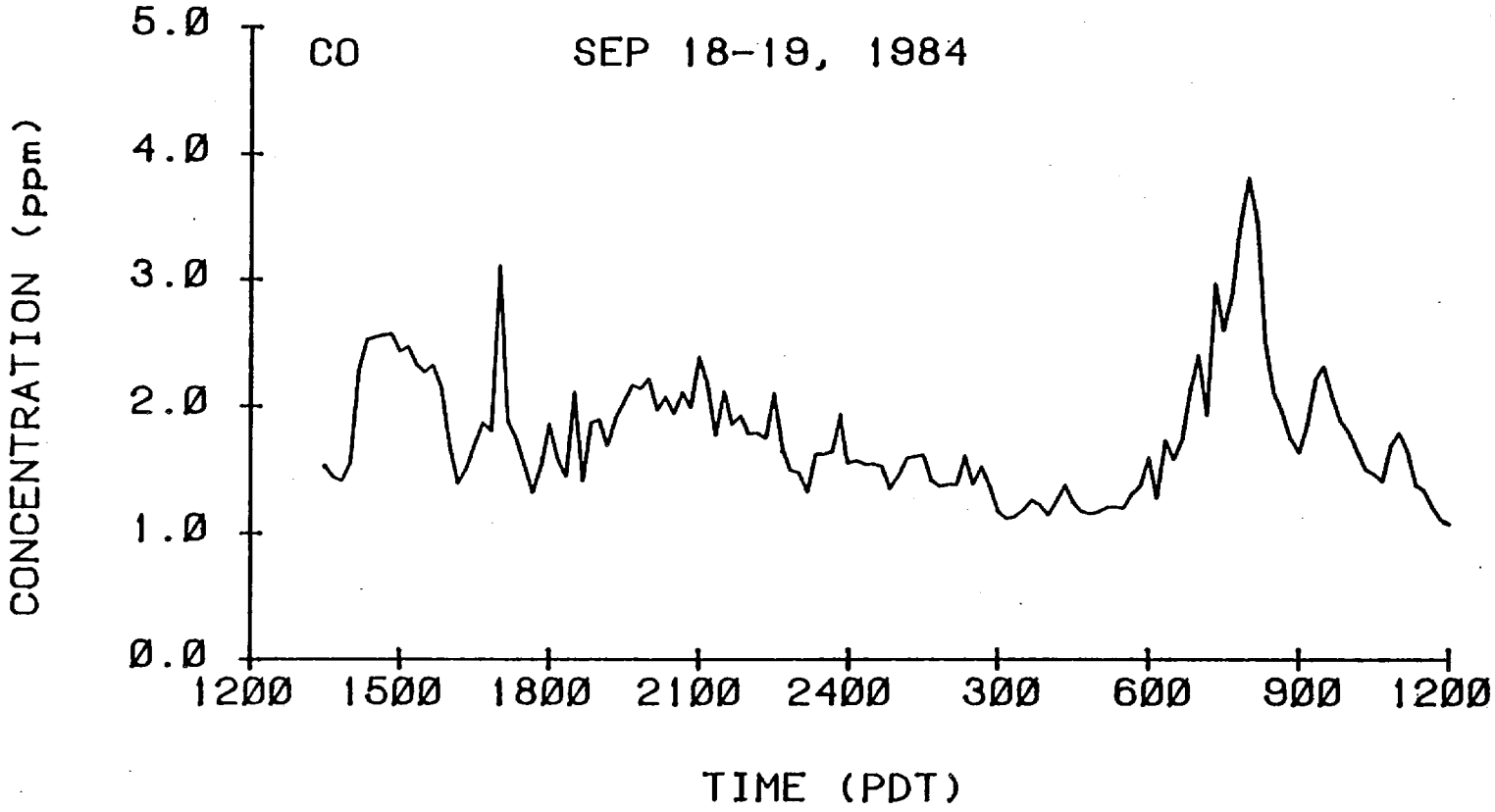

Figure III-1. Carbon monoxide concentration at U.C. Riverside for 1200 PDT September 18 to 1200 PDT September 19, 1984.

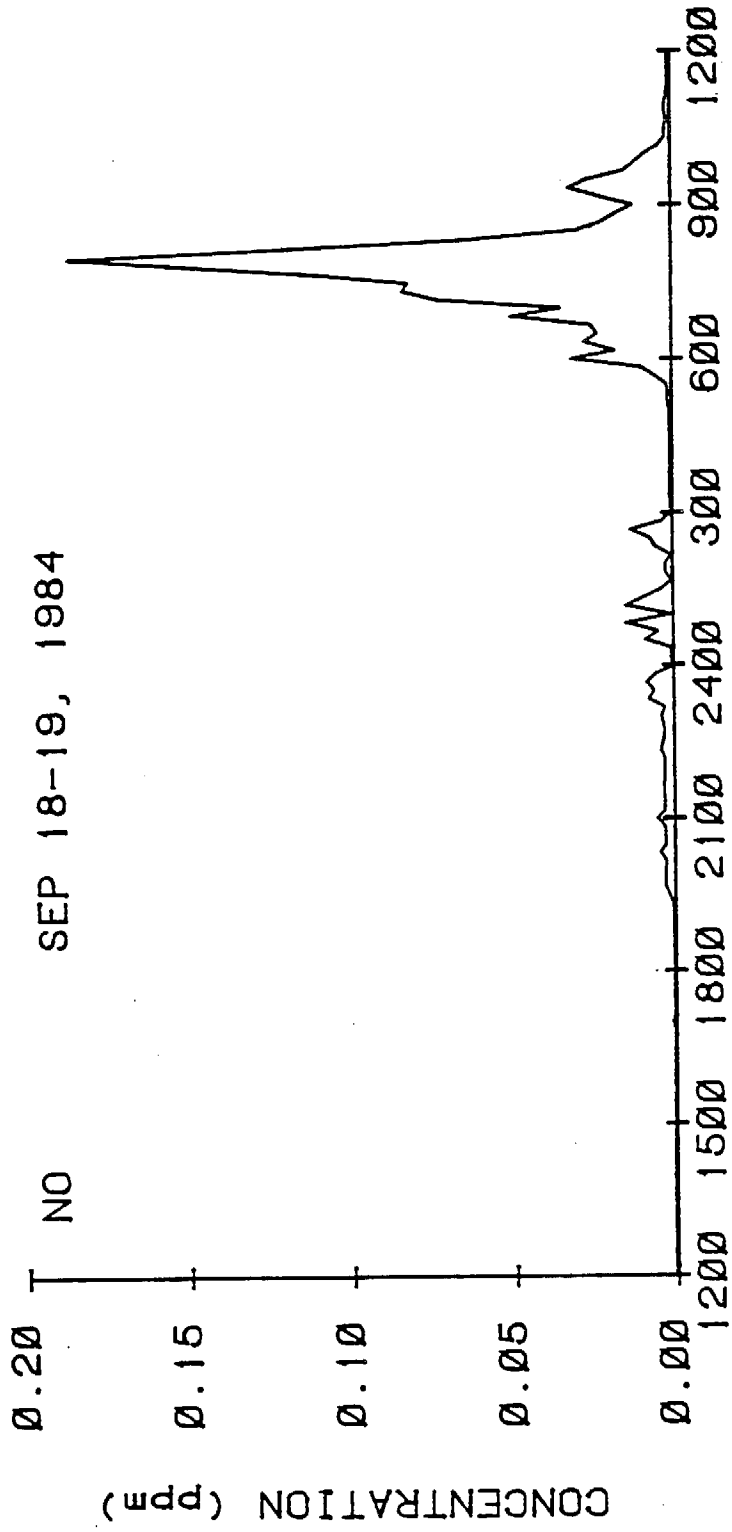

Figure III-2. Nitric oxide concentration at U.C. Riverside for 1200 PDT September 18 to 1200 PDT September 19, 1984.

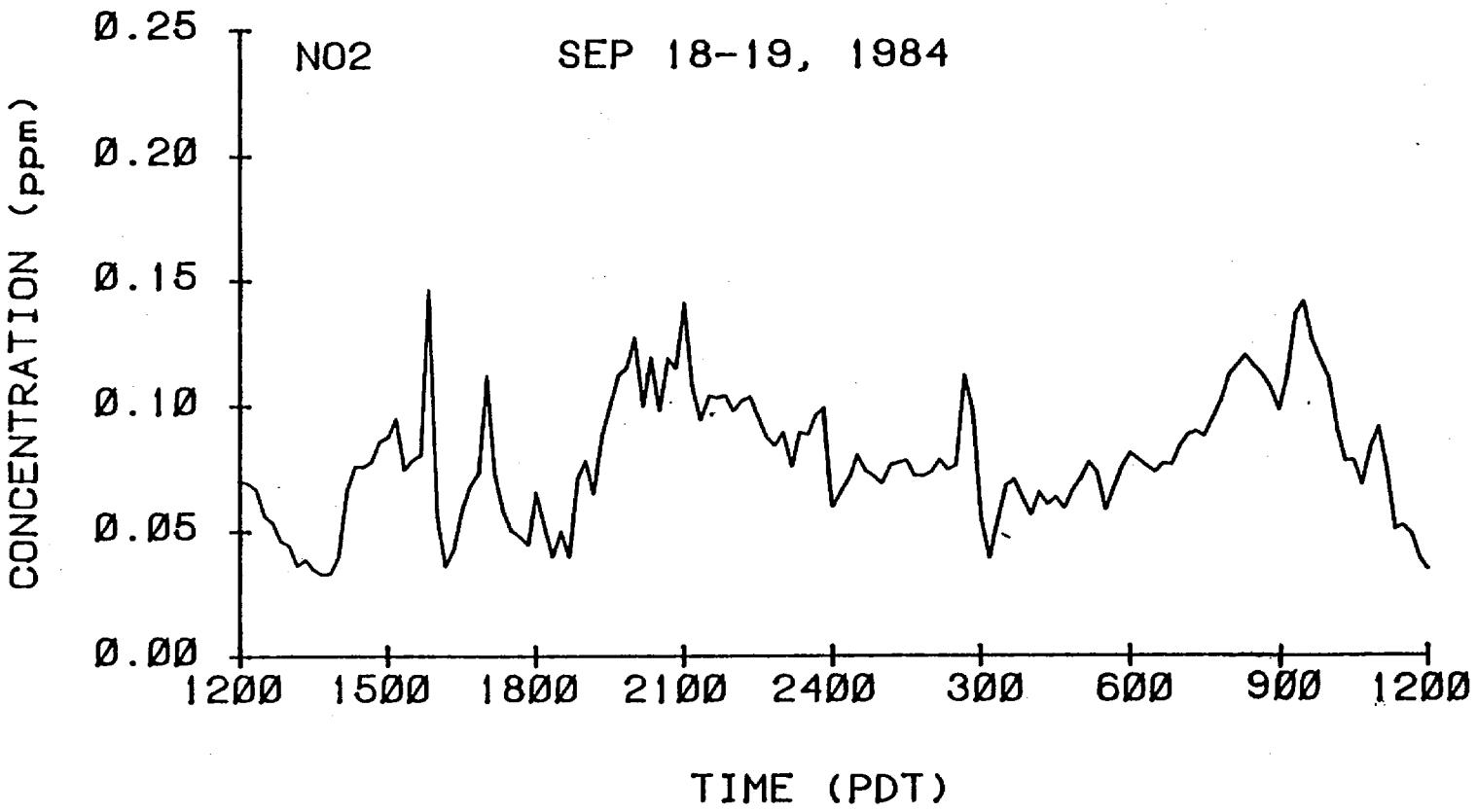

Figure III-3. Nitrogen dioxide concentration at U.C. Riverside for 1200 PDT September 18 to 1200 PDT September 19, 1984 (chemiluminescence detection, uncorrected for interferences).

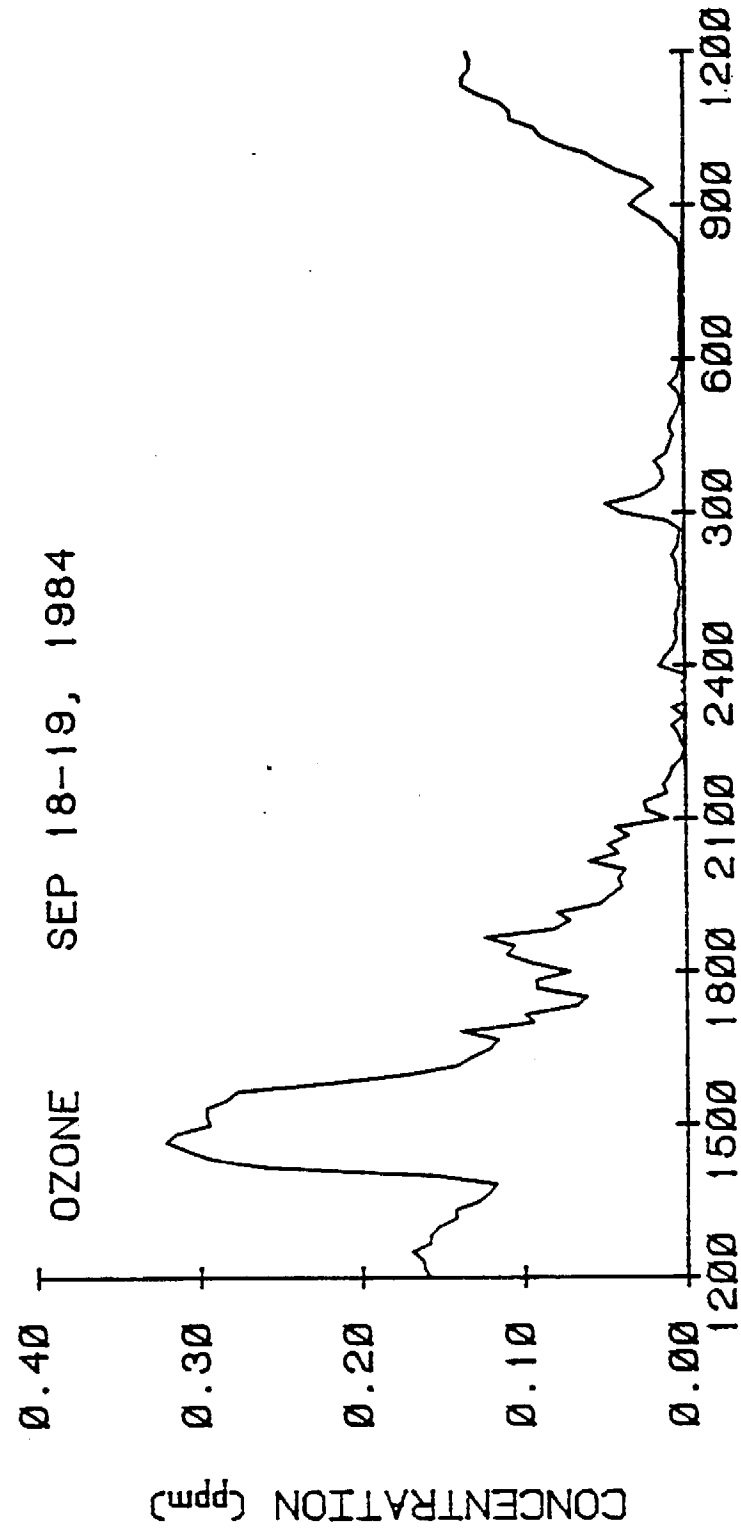

Figure III-4. Ozone concentration at U.C. Riverside for 1200 PDT September 18 to 1200 PDT September 19, 1984.

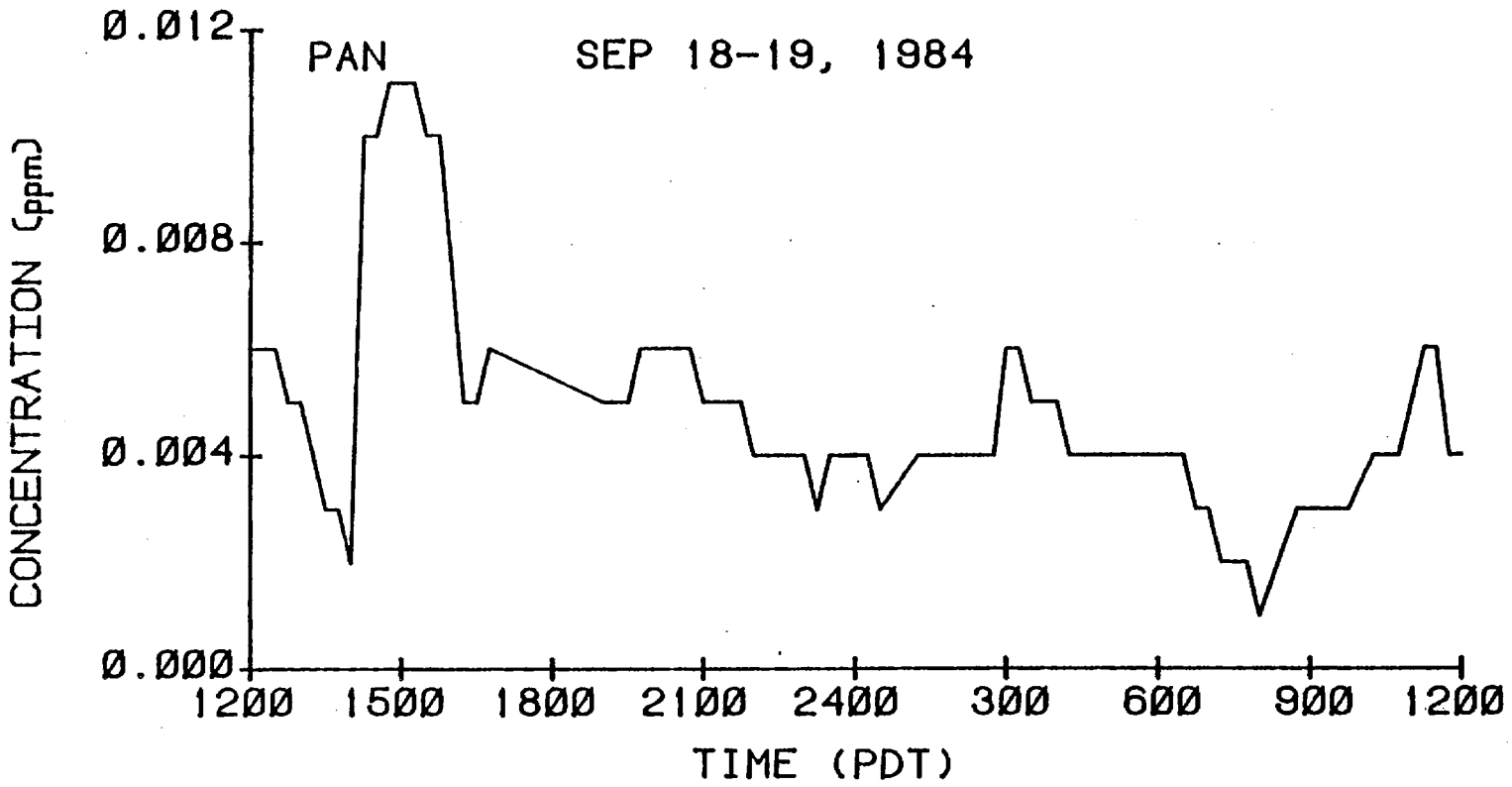

Figure III-5. Peroxyacetyl nitrate concentration at U.C. Riverside for 1200 PDT September 18 to 1200 PDT September 19, 1984.

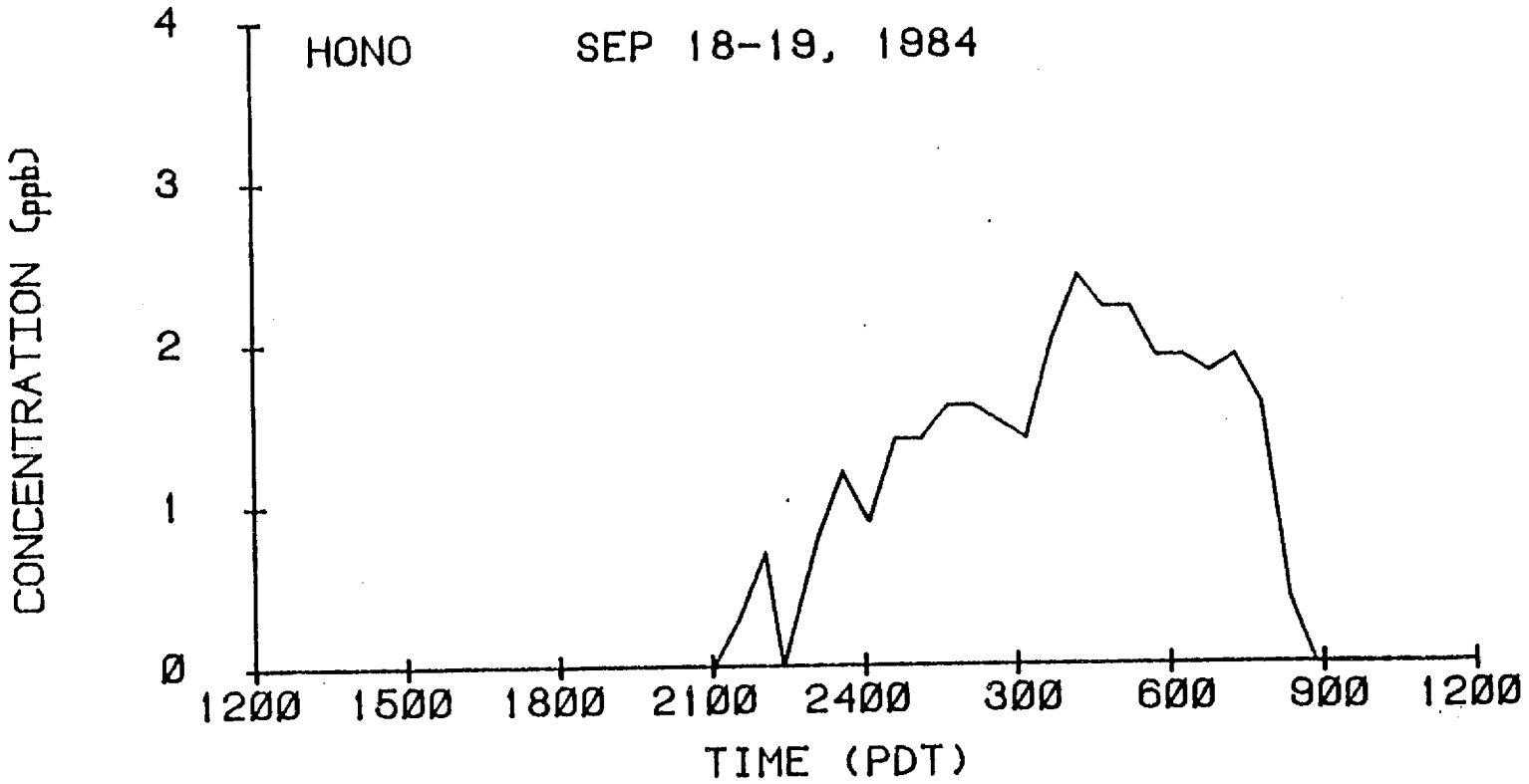

Figure III-6. Nitrous acid concentration at U.C. Riverside for 1200 PDT September 18 to 1200 PDT September 19, 1984, as measured by differential optical absorption spectroscopy.

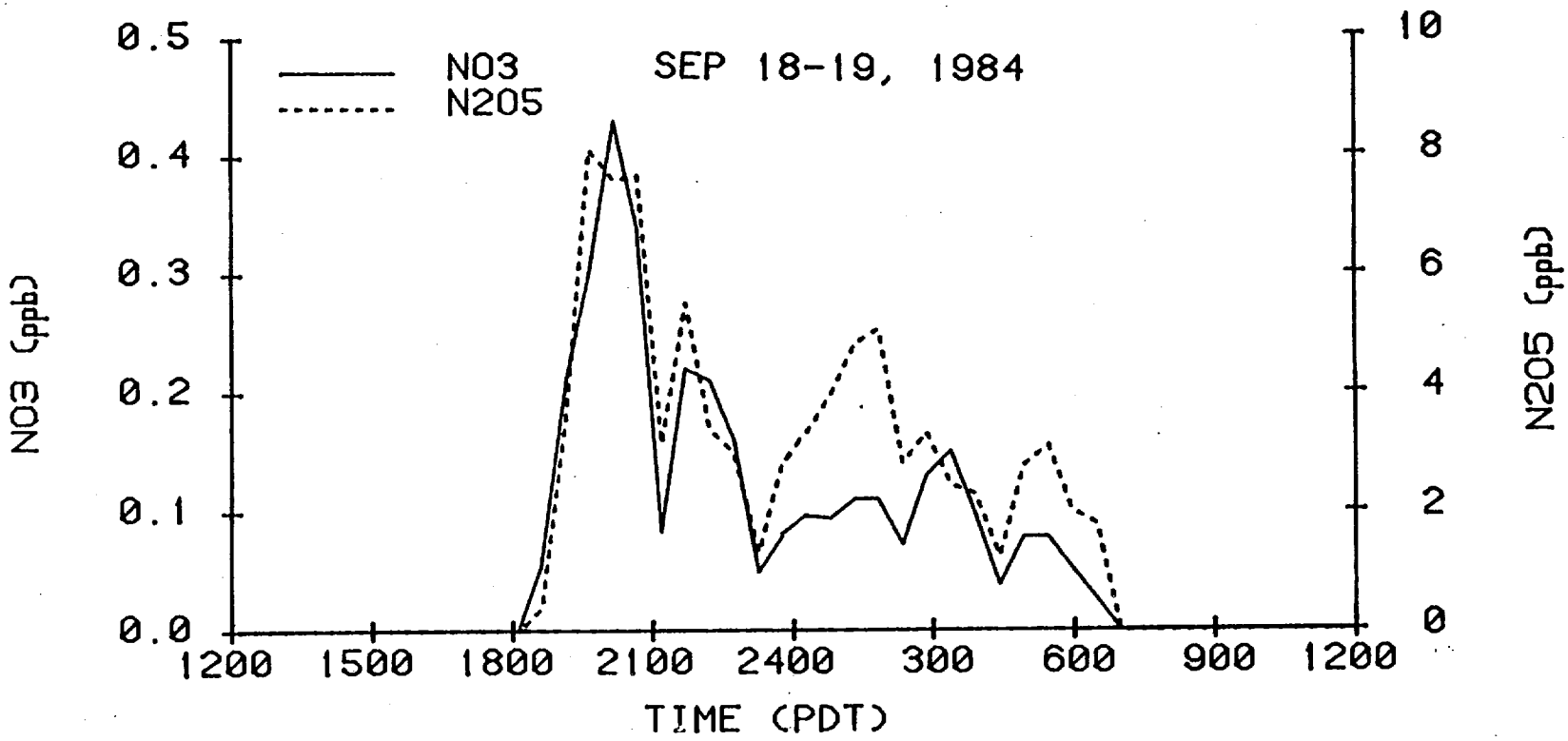

Figure III-7. Nitrate radical concentration (measured by DOAS) and dinitrogen pentoxide (N_2O_5) concentration (calculated) at U.C. Riverside for 1200 PDT September 18 to 1200 PDT September 19, 1984.

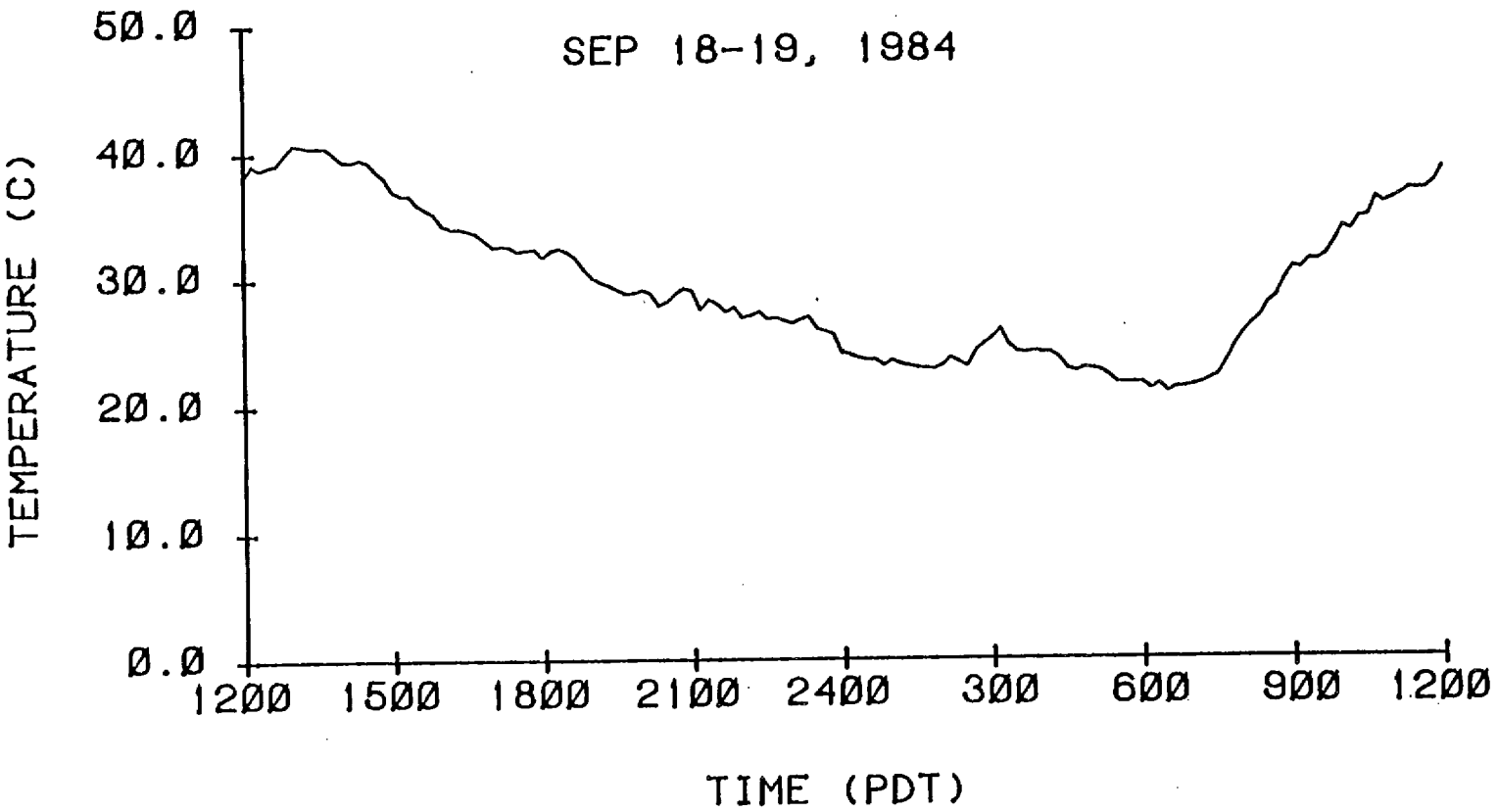

Figure III-8. Temperatures measured at U.C. Riverside for 1200 PDT September 18 to 1200 PDT September 19, 1984.

our study period. We have individually extracted and analyzed filters from this period utilizing HPLC and GC-MS with multiple ion detection (MID). Preliminary mutagen assays ("spot tests") of these extracts on TA98 (for both passive and active exposures), TA98NR and TA98/1,8-DNP_6 (only for active exposures) have also been done. In these preliminary tests $\lesssim$10% of the extract was utilized for testing with three or four doses on single plates.

Tables III-3 and III-4 show the recovery of FL, PY, BaP and PER from GF and TIGF filters after active and passive exposures to ambient air, respectively. For both types of exposure during all time periods, <1% conversion to NO_2-PAH occurred, based upon our detection limit. However, we cannot exclude the possibility that the pre-filters used to remove POM during the active exposures may also have removed HNO_3 and other reactive species such as N_2O_5. The presence of HNO_3 is essential in nitroarene formation, as a catalyst in the reaction with NO_2 or as the reagent species (Pitts et al. 1978a, Grosjean 1983). The absence of nitroarenes in the passive exposures seems to indicate that the four PAH we studied adsorbed on filter surfaces do not react to any detectable extent with ambient levels of nitrogenous species. However, the likelihood of the most volatile PAH, FL and PY, reacting in the gas phase has to be considered. Thus we have obtained preliminary laboratory data indicating that N_2O_5 may react with fluoranthene and pyrene in the gas phase (Pitts et al. 1984d). In an ambient exposure the products of a reaction in the gas phase would be unlikely to be readsorbed back onto the filters.

In the passive exposures the losses of FL and PY closely paralleled the temperaure profile, suggesting that these losses were due to volatilization. While laboratory data (Pitts and Lokensgard 1982) indicate that reaction with ozone could also have occurred, the small yield of products observed for FL suggests that volatilization was the major loss process for this PAH. For PY the filter extracts from the 1200-1800 hr time period contained oxygenated products, indicating reaction with ozone and thus making it difficult to evaluate the relative importance of volatilization losses.

The high volatility of FL and PY was consistent with the low recovery of these PAH during the active exposures. That the low observed

Table III-3. PAH Recovered (HPLC Analyses) from 1200 hr September 18 to 1200 hr September 19. Active Exposures on TIGF and GF Filters

PAH	μg PAH Recovered After Exposure[a]							
	1200–1800 hr		1800–2400 hr		0000–0600 hr		0600–1200 hr	
	TIGF	GF	TIGF	GF	TIGF	GF	TIGF	GF
Pyrene	~5	~20	~10	~30	~20	40	~7	~15
Fluoranthene	<3	~8	~9	~13	~12	120	~6	~8
Benzo(a)pyrene	260	270	560	470	760	880	540	640
Perylene	890	660	970	1400	b	1600	1000	1200

[a] ~1,000 μg was placed on each filter.
[b] No data available.

Table III-4. PAH Recovered (HPLC Analyses) from 1200 hr September 18 to 1200 hr September 19. Passive Exposures on TIGF and GF Filters

PAH	μg PAH Recovered After Exposure[a]							
	1200–1800 hr		1800–2400 hr		0000–0600 hr		0600–1200 hr	
	TIGF	GF	TIGF	GF	TIGF	GF	TIGF	GF
Pyrene	110	180	680	790	860	870	580	720
Fluoranthene	40	85	600	b	790	850	430	630
Benzo(a)pyrene	310	300	570	700	810	850	560	640
Perylene	780	820	640	650	770	680	790	960

[a] ~1,000 μg was spiked on each filter.
[b] No data available.

recoveries was due chiefly to "blow-off" from the filters was suggested by the fact that the recovery was consistently low while the concentrations of the reactive gas phase specifies, e.g., ozone, varied with time. In addition, few product peaks were evident in the HPLC traces.

The low recovery of BaP in both active and passive exposures for the 1200-1800 hr time period was probably the result of reaction with ozone

(Pitts et al. 1980, Wu et al. 1984). Indeed, the HPLC traces indicated that the filter extracts contained relatively large quantities of isomeric BaP-diones.

The results of preliminary Ames Salmonella assays ("spot tests") are shown in Table III-5 (active exposures) and in Table III-6 (passive exposures, strain TA98 only). The mutagenicities are presented as total revertants per filter.

For the active exposures (Table III-5) the highest mutagenic activity was found for BaP deposited on GF filters exposed during the 1200-1800 hr time period. Significant activity, with higher values on the GF than on the TIGF filters, was also observed for BaP exposed on filters in the

Table III-5. Mutagenic Activity for Active Exposures - Spot Test Results (Total Revertants per Filter)

	1200-1800 hr		1800-2400 hr		0000-0600 hr		0600-1200 hr	
PAH	TIGF	GF	TIGF	GF	TIGF	GF	TIGF	GF
TA98 Activity								
Pyrene	14,000	2,500	9,000	8,000	4,800	a	3,800	4,000
Fluoranthene	c	2,100	d	d	2,500	d	c	c
Benzo(a)pyrene	21,000	58,000	14,000	24,000	6,000	4,500	12,000	14,000
Perylene	23,000	18,000	15,000	6,000	a	1,500	a	9,000
TA98NR Activity								
Pyrene	9,000	d	6,000	5,000	3,000	1,600	2,000	1,800
Fluoranthene	c	1,600	d	d	c	d	d	d
Benzo(a)pyrene	16,000	33,000	12,000	16,000	7,000	4,000	11,000	10,000
Perylene	26,000	17,000	b	5,000	a	d	8,000	11,000
TA98/1,8-DNP_6 Activity								
Pyrene	c	d	c	c	d	d	d	d
Fluoranthene	d	d	d	d	d	d	d	d
Benzo(a)pyrene	5,000	7,000	3,000	4,000	c	c	1,600	3,000
Perylene	5,000	2,800	4,000	d	a	d	c	2,000

[a]No data available.
[b]Possible toxicity.
[c]Activity significant, but too low to be of quantitative use.
[d]Not significant (less than twice the spontaneous background revertants).

Table III-6. TA98 Activity for Passive Exposures - Spot Test Results (Total Revertants per Filter)

PAH	1200-1800 hr		1800-2400 hr		0000-0600 hr		0600-1200 hr	
	TIGF	GF	TIGF	GF	TIGF	GF	TIGF	GF
Pyrene	50,000	10,000	5,000	b	4,200	b	30,000	2,700
Fluoranthene	4,000	c	c	a	c	b	8,200	b
Benzo(a)pyrene	17,000	9,200	4,800	1,900	c	c	8,000	8,700
Perylene	15,000	c	4,000	b	2,100	b	6,700	b
Blanks	b	b	b	b	a	b	b	b

[a]No data available.
[b]Not significant (less than twice the spontaneous background revertants).
[c]Activity significant, but too low to be of quantitative use.

1800-2400 hr and 0600-1200 hr time periods. While PER and PY also showed significant mutagenic activity, the activity was generally higher on the TIGF than on the GF filters. It is interesting to note that strains TA98NR and TA98/1,8-DNP_6 often showed reduced activity, despite the absence of mononitro-PAH products on the filters.

For the passive exposures the highest mutagenic activity was observed for PY deposited on TIGF filters exposed during the 1200-1800 hr and 0600-1200 hr time periods when the ozone concentrations were high. Benzo(a)-pyrene and PER adsorbed on TIGF filters also showed significant activity in these time periods. Lower activity was seen for BaP, PY and PER adsorbed on GF filters during some of the 6-hr exposure periods.

The large differences in mutagenic activities on TA98 observed for extracts from TIGF and GF filters would seem to indicate a filter surface effect (or filter artifact) on the yields or recoveries of mutagenic products in both active and passive exposures. Extracts from TIGF filters coated with PY, PER and BaP always showed significantly higher activity than extracts from GF filters, with one exception - the active exposures of BaP. The ratio of the mutagenic activities for the two filter types (GF/TIGF) for the BaP active exposures seemed to follow the atmospheric level of ozone with the highest ratio (2.8) being observed for the 1200-1800 hr exposure and the lowest (0.7) for the 2400-0600 hr time period. This behavior for the mutagenicity ratio for BaP on the two types of

filters parallels that observed for collected ambient POM as discussed earlier in Section II.

Following the September 1984 field study, insufficient time was available to carry out extensive fractionation of the mutagenic extracts from the four PAH coated-filter exposures. However, HPLC fractionation (ultrasphere ODS semi-prep column) of the mutagenic extracts from PY-coated GF and TIGF filters, followed by mutagen assay of the fractions, showed that the mutagenic product(s) were contained in the polar fractions. Since we have shown in an earlier SAPRC/ARB program (Pitts et al. 1984e) that a large portion of the mutagenicity of extracts of ambient POM is contained in the polar fractions, and little is known about the identities of these polar mutagens, it would be of interest to identify the compound(s) responsible for the mutagenicity observed for the PY exposure extract.

D. Conclusions

- No NO_2-PAH were found during four 6-hr exposures of PAH coated on GF or TIGF filters in either active or passive exposures to ambient pollutants. Based upon our detection limit, this shows that less than 1% conversion of the parent PAH to NO_2-PAH occurred.

- From an examination of the PAH recoveries from both the active and passive exposures and the corresponding co-pollutant and meteorological data we conclude that: (a) In the active exposures the low recovery of the volatile PAH, PY and FL resulted mainly from blow-off of these PAH; (b) in the passive exposures, the low recovery of PY and FL for the 1200-1800 hr time period may have been the result of high temperature (volatilization) and/or reaction with ozone; and (c) in both the active and passive exposures the low recovery of BaP for the 1200-1800 hr time period was probably the result of reaction with ozone.

- The product (or products) formed from PY and BaP during the period of high O_3 concentration (1200-1800 hr) were highly mutagenic.

- The mutagenic activity of the extracts from PY-coated TIGF and GF filters exposed in the passive mode (1200-1800 hr) was shown to be in the polar fraction.

- There was an apparent filter surface effect (or filter artifact) on the mutagenic product yields or recoveries observed in both active and passive exposures.

IV. INVESTIGATION OF MUTAGENICITY AND NITROARENE LEVELS IN AMBIENT PARTICULATE

A. Introduction

It has been shown that collected respirable ambient POM exhibits strong, direct-acting mutagenicity in the Ames bacterial assay (Pitts et al. 1977, Talcott and Wei 1977, Tokiwa et al. 1977). The PAH themselves are not directly mutagenic, requiring microsomal activation, and it has been postulated that this observed direct mutagenicity of POM may be due, at least in part, to the presence of mono- and dinitroarenes (Jäger 1978, Ramdahl et al. 1982, Tokiwa et al. 1983). A major source of these nitroarenes in POM appears to be due to their direct emission in combustion generated fine particles such as auto and diesel exhaust particulate (Pitts et al. 1982a, Schuetzle et al. 1982, Xu et al. 1981,1982) and soot from wood-burning fireplaces (Gibson 1982, 1983). These nitroarenes are of special interest because of their worldwide distribution in polluted atmospheres (see the reviews by Nielsen et al. 1983 and Pitts 1983), and because their presence in ambient POM may pose health risks (Rosenkranz and Mermelstein 1983, Rosenkranz 1984 and references therein).

To date, however, there are only a few reports in the literature on the detection and quantification of NO_2-PAH and di-NO_2-PAH in ambient POM (Ramdahl et al. 1982, Gibson 1982, 1983, Nielsen 1983, Tokiwa et al. 1983). The NO_2-PAH most frequently identified in ambient POM have been 3-nitrofluoranthene and 1-nitropyrene, the latter being the most abundant NO_2-PAH in diesel POM (Salmeen et al. 1984). Although dinitropyrenes have been found only in very low levels (Gibson 1982, 1983, Tokiwa et al. 1983), their presence in ambient POM is important due to their extremely high mutagenic activities. Recently, 2-nitropyrene has been identified in an ambient POM extract and an atmospheric mechanism for its formation proposed (Nielsen et al. 1984). Therefore we undertook to determine the concentration of the important mutagenic species, 1-nitropyrene (1-NO_2-PY), 3-nitrofluoranthene (3-NO_2-FL) and isomeric di-NO_2-PY, in southern California ambient POM and to investigate the presence of additional isomers such as 2-nitropyrene. In order to enhance the selectivity and sensitivity of detection, as well as the recovery of NO_2-PAH from POM, we

employed deuterated internal standards of the NO_2-PAH of interest, 1-NO_2-PY-d_9, 3-NO_2-FL-d_9 and a mixture of isomeric di-NO_2-PY-d_8.

Additionally, we investigated the problem of "filter artifacts" during our September 1984 field studies by employing four different filter types for POM collection. The dichloromethane and acetonitrile extracts of each filter were separately tested for mutagenic activity in an effort to make any "filter artifacts" more evident.

B. Experimental

1. Mega-Sampler Ambient POM Collection

Parallel to the PAH "active" and "passive" exposures described in Section III above, ambient POM was collected with the SAPRC-designed and constructed ultra-high volume "mega-sampler" (Fitz et al. 1983). In order to investigate filter artifacts, the four cartridges of the megasampler were loaded with four different filters, namely Teflon impregnated glass fiber filters (TIGF), Pallflex T60A20 and Pallflex TX40HI20WW (high efficiency), Gelman glass fiber filters (GF) and Pallflex QA02500 Quartz filters.

Both TIGF and GF filters were prewashed by Soxhlet extraction with CH_2Cl_2 and CH_3OH. The quartz filters were used as received, without prewashing. All filters were equilibrated (at 50% relative humidity and 21 C and weighed before and after use. Following sampling, they were immediately sealed in aluminum foil, sealed in plastic bags and stored at dry ice temperature in the field and at -10 C in the laboratory prior to weighing and extraction.

Ambient POM Extraction. The four 6-hr samples collected from 1200 September 18 to 1200 September 19, 1984 were analyzed. The extracts of POM were prepared by Soxhlet extraction of filters with CH_2Cl_2 for 17 hr followed by CH_3CN extraction for an additional 17 hr. Both extracts were reduced in volume, filtered through 0.5 μm Millex-SR cartridges and dried to a constant weight under a stream of N_2. Approximately 25% of each sample (by weight) was then subjected to the Ames test.

Mutagenicity Bioassay Procedures. The Ames assay (Ames et al. 1975) was carried out in our microbiological facility using our modified procedure developed with earlier CARB support (Belser et al. 1981, Pitts 1981). Ames Salmonella typhimurium strain TA98 (-S9) was used in these

assays. See Section II.C for details on the experimental procedures followed.

2. Synthesis of Nitroarene Standards

Commercially available 1-nitropyrene (Pfaltz and Bauer) was purified according to a method described by Paputa-Peck et al. (1983) utilizing modified Soxhlet extraction through neutral aluminum with iso-octane:toluene (2:1). 2-Nitropyrene was a gift from Dr. D. Schuetzle (Ford Motor Company). Fluoranthene was of commercial purity (Aldrich, 98%) and was used without purification. Pyrene-d_{10} (KOR Isotopes Inc.) and fluoranthene-d_{10} (MSD Isotopes Inc.) were of >99% isotopic purity. NO_2/N_2O_4 was of commercial purity (J. T. Baker Chemical Co.) and its solution in CH_2Cl_2 (Burdick & Jackson Laboratories) was prepared by differential weighing. N_2O_5 was prepared by the method of Schott and Davidson (1958).

The 3- and 8-nitrofluoranthene isomers were synthesized by nitration of fluoranthene with concentrated nitric acid in glacial acetic acid (Kloetzel et al. 1955).

2-Nitrofluoranthene was synthesized by nitration of fluoranthene with N_2O_5 in CCl_4 solution. Freshly prepared N_2O_5 (~0.05 mmol) in 5 mℓ of CCl_4 was added slowly to a stirred solution of FL (0.1 mmol) in 20 mℓ of CCl_4. The reaction was carried out at room temperature and in the dark in a dry box under an atmosphere of N_2. The only mononitroisomer formed was 2-nitrofluoranthene (yield ~50%) which was purified by open column chromatography (as described below) and crystallized from ethanol. The pure compound was identified on the basis of its mass spectrum and a comparison of its NMR spectrum with that reported in the literature (Paputa-Peck et al. 1983). A preliminary mutagen assay of 2-NO_2-FL on Salmonella strain TA98 (-S9) was carried out for three doses (single plates with 0.0 μg, 0.1 μg and 1 μg 2-NO_2-FL).

1-Nitropyrene-d_9(1-NO_2-PY-d_9) and nitrofluoranthene-d_9 (NO_2-FL-d_9) isomers were synthesized according to methods described by Pitts et al. (1982c) and Radner (1983). Pyrene-d_{10} (0.47 mmol) in 50 mℓ CH_2Cl_2 and N_2O_4 (0.25 mmol) in 1 mℓ CH_2Cl_2 were mixed and stirred at room temperature for 0.5 hr. CH_3SO_3H [0.02 mmol (~1.5 μℓ)] was added to the solution of fluoranthene-d_{10} (0.1 mmol) in CH_2Cl_2 prior to addition of 0.05 mmol of N_2O_4 in 1 mℓ of CH_2Cl_2. The mixture was allowed to react for 0.4 hr.

Both nitro-PAH were purified by open column chromatography. After reaction was complete, 0.5 g of silica gel 60 (Merck) was added to the solution and the solvent evaporated under vacuum. The yellowish powder was placed on the top of a column packed with silica gel (1 x 30 cm) and eluted with benzene:hexane (2:1) in the case of 1-nitropyrene-d_9 and with CCl_4:CH_2Cl_2 (9:1) in case of the nitrofluoranthene-d_9 isomers. After evaporation of the solvent, the nitro-PAH's were recrystallized from ethanol-benzene with yields of ~70% for 1-NO_2-PY-d_9 and ~90% for NO_2-FL-d_9.

Isomeric di-nitropyrenes-d_8 (di-NO_2-PY-d_8) were synthesized according to the method described by Vollmann et al. (1937). A 0.75 mℓ aliquot of concentrated HNO_3 (70%) was added to a solution of 100 mg (0.47 mmol) of pyrene-d_{10} in 1 mℓ of glacial acetic acid at 90 C with stirring. The temperature was raised to 100 C and stirring continued for an additional 0.5 hr. The reaction mixture was allowed to cool, the precipitate was filtered and washed extensively with ethanol. The yield was ~140 mg.

GC-MS Analyses. The purified reaction products were analyzed by GC/MS (Finnigan Model 3200) using DB-5 fused silica capillary columns (20 or 60 m x 0.25 mm). The only product of pyrene-d_{10} nitration by N_2O_4 was 1-NO_2-PY-d_9 (>99% isotopic purity). The nitrofluoranthene-d_9 isomers contained 3-NO_2-FL-d_9 and 8-NO_2-FL-d_9 in the ratio ~4:1. The di-NO_2-PY-d_8 contained a mixture of 1,3- 1,6- and 1,8-dinitropyrenes (identified on the basis of their retention indices) together with small amounts of 1-NO_2-PY-d_9 (8.5%, as determined by HPLC, using triphenylbenzene as internal standard).

The mass spectra of the deuterated and non-deuterated nitro-PAH standards are given in Appendix IX.D. The chromatographic resolution of the nitrofluoranthene and nitropyrene isomers on the 60-m DB-5 capillary column used in these nitroarene determinations is shown in Figure IV-1.

3. Experimental Procedure for Determination of Selected Nitroarene Concentrations in Ambient POM

Extract Fractionation. Recently we successfully tested and employed a new procedure for separation of the nitroarene fraction from ambient POM. The first step of this procedure (outlined in Figure IV-2) is a modification of that published by Spitzer and Dannecker (1984) utilizing XAD-2 resins for PAH separation. The second step is a semi-preparative HPLC separation as described by Schuetzle et al. (1981).

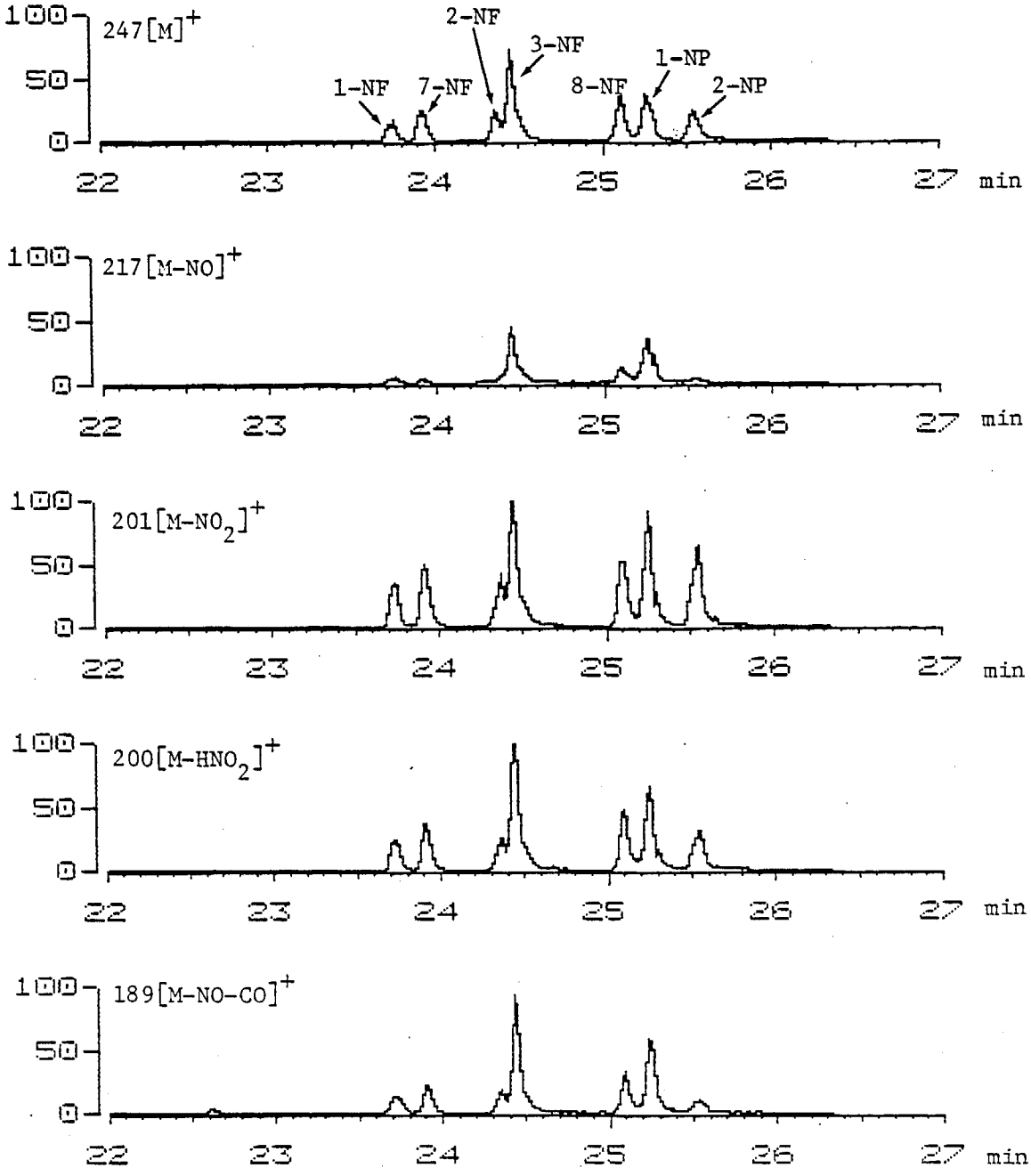

Figure IV-1. MID traces showing resolution of nitrofluoranthene and nitropyrene isomers on 60-m DB-5 capillary column. The isomers in order of elution are: 1-nitrofluoranthene (1-NF), 7-nitrofluoranthene (7-NF), 2-nitrofluoranthene (2-NF), 3-nitrofluoranthene (3-NF), 8-nitrofluoranthene (8-NF), 1-nitropyrene (1-NP) and 2-nitropyrene (2-NP). All ions shown to same scale. Column conditions: 50 to 200 C at 20 C min^{-1}, then increased at 6 C min^{-1}.

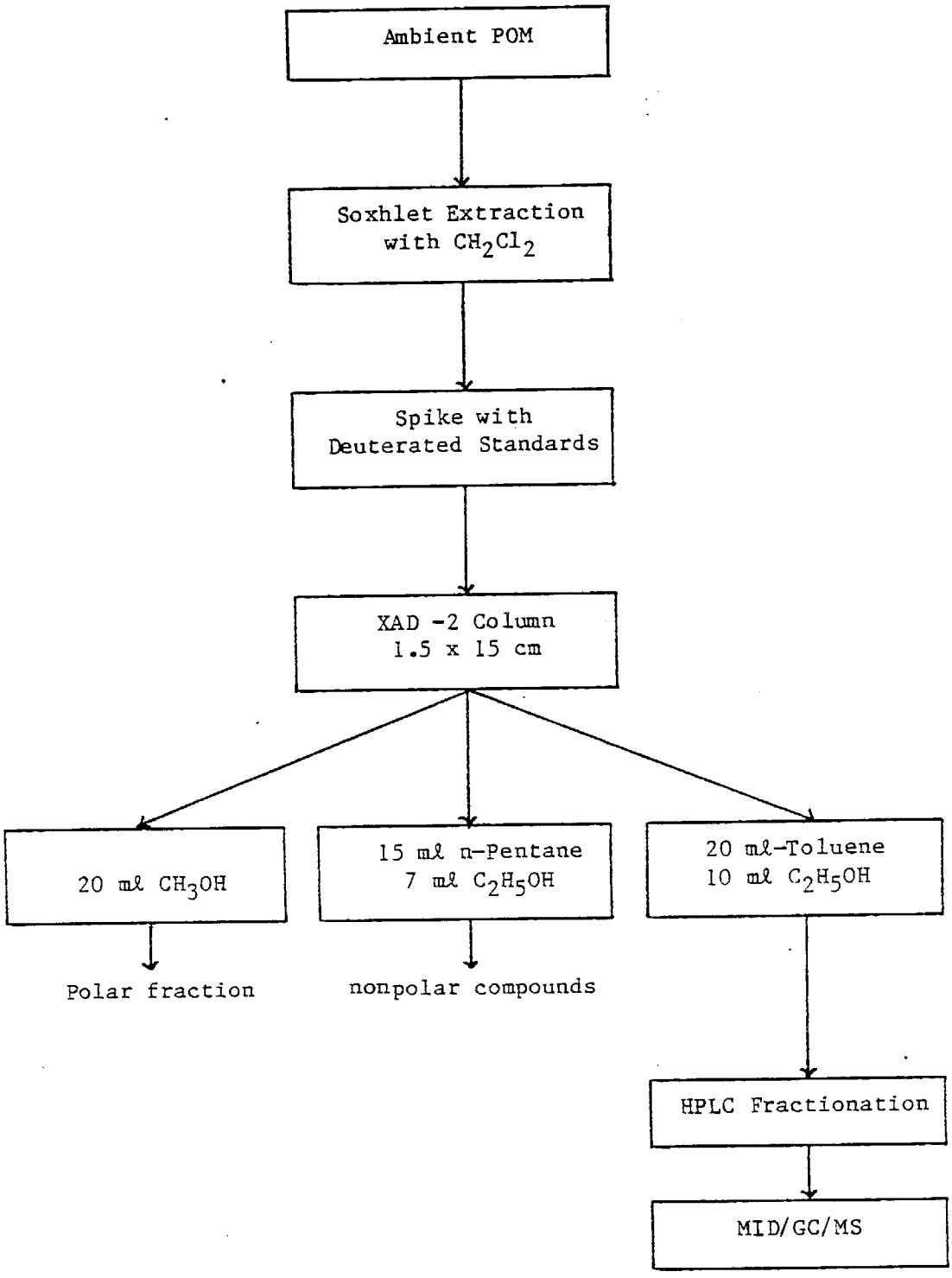

Figure IV-2. Outline of chemical analysis for nitro-PAH.

The four 6-hr POM collections from 1200 hr September 18, 1984 to 1200 hr September 19, 1984 were analyzed for nitroarenes. The CH_2Cl_2 extracts from POM simultaneously collected on TIGF and quartz filters utilizing the SAPRC "megasampler" were combined and redissolved in methanol. Deuterated NO_2-PAH standards (10 μg 1-NO_2-PY-d_9, 8.5 μg of a mixture of 3- and 8-NO_2-FL-d_9 and 20 μg of isomeric di-NO_2-PY-d_8) were added. The XAD-2 resins (Sigma), precleaned by sequential Soxhlet extraction with CH_3OH (8 hr) and CH_3CN (8 hr) (Junk et al. 1974) were packed into a column (1.5 x 15 cm) and equilibrated with 20 mℓ of CH_3OH. The sample was transferred to the top of the column and a polar fraction was eluted with 20 mℓ of CH_3OH. Nonpolar material was then eluted with 15 mℓ of n-pentane followed by 7 mℓ of ethanol. The fraction which contained the NO_2-PAH (and most of the PAH) was eluted with 20 mℓ of toluene followed by 10 mℓ of ethanol. The fractions were then concentrated in volume using a rotary evaporator, transferred to tared vials and dried under N_2 to a constant weight. Typically, 90% of the sample was eluted in two first fractions and ~10% in the last toluene fraction.

The toluene fraction was redissolved in small amounts of CH_2Cl_2 and further fractionated by HPLC, using a semi-prep (10 mm x 25 cm) ultrasphere Si column (Altex). The HPLC system was composed of a Spectra-Physics Model 8100 chromatograph, Model 4100 computing integrator, Model 8400 variable wavelength UV/VIS detector and ISCO fraction collector. The mobile phase program used during these elutions is shown in Figure IV-3 together with a typical chromatogram obtained by monitoring at a detection wavelength of 254 nm. Starting from 18 min elution time, four 2.0-min fractions were collected at a flow rate of 3 mℓ min^{-1}. As established by chromatography of standard mixtures the mono- and di-nitro-PAH of interest were eluted in these fractions. These fractions were subjected to GC/MS analysis as described below.

The method described above is fast, convenient and cost-effective. XAD-2 resins are not expensive and can be used, after regeneration, several times. The amounts of solvent used for the separation is low and the recovery of deuterated mono- and di-NO_2-PAH is good.

MID/GC-MS. The HPLC fractions were analyzed for mononitro-FL and PY isomers and di-NO_2-PY isomers. For the nondeuterated NO_2-FL and NO_2-PY isomers, the ions monitored were molecular ions as well as characteristic

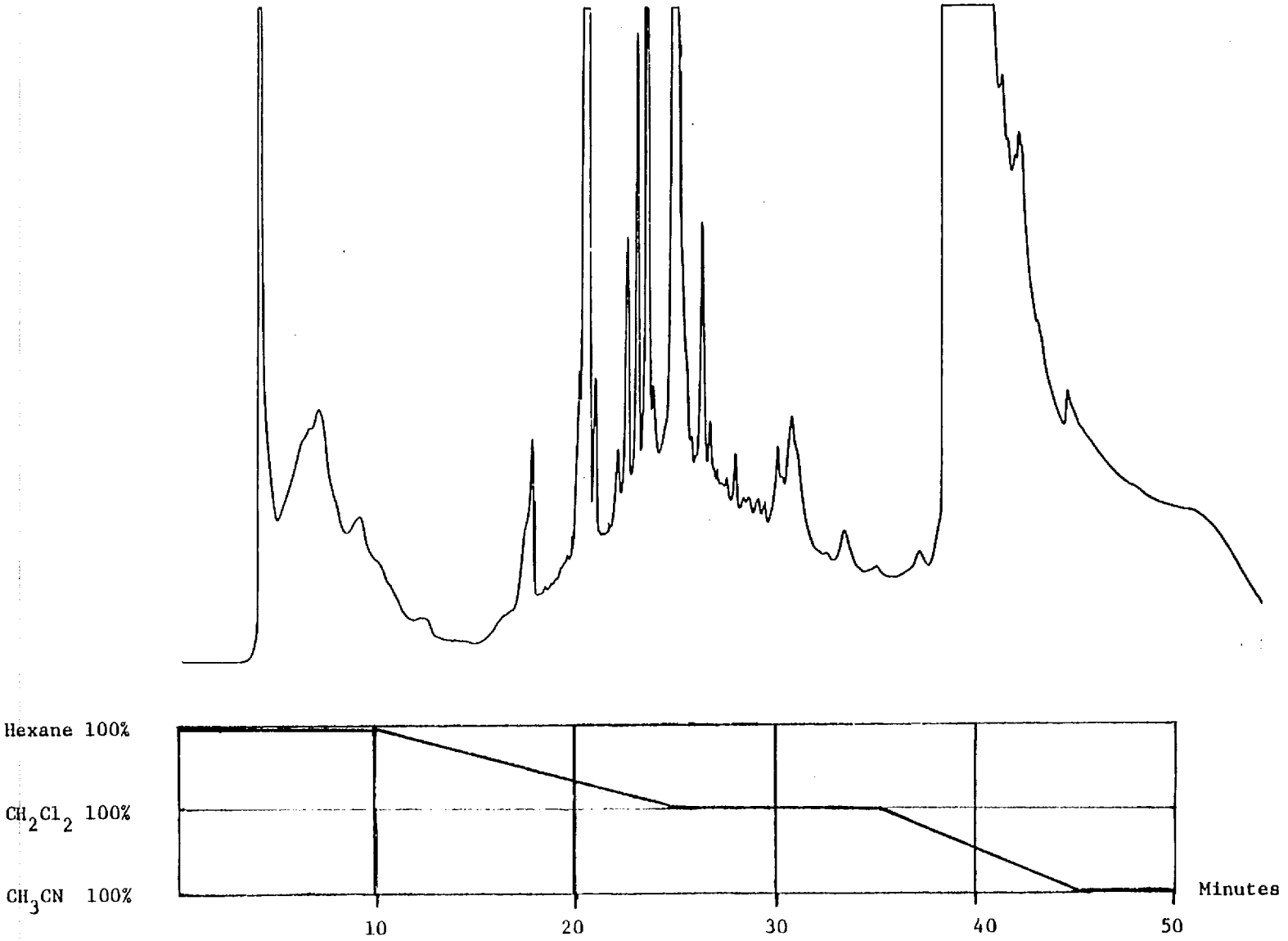

Figure IV-3. HPLC trace (254 nm) and gradient program for separation of ambient sample.

fragment ions, as follows: m/e 247($[M]^+$); 217($[M-NO]^+$); 201($[M-NO_2]^+$); 200($[M-HNO_2]^+$). For the deuterated species, the corresponding ions were 9 or, for ($[M-DNO_2]^+$), 8 amu higher. In addition, chrysene was added as an internal standard and its molecular ion at m/e 228 was also monitored. The ratios of the areas of the molecular ion peaks of the nitro-PAH to that of the internal standard were used to quantify the NO_2-PAH in the ambient extracts by comparison with a standard mixture. That is, the ratios $[256]^+/[228]^+$ were utilized to determine the recovery of 1-NO_2-PY-d_9 after the XAD-2 and HPLC fractionation steps, and the ratios $[247]^+/[228]^+$ were employed to quantify the NO_2-FL and NO_2-PY isomers.

Figure IV-4 shows the MID traces of the deuterated standard and illustrates that the deuterated standard was isotopically pure and there were no interfering peaks for the nondeuterated molecular ion used in quantification (m/e 247) or the m/e 217($[M-NO]^+$) characteristic fragment ion. The $[M-NO]^+$ fragment ion proved important in isomer identification. In particular, as evidenced from its mass spectrum (Appendix IX.D) and the MID traces shown in Figure IV-1, the 2-nitrofluoranthene isomer has a very low (<2%) $[M-NO]^+$ abundance.

Figure IV-5 shows the MID traces of the standard solution utilized for quantification. It contained 3-NO_2-FL and 3-NO_2-FL-d_9, 8-NO_2-FL-d_9, 1-NO_2-PY and 1-NO_2-PY-d_9, and 2-NO_2-PY (note that the deuterated species elute slightly before the corresponding non-deuterated isomers).

For the dinitropyrenes the ions monitored were: m/e 292($[M]^+$); 200($[M-2NO_2]^+$) and the corresponding ions for the deuterated species: m/e 300 and m/e 208, as well as m/e 228 for the internal standard (chrysene). Since the di-NO_2-PY abundance was expected to be low, the integration time used for m/e 292 and 200 ions was 10 times that of the other ions monitored. Figure IV-6 shows the MID traces of the deuterated standard. Again there was no interference with the molecular ion of the nondeuterated species and this ion was used for quantification.

C. Results

1. Mutagenicity of Ambient POM Extracts

As described above, the filters from the "mega-sampler" POM collections were extracted individually with CH_2Cl_2 and CH_3CN and both extracts were analyzed separately for direct mutagenic activity (TA98).

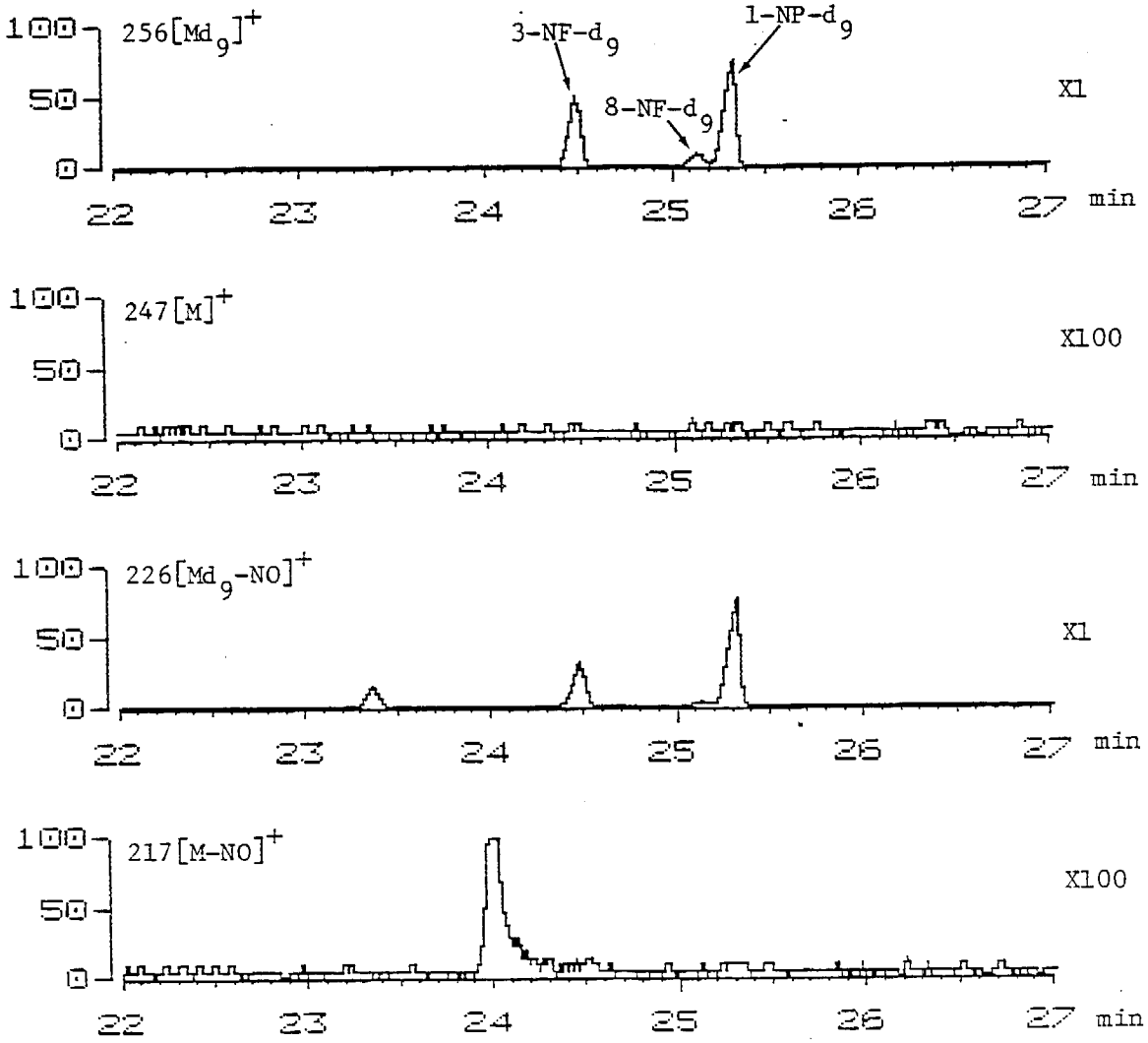

Figure IV-4. MID traces of deuterated mononitro-PAH used to spike ambient samples prior to the separation procedure. Samples were spiked with 8.5 μg 3- and 8-nitrofluoranthene-d_9 and 10 μg 1-nitropyrene-d_9. Note the lack of interfering ion peaks at 247($[M]^+$) and 217($[M-NO]^+$) [the scale to which these ions are plotted is 100X more sensitive than for the deuterated ions]. GC conditions: 60-m DB-5 column, 50 to 200 C at 20 C min^{-1}, then increased at 6 C min^{-1}.

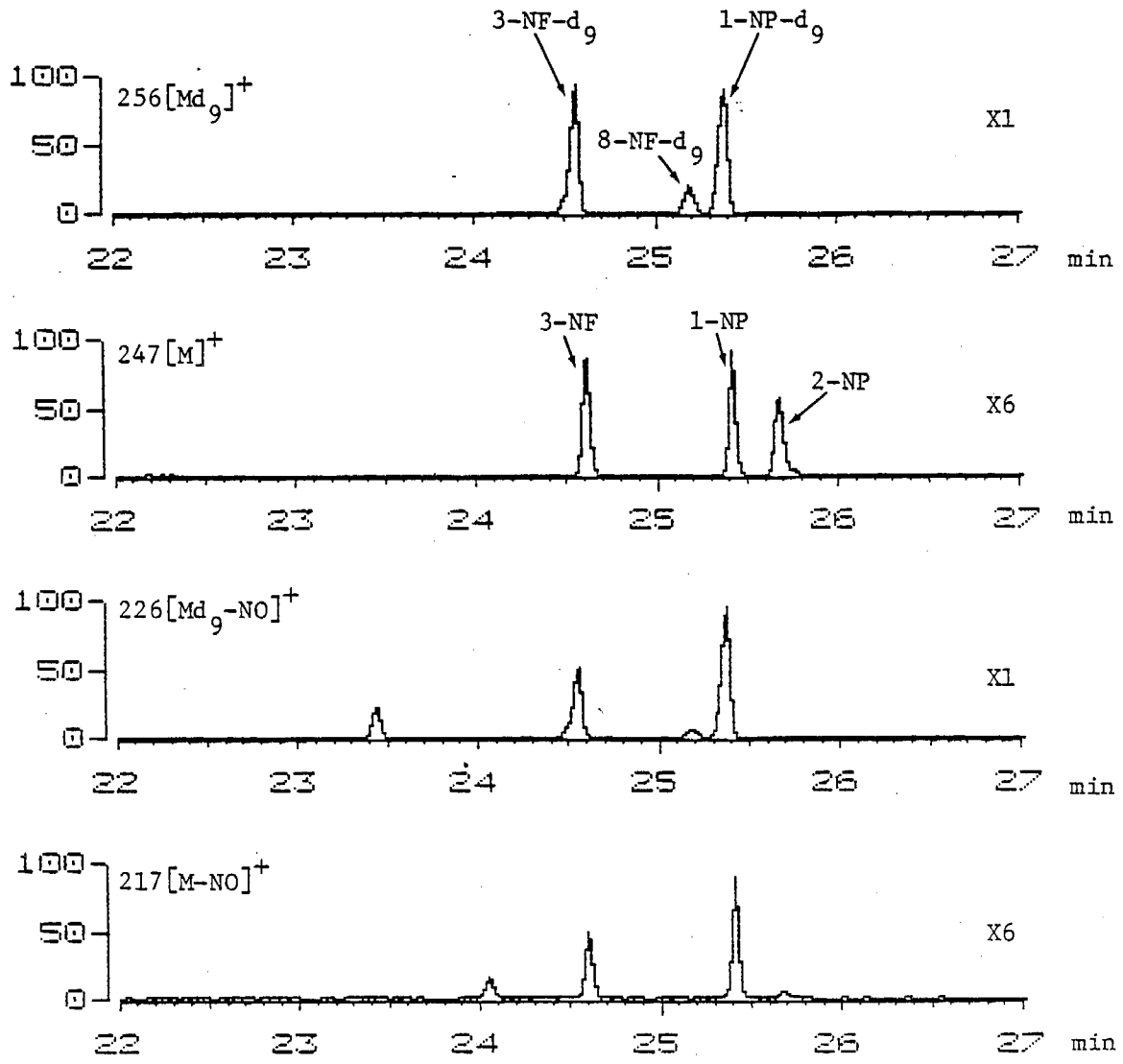

Figure IV-5. Nitro-PAH standard used for quantification. Standard contained 3-nitrofluoranthene, 3-nitrofluoranthene-d_9, 8-nitrofluoranthene-d_9, 1-nitropyrene, 1-nitropyrene-d_9 and 2-nitropyrene. Note that the retention times of the deuterated species is slightly lower than the corresponding non-deuterated isomer. GC conditions as given in Figure IV-4.

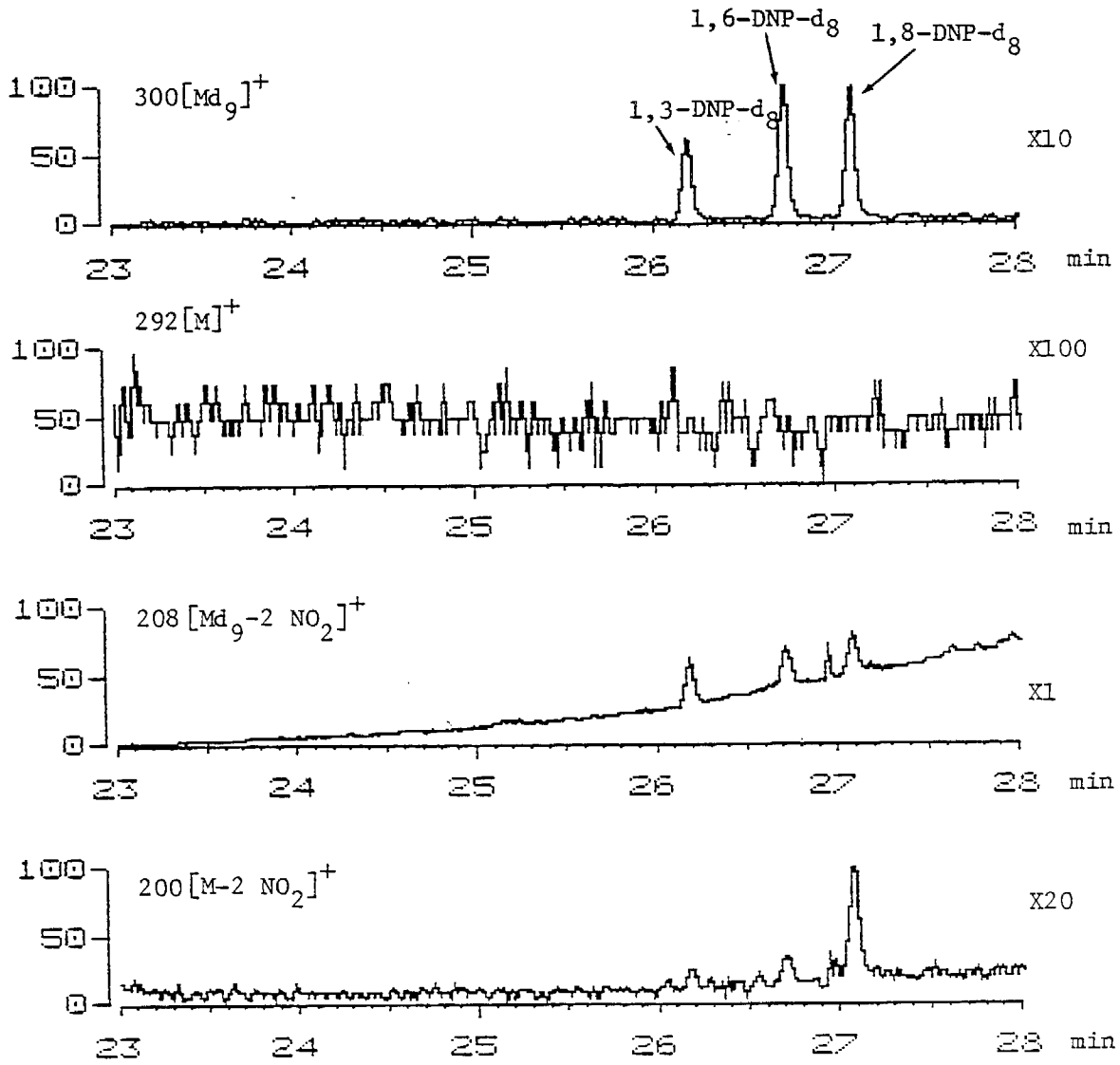

Figure IV-6. MID traces of deuterated dinitropyrene isomers. The isomers in order of elution are: 1,3-dinitropyrene-d_8, 1,6-dinitropyrene-d_8; 1,8-dinitropyrene-d_8. Samples were spiked with 20 µg of this mixture. GC conditions: 60-m DB-5 column, 50 to 200 C at 20 C min^{-1} then increased at 8 C min^{-1}. Ions m/e 292 and m/e 200 integrated 10X other ions.

Table IV-1. Mutagen Density [rev m^{-3}, Strain TA98 (-S9)] of CH_2Cl_2 and CH_3CN Extracts from Ambient POM Collected on Different Filter Substrates from 1200 hr September 18 to 1200 hr September 19, 1984 and Particulate and Extract Weights (mg)

Filter Type and Extract		Collection Time: 1200-1800 hr			1800-2400 hr			2400-0600 hr			0600-1200 hr		
			Weight (mg)			Weight (mg)			Weight (mg)			Weight (mg)	
		TA98 rev m^{-3}	Extract	Particulate	TA98 rev m^{-3}	Extract	Particulate	TA98 rev m^{-3}	Extract	Particulate	TA98 rev m^{-3}	Extract	Particulate
TIGF T60A20	CH_2Cl_2	4.7	26	204	9.7	21	110	9.5	20	124	18.8	20	146
	CH_3CN	18.7	48		12.9	18		15.5	38		20.7	25	
TIGF TX40	CH_2Cl_2	5.6	22	190	12.9	18	104	12.6	16	116	23.0	18	132
	CH_3CN	13.4	45		9.7	21		16.7	41		17.8	27	
Quartz	CH_2Cl_2	6.7	27	196	12.6	24	100	16.0	24	121	20.0	22	136
	CH_3CN	10.7	45		4.8	16		6.5	37		11.8	25	
GF	CH_2Cl_2	4.0[b]	17	246	7.0	13	122	5.3	13	124	9.0	13	177
	CH_3CN	16.1	82		4.0[b]	28		4.9[b]	38		6.9	53	

[a]Standard mutagen activities: 2-nitrofluorene = 250 rev μg^{-1}; quercetin = 8.2 rev μg^{-1}.
[b]Values from spot test.

Approximately 25 to 50% of each sample was submitted for Ames testing on Salmonella strain TA98 (-S9). Table IV-1 shows the weights of particulate collected on the different filter substrates from 1200 hr September 18 to 1200 hr September 19 and the weights of their CH_2Cl_2 and CH_3CN extracts, as well as the mutagen density of these extracts.

The activities of the standard mutagens tested with these samples (given in Table IV-1) were somewhat lower than for previous tests (see, for example, Table II-7), and the mutagen density (rev m^{-3}) of the ambient POM extracts were at the lower end of the range normally found in Riverside during smog episodes. The lowest mutagenic activities for the CH_2Cl_2 extracts of the four filter types examined were observed for the 1200-1800 hr POM collection. The GF filters had the lowest CH_2Cl_2 extract mutagenicities for all time periods. It can be seen from the data in Table IV-1 that the mutagen densities calculated from the activities of the CH_3CN extracts of POM collected on GF filters were always lower than for POM collected on TIGF filters, with the exception of the GF filter collection during the period of high ozone (1200-1800 hr). In this time period the CH_3CN extract from the GF filter showed higher or comparable activity with the other filters. This finding is consistent with the GF filter "artifact" observed in our September 1983 field study (see Section II.D).

The CH_2Cl_2 extract weights were the lowest and the CH_3CN the highest for the GF filters in all time periods except 2400-0600 hr. In this time period the values were similar for all filters. The extract weights and mutagenic activities of the TIGF filters were in good agreement with the quartz filter for the CH_2Cl_2 extracts. For the CH_3CN extracts the quartz filters had somewhat lower mutagenic activity than the TIGF filters.

2. Nitroarene Identification and Quantification

Since the mutagenic activites of CH_2Cl_2 extracts of T60A20, TX40HI20WW and Quartz filters (Table IV-1) were similar, we combined these extracts for a given time period and analyzed them for the presence and concentration of NO_2-FL and mono- and di-NO_2-PY. After the addition of standard deuterated NO_2-PAH, the combined extracts were prefractionated on an XAD-2 column and then further fractionated by semi-preparative HPLC, as described above. The fractions containing the mono- and di-NO_2-PAH of interest were analyzed by MID/GC-MS. Figures IV-7 to IV-11 show the MID traces of the HPLC fractions containing the NO_2-FL and NO_2-PY isomers.

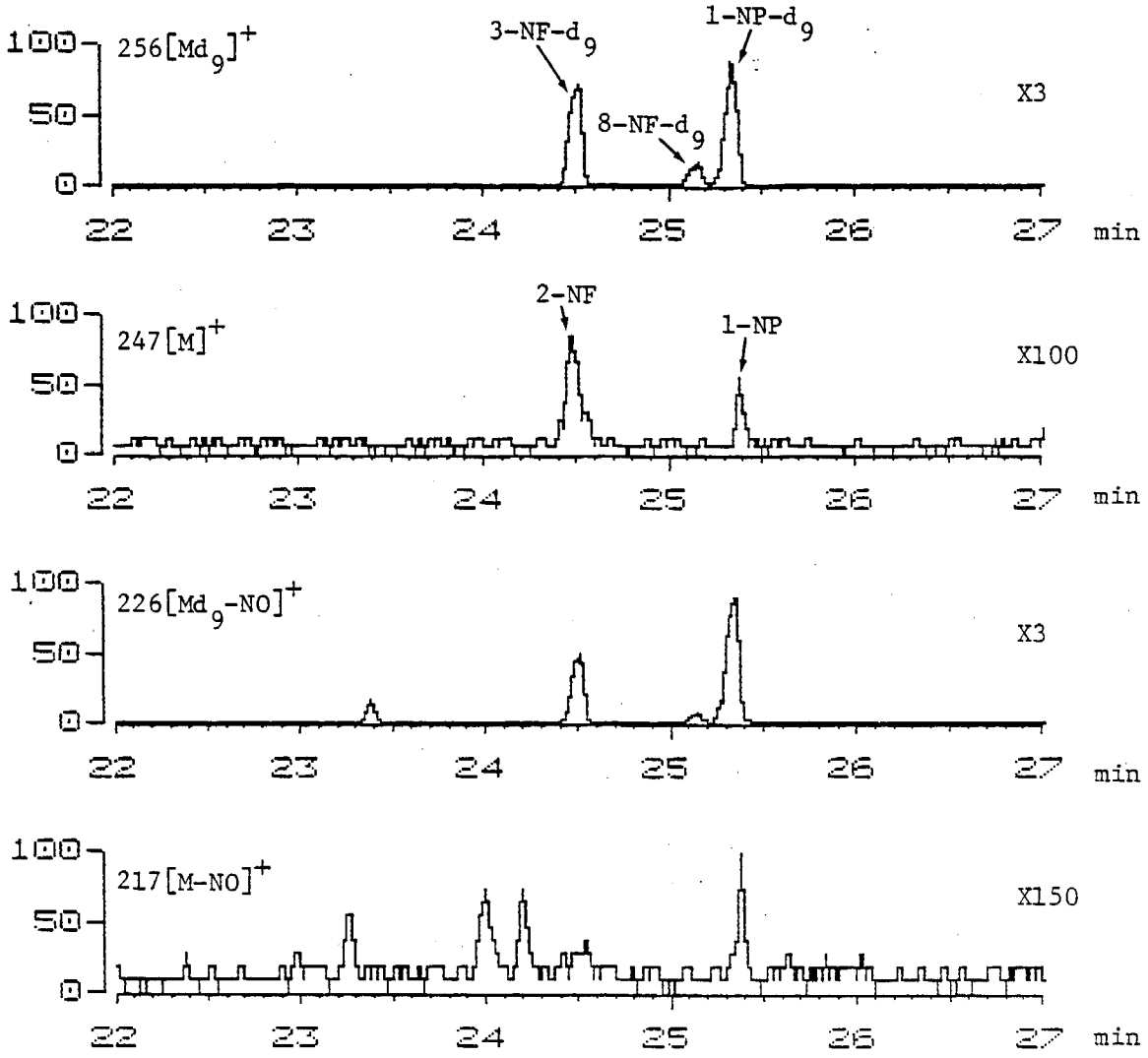

Figure IV-7. MID traces of CH_2Cl_2 extract from ambient, POM 1200-1800 hr September 18, 1984 collection period. HPLC fraction containing mononitro-isomers is shown. GC conditions as given in Figure IV-4.

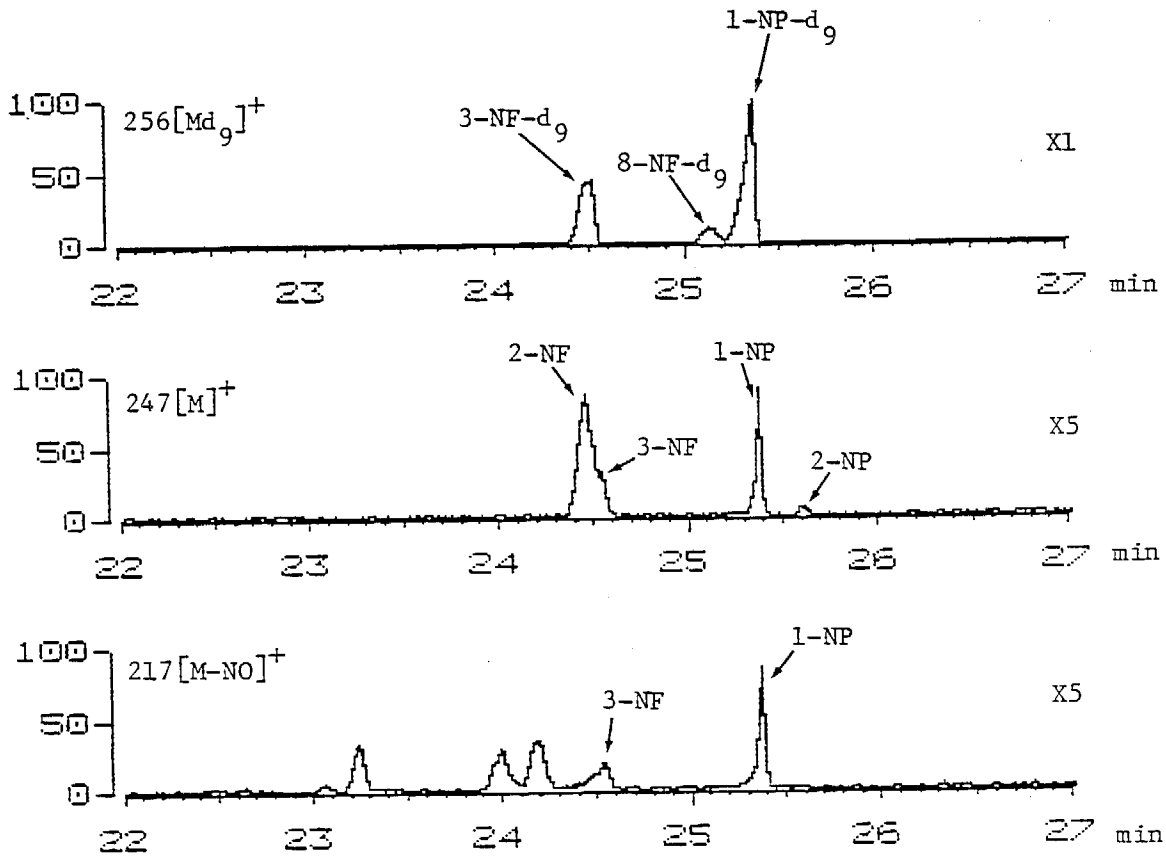

Figure IV-8. MID traces of POM extract shown in Figure IV-7. Ten times longer integration times were used for m/e 247 and 217 than for m/e 256.

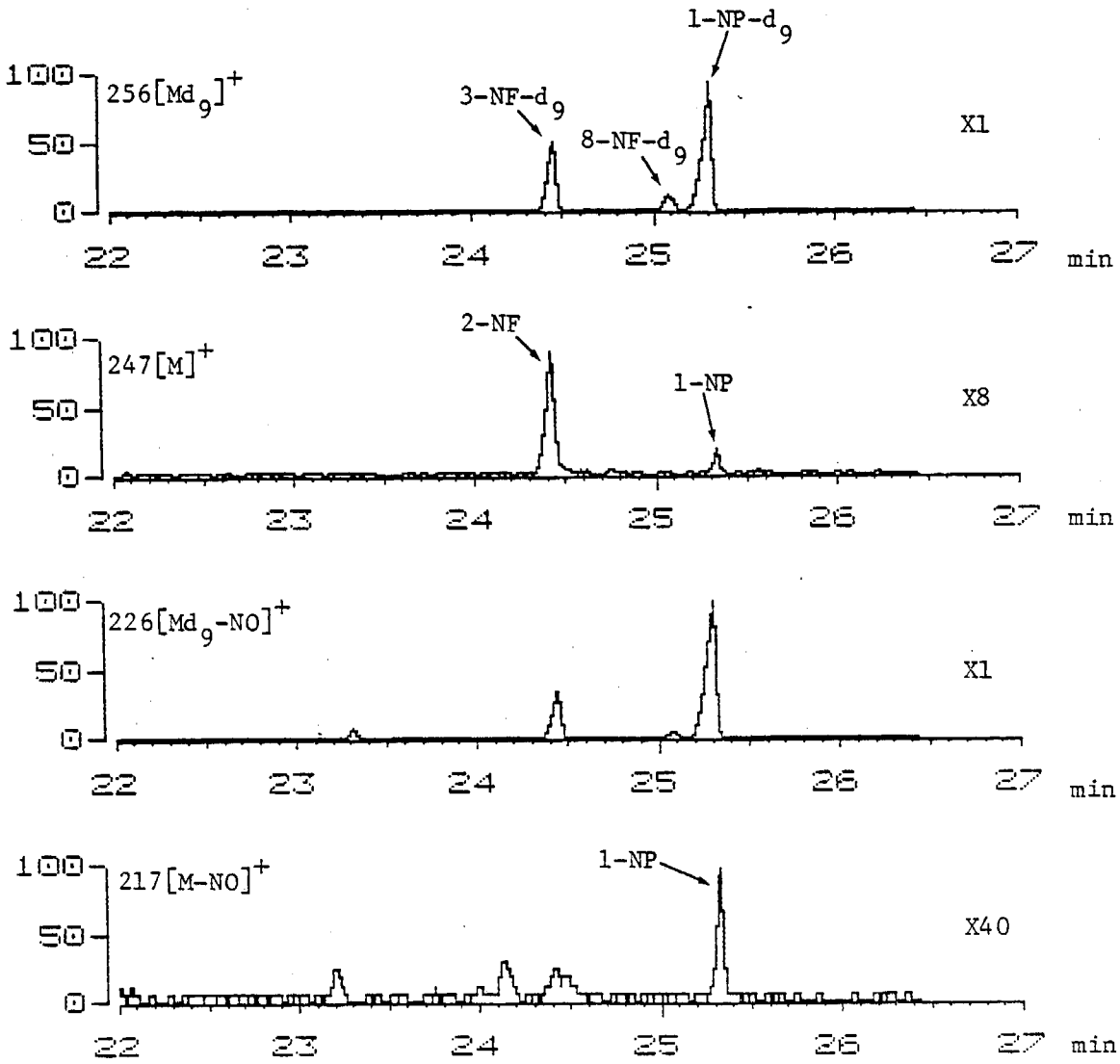

Figure IV-9. MID traces of CH_2Cl_2 extract from ambient POM, 1800-2400 hr September 18, 1984 collection period. HPLC fraction containing mononitro-isomers is shown. GC conditions as given in Figure IV-4.

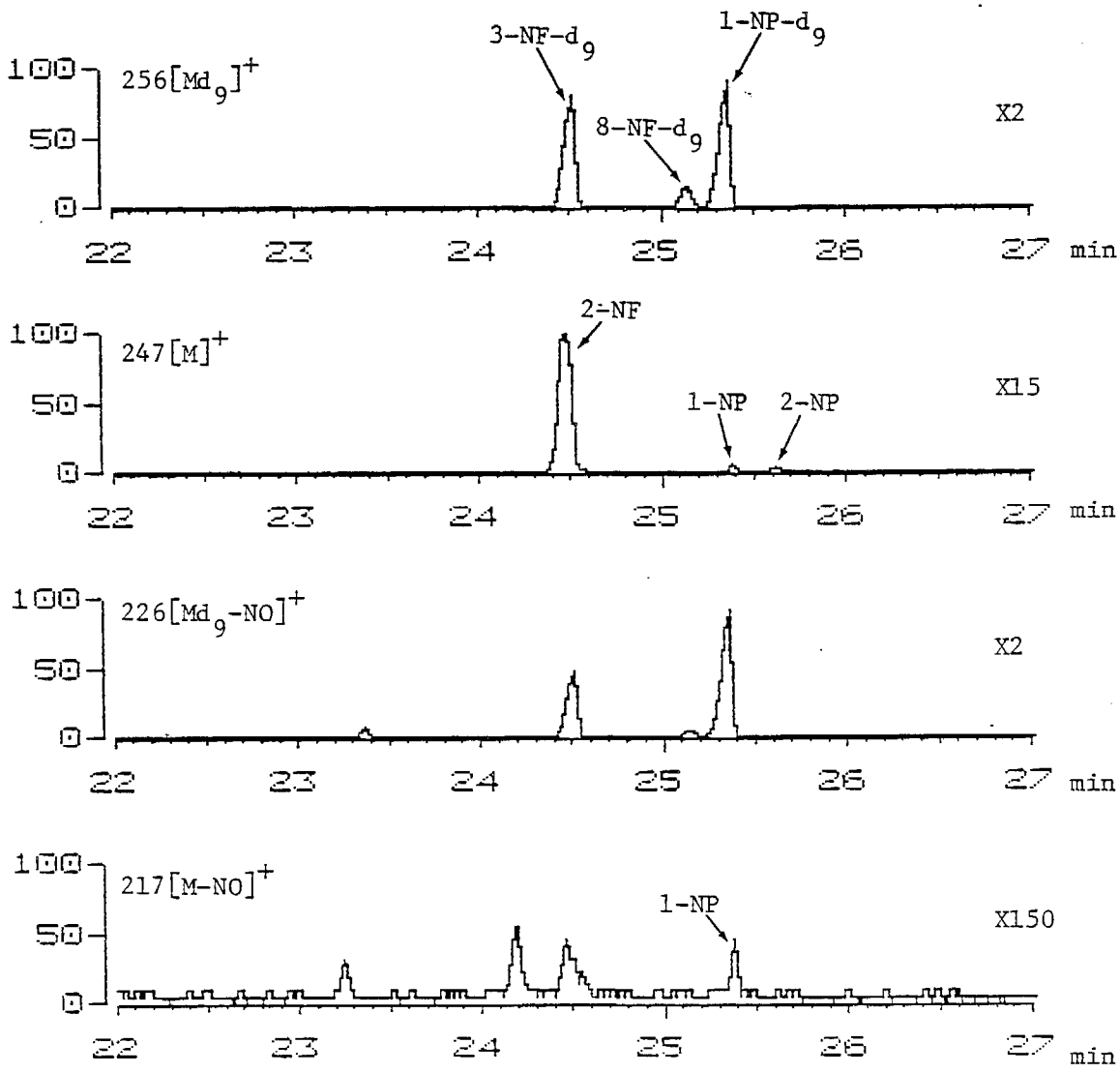

Figure IV-10. MID traces of CH_2Cl_2 extract from ambient POM, 0000-0600 hr September 19, 1984 collection period. HPLC fraction containing mononitro-isomers is shown. GC conditions as given in Figure IV-4.

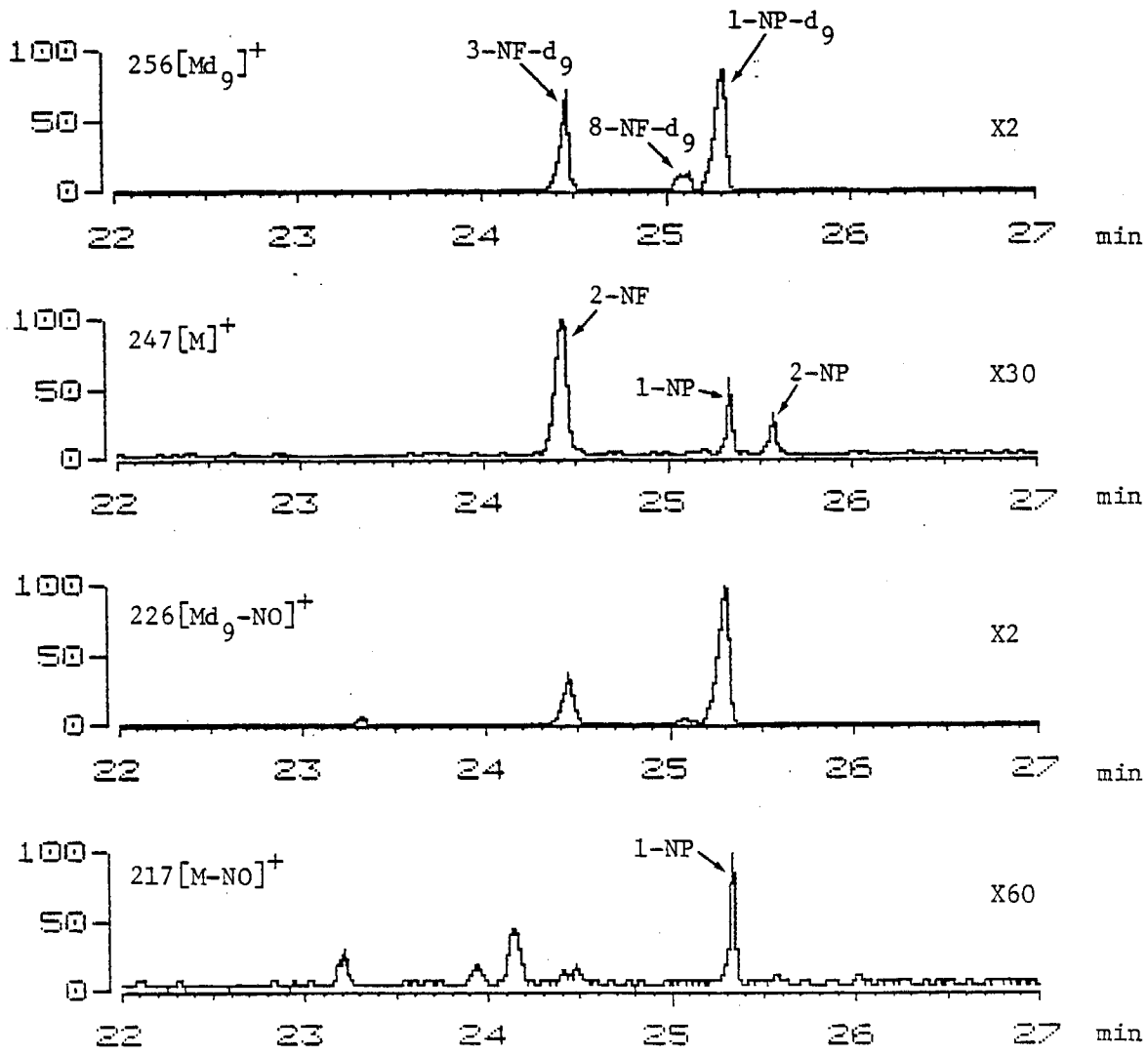

Figure IV-11. MID traces of CH_2Cl_2 extract from ambient POM, 0600-1200 hr September 19, 1984 collection period. HPLC fraction containing mononitro-isomers is shown. GC conditions as given in Figure IV-4.

The molecular ions and the characteristic $[M-NO]^+$ fragment ions for the deuterated and non-deuterated species are shown. It is evident from Figure IV-7 that the POM extract for the 1200-1800 hr sampling period contained 1-NO_2-PY and a nitrofluoranthene isomer. We have identified this isomer as 2-NO_2-FL (note that it elutes just before the 3-NO_2-FL-d_9 peak) on the basis of its retention time and the low abundance of the m/e 217($[M-NO]^+$) ion peak. This result was unexpected since all previous reports of nitrofluoranthene in ambient POM extracts have identified the isomer present as 3-NO_2-FL (Jäger 1978, Ramdahl et al. 1982, Nielsen 1983). Since it appeared that traces of 3-NO_2-FL might also be present in this sample, it was reanalyzed using an integration ratio of 1:10:10 for m/e 256, 247, and 217, respectively. As can be seen in Figure IV-8, traces of 3-NO_2-FL are probably present along with a small amount of 2-NO_2-PY.

The MID traces shown in Figure IV-9 indicate that 2-NO_2-FL and 1-NO_2-PY were present in the 1800-2400 hr ambient POM extract. From the MID traces in Figure IV-10, it is clear that the main nitro-isomer in the 0000-0600 hr ambient POM extract is 2-NO_2-FL with small and nearly equal amounts of 1- and 2-NO_2-PY also present. MID traces for the extracts of the final POM collection period analyzed, 0600-1200 hr, are given in Figure IV-11. 2-Nitrofluoranthene, and 1- and 2-NO_2-PY can be seen to be present.

Table IV-2 gives the quantities (ng m^{-3}) of the nitro-PAH observed in the four POM collections along with the recovery for the deuterated carrier, 1-NO_2-PY-d_9. The possible sources of the 1-NO_2-PY detected in POM are direct emission and atmospheric transformation, for example, the reaction with gaseous N_2O_5 (see Section V below). The highest concentration of 1-NO_2-PY was observed in POM collected in the 1800-2400 hr time period, during which N_2O_5 peaked (Figure III-7) and in the 0600-1200 hr time period, when a morning traffic peak occurred.

Dinitropyrenes were detected only in ambient POM collected during the 0600-1200 hr time period suggesting that direct emissions from traffic may be responsible for the relatively high concentrations of these isomers. The three di-NO_2-PY isomers were split between two HPLC fractions. The MID traces showing the molecular ions of deuterated and nondeuterated di-NO_2-PY isomers are given in Figure IV-12. The estimated concentration of di-NO_2-PY isomers in POM collected in this time period was ~0.1 ng m^{-3}.

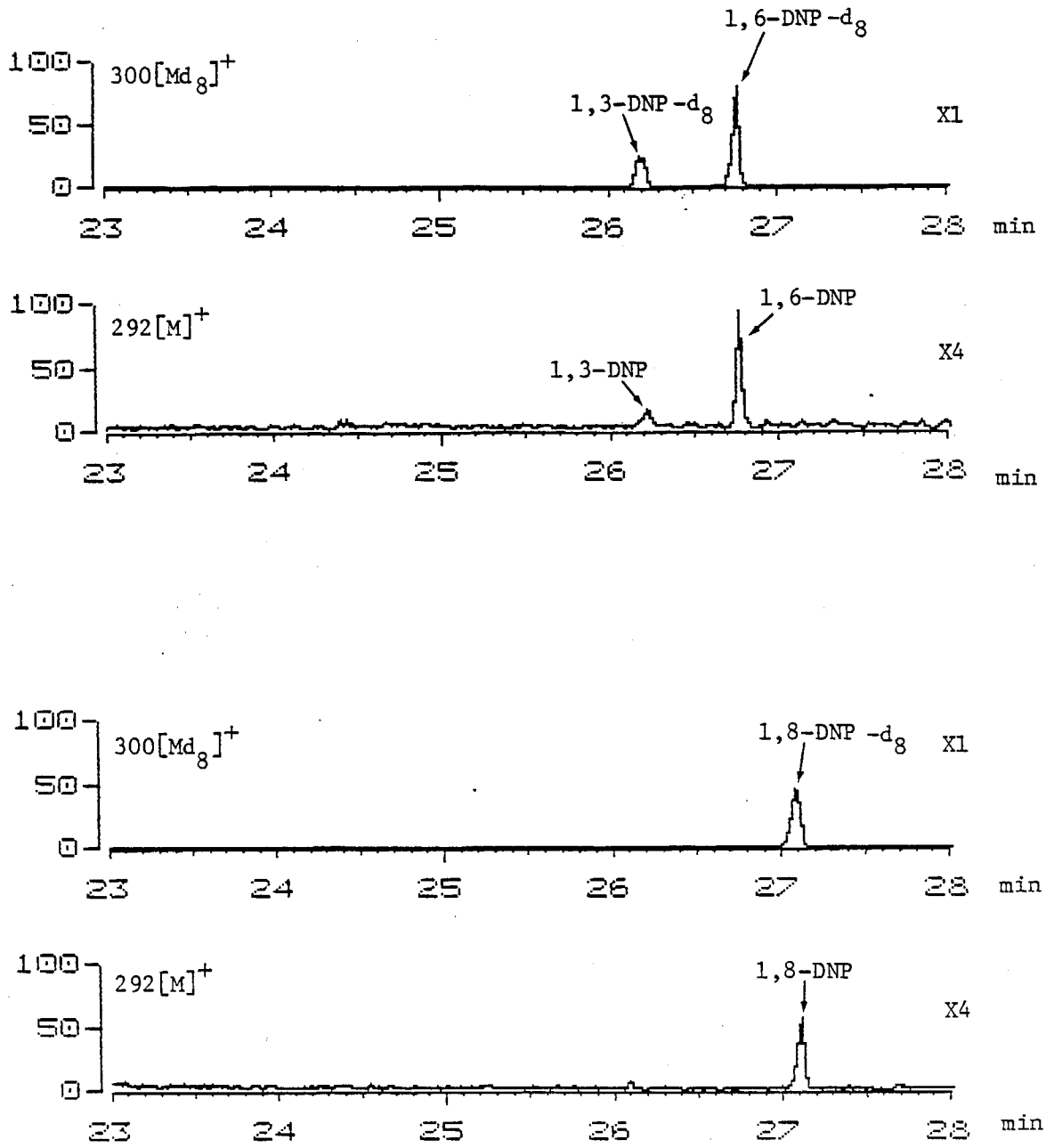

Figure IV-12. MID traces of CH_2Cl_2 extract from ambient POM, 0600-1200 hr September 19, 1984 collection period. Two HPLC fractions containing di-NO_2-PY isomers are shown. GC conditions as given in Figure IV-6.

Table IV-2. Concentration of Nitro-PAH in Ambient POM[a]

Date	Collection Time (hr)	Recovery of $1\text{-}NO_2\text{-}PY\text{-}d_9$ (%)	Concentration (ng m^{-3})		
			$1\text{-}NO_2\text{-}PY$	$2\text{-}NO_2\text{-}PY$	$2\text{-}NO_2\text{-}FL$[b]
9/18/84	1200-1800	94	0.02	0.003	0.07
9/18/84	1800-2400	85	0.03	c	0.2
9/19/84	0000-0600	98	0.008	0.01	0.3
9/19/84	0600-1200	77	0.03	0.02	0.2

[a]TX40HI20WW, T60A20, and Quartz CH_2Cl_2 filter extracts combined.
[b]Using response factor measured for $3\text{-}NO_2\text{-}FL$.
[c]None detected.

Consistent with the presence of $di\text{-}NO_2\text{-}PY$ isomers, the mutagen densities calculated from the activity of the CH_2Cl_2 extracts were highest during this 0600-1200 hr collection period. However, the mutagen density based on the activity of the GF filter CH_2Cl_2 extract was more than a factor of two lower than for the other filters suggesting $di\text{-}NO_2\text{-}PY$ isomers may not be fully recovered from GF filters.

A preliminary mutagenicity assay, involving single plates of three doses (0.01, 0.1 and 1 μg) showed that $2\text{-}NO_2\text{-}FL$ is a direct acting mutagen with an estimated activity of 4000 rev μg^{-1}. This activity can be compared with 2000 and 9000 rev μg^{-1} for $1\text{-}NO_2\text{-}PY$ and $2\text{-}NO_2\text{-}PY$ respectively (Rosenkranz and Mermelstein 1983).

D. Discussion

To date, neither $2\text{-}NO_2\text{-}FL$ nor $2\text{-}NO_2\text{-}PY$ have been detected in particles directly emitted from such sources as auto and diesel exhaust, wood-burning fireplaces or fossil-fueled power plants. Our observation of $2\text{-}NO_2\text{-}FL$, and $2\text{-}NO_2\text{-}PY$ in collected ambient POM suggests that transformations of PY and FL to their mutagenic 2-nitro-derivatives occur during transport through the atmosphere, during POM collection or both. Based on studies in simulated atmospheres there appears to be at least three mechanisms which could lead to nitro-PAH formation during transport or collection. These involve (a) the nitration of PAH by NO_2 in the presence of trace amounts of HNO_3, or by HNO_3 alone, a mechanism which

would be operative throughout the day and night (Pitts et al. 1978a, Grosjean et al. 1983, Pitts 1983, and references therein); (b) the nighttime nitration of PAH by N_2O_5 (Pitts et al. 1984a,c,d), and (c) the daytime addition reaction of OH radicals with the PAH, followed by reaction of NO_2 with the OH-PAH adduct to yield the nitro-PAH (Kenley et al. 1978, Atkinson et al. 1980, Nielsen et al. 1983).

The only known product of nitration of PY by NO_2 and/or HNO_3 in either solution phase or in the adsorbed state is 1-NO_2-PY (Vollmann et al. 1937, Dewar et al. 1956, Radner 1983, Jäger and Hanus 1980, Ramdahl et al. 1984, Pitts et al. 1984a). For FL, while few data are available concerning the nitrofluoranthene isomers formed from the exposure of adsorbed PAH to NO_2 containing traces of HNO_3, 3- and 8-NO_2-FL have been reported by Tokiwa et al. (1981). In solution, nitration by NO_2/N_2O_4 and by the NO_2^+ ion leads to the 1-,3-,7- and 8-NO_2-FL isomers, with an isomeric distribution of 3 > 8 >> 1 ~ 7 (Radner 1983, Streitweisser and Fahrey 1962). Thus the possible reaction of adsorbed PAH with NO_2 containing traces of HNO_3 cannot explain the formation of 2-NO_2-PY and 2-NO_2-FL during atmospheric transport. Further, this reaction cannot lead to artifactual formation of the 2-NO_2-PY and 2-NO_2-FL isomers during collection of ambient POM on filters.

With respect to the possible nighttime nitration of PAH by N_2O_5, we have investigated this reaction under a variety of experimental conditions including reactions with PAH in solution, in the gas phase and coated on glass fiber filters (Pitts et al. 1984a,c,d). For pyrene in CCl_4 solution and coated on filters, the only isomer observed from reaction with N_2O_5 was 1-NO_2-PY (Pitts et al. 1984a,d). While for fluoranthene in CCl_4 solution, reaction with N_2O_5 yields only the 2-NO_2-FL isomer, reaction with FL coated on GF filters yields the 1-,3-,7- and 8-NO_2-FL isomers in essentially equal yields (Pitts et al. 1984d). Clearly further experimental work concerning the reactions of N_2O_5 with fluoranthene in the gaseous, adsorbed and liquid phases is necessary before the atmospheric relevance of these reactions can be assessed.

The only data available concerning the OH radical-initiated reactions of PAH coated on glass fiber filters are those from a preliminary study carried out in this laboratory (Pitts 1984) in which OH radicals were produced from the photolysis of CH_3ONO-NO-air mixtures (Atkinson et al.

1981). For the reaction involving PY, both the 1-NO_2-PY and 2-NO_2-PY isomers were observed. The following reaction mechanism involving OH radical addition at the site of highest electron density (Dewar et al. 1956) could explain the formation of 2-NO_2-PY:

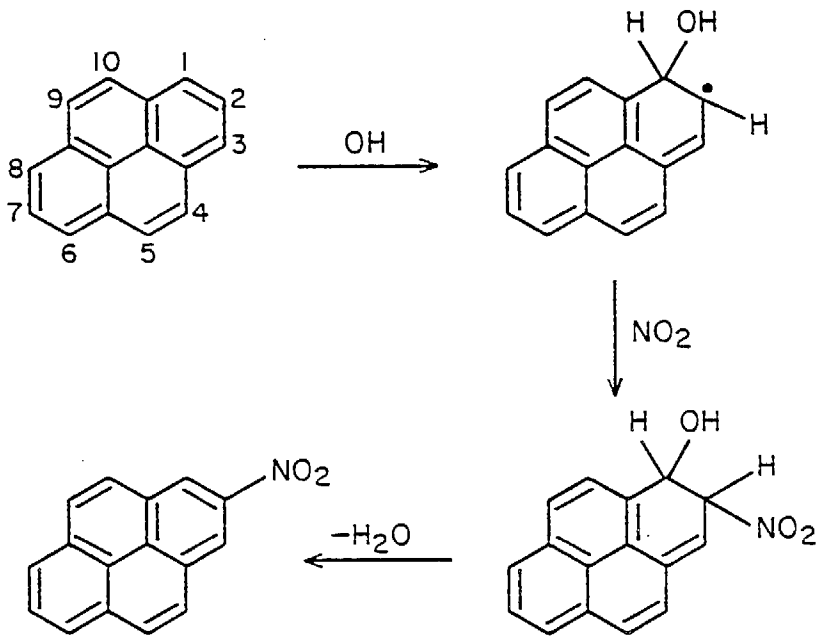

This reaction sequence was postulated for the formation of m-nitrotoluene from toluene by Kenley et al. (1978) and Atkinson et al. (1980), and has been more recently suggested as a pathway for the atmospheric formation of 2-nitropyrene from pyrene by Nielsen et al. (1984). An analogous reaction scheme could lead to the formation of 2-NO_2-FL from FL:

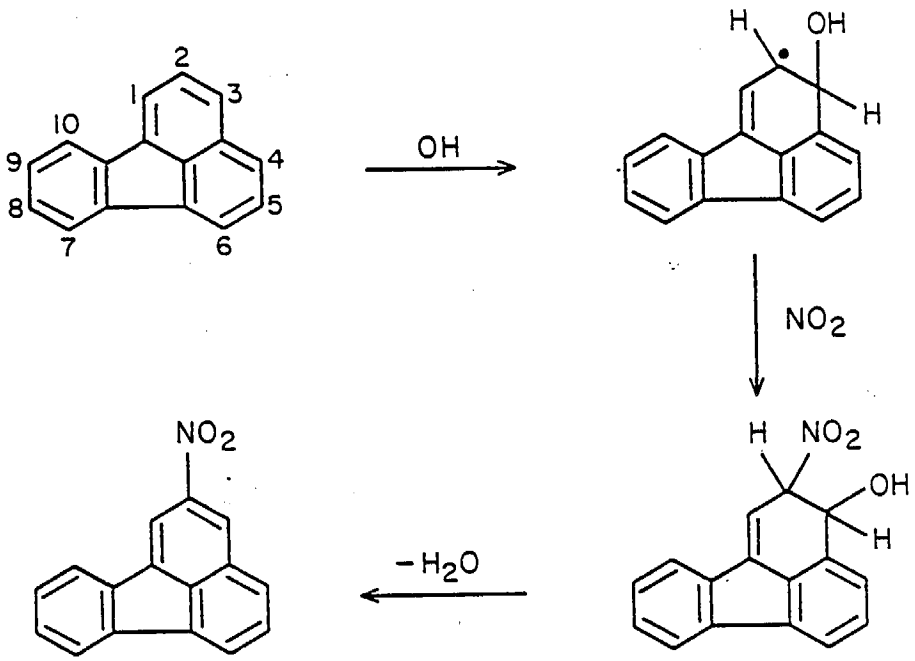

As noted earlier, we measured either directly the concentrations of the relevant gaseous co-pollutants (e.g., NO_2, NO_3 radical, O_3) or calculated them (e.g. N_2O_5) for the four 6-hour time periods shown in Table IV-1. Therefore, in principle the concentration data given in this table for 2-NO_2-PY and 2-NO_2-FL should be useful in elucidating the possible reaction pathways leading to the formation of these isomers. However, at least two factors complicate such interpretations.

First, it is difficult to account for the influence which air parcel transport and atmospheric residence time might have had on the observed time dependence of the 2-NO_2-PY and 2-NO_2-FL concentrations.

A second factor concerns the influence of ambient temperature on the volatility of both PY and FL and their nitro products, and hence on the partitioning between the gas and adsorbed phases. Thus, it is possible that the PAH reactions with N_2O_5 and OH radicals, leading to the observed isomers, proceed partly or entirely in the gas phase, followed by condensation of the products. Thus, further interpretation of the observed 2-NO_2-FL and 2-NO_2-PY concentrations as a function of time (Table 1) is unwarranted at this time.

Clearly, much further experimental work is necessary to elucidate the mechanism of formation of 2-nitrofluoranthene and 2-nitropyrene from their respective parent PAH. Also needed, in view of identification of these strong direct mutagens in ambient POM, are animal tests to assess the carcinogenicity of these compounds.

E. Conclusions

For the first time 2-nitrofluoranthene and 2-nitropyrene (strong direct mutagens) were detected and quantified in ambient POM collected in Southern California. The presence of these nitro-PAH in ambient POM provides strong evidence for the transformation of PAH to mutagenic nitroarenes during transport through the atmosphere. In addition, highly mutagenic and carcinogenic (in animals) dinitropyrene isomers were shown to be present in ambient POM collected during peak morning traffic hours. 1-Nitropyrene, an animal carcinogen, was also identified in all ambient POM samples analyzed. These results support the view that reliable assessments of the health impacts of POM cannot be based solely on testing of directly emitted material but must also take into account transformations of PAH adsorbed on such POM during transport through the atmosphere.

V. CALCULATIONS OF NIGHTTIME N_2O_5 CONCENTRATIONS AND IMPLICATIONS FOR PAH TRANSFORMATIONS

A. Introduction

In recent years, the salient features of the major chemical cycles occurring in the atmosphere have become, on a qualitative or semi-quantitative basis, reasonably well understood.

However, it is only in the past approximately five years that the chemistry occurring during nighttime hours in both the clean troposphere and polluted urban atmospheres has been investigated. There are, despite numerous ambient atmospheric studies (Platt et al. 1980a, 1981, 1982, 1984, Noxon et al. 1980), still significant uncertainties, especially involving N_2O_5 and its role in nighttime atmospheres.

Thus in the ambient atmosphere, the reaction of NO_2 with O_3

$$NO_2 + O_3 \rightarrow NO_3 + O_2 \qquad (1)$$

leads to the formation of the NO_3 radical whose subsequent reaction with NO_2

$$NO_2 + NO_3 \xrightarrow{M} N_2O_5 \qquad (2)$$

forms N_2O_5. Since N_2O_5 thermally decomposes to NO_2 and NO_3 (Malko and Troe 1982, Atkinson and Lloyd 1984)

$$N_2O_5 \xrightarrow{M} NO_2 + NO_3 \qquad (3)$$

and the NO_3 radical rapidly photolyzes (Graham and Johnston 1978, Magnotta and Johnston 1980)

$$NO_3 + h\nu \rightarrow NO_2 + O(^3P) \qquad (4a)$$

$$\rightarrow NO + O_2 \qquad (4b)$$

the concentrations of NO_3 radicals and N_2O_5 remain negligible during daylight hours. However, at night, when reactions (4a and 4b) are

negligible, and in the absence of NO, the NO_3 radical and N_2O_5 concentrations are expected to increase to significant levels.

Ambient atmospheric measurements have shown this to be the case for the NO_3 radical. Thus the spectroscopic identification of the NO_3 radical and measurement of its concentrations in ambient nighttime atmospheres during the past five years at a variety of locations in the United States (Platt et al. 1980, 1982, 1984, Noxon et al. 1980, Pitts et al. 1984b and Section VI below) Germany (Platt et al. 1981, 1982) and over the mid-Pacific ocean (Noxon 1983) has shown that the NO_3 radical is a common constituent of both the polluted and the clean troposphere. To date, however, N_2O_5 has not been detected in the ambient atmosphere.

All ambient measurements of NO_3 radical concentrations in the troposphere (Platt and Perner 1980, Noxon et al. 1980, Platt et al. 1980a, 1981, 1982, 1984, Noxon 1983, Pitts et al. 1984b) have been made using longpath differential optical absorption at the strong 662 nm (and in some cases the 623 nm) absorption band of the NO_3 radical (Graham and Johnston 1978, Marinelli et al. 1982). This technique utilizes the fact that species whose ultraviolet and visible absorption spectra exhibit distinct banded structure, such as HONO, NO_2, HCHO, SO_2, O_3 and the NO_3 radical, can be monitored by a single beam, single pass configuration. Three variations of this technique have been used. Platt et al. (1980a, 1981, 1982, 1984), Platt and Perner (1980) and Pitts et al. (1984a,b) have used a rapid scan spectrometer with the source set ~1-17 km from the spectrometer, with corresponding NO_3 radical concentration detection limits of ~10 ppt at 1 km pathlength to ~1 ppt at 17 km pathlength. Noxon and co-workers have used a slow scan spectrometer either with a light source ~10 km from the detection system (Noxon et al. 1980), or more recently (Noxon 1983) with the setting sun as a source, deriving NO_3 radical concentrations at 3 km altitude along a 220 km pathlength from Mauna Loa, Hawaii, with a detection sensitivity of ~0.15 ppt.

B. Ambient Atmospheric Data

Measurements of NO_3 radical concentrations in continental air masses have been made at a variety of locations ranging from relatively clean air sites such as Death Valley, CA (Platt et al. 1984), to heavily polluted urban areas downwind and east of Los Angeles, CA (Platt et al. 1980a, and

Sections VI and IX.B of this report). Measurements of NO_3 radical concentrations have also been carried out (Noxon 1983) in clean maritime air in the mid-Pacific, as noted above, and upper limits have been determined at Loop Head, Ireland (Platt and Perner 1980). The relevant data from these studies, including NO_2, O_3, NO_3 radical and H_2O concentrations, and temperature (where available), are summarized in Table V-1.

From this table it can be seen that over continental areas the observed NO_3 concentrations range from below the detection limit of ~1 ppt up to 430 ppt, the latter value being observed in Riverside, CA in September 1984 during conditions of elevated concentrations of secondary air pollutants (e.g., NO_2 and O_3). Of particular relevance are our observations of consistent NO_3 radical levels of ~10-100 ppt at a variety of desert and semi-arid sites in California under slightly polluted to clean air conditions (Platt et al. 1984).

Since, as noted above, the NO_3 radical and NO_2 are in equilibrium with N_2O_5 via reactions (2) and (3), with this equilibrium being attained in $\lesssim$1 min at 298 K and 760 torr total pressure (Atkinson and Lloyd 1984), then N_2O_5 concentrations can be readily calculated from the observed NO_3 radical and NO_2 concentrations and the appropriate equilibrium constant for reactions (2) and (3). We have used the equilibrium constant $K_{2,3}$ recently derived by Kircher et al. (1984), from their measured rate constants for reaction (2) and literature values for reaction (3), of $K_{2,3} = 3.15 \times 10^{-30} \; T \; e^{11350/T}$ cm^3 molecule^{-1} = 3.26×10^{-11} cm^3 molecule^{-1} at 298 K [which is in excellent agreement with the value of $K_{2,3} = (3.44 \pm 0.81) \times 10^{-11}$ cm^3 molecule^{-1} at 298 K recently determined directly by Tuazon et al. (1984)] to derive the calculated N_2O_5 concentrations at the time of the maximum NO_3 radical concentrations shown in Table V-1. These calculated N_2O_5 concentrations range up to ~15-20 ppb for the nights of September 18, 1979 in Riverside and April 16, 1980 in Deuselbach, Germany. [It should be noted that use of the equilibrium constant of Malko and Troe (1982) would lead to N_2O_5 concentrations a factor of 1.7 lower.]

These estimated nighttime N_2O_5 concentrations (which are expected to be close to the maximum values), of which ~30% are $\gtrsim$1 ppb, are significantly higher than previous estimates (see, for example, Pitts et al. 1983). Indeed, it is now apparent that for several nights of those in Table V-1 for which N_2O_5 concentrations can be estimated, the N_2O_5

Table V-1. Reported Ambient Atmospheric NO_3 Radical Concentration Data, Other Relevant Parameters, and Estimates of the Rate Constant k_7 and the NO_3 Radical Decay Rate $k_5[X]$

Location and Investigators	Date (night of)	Concentration[a] O_3 (ppb)	NO_3[b] (ppt)	NO_2 (ppb)	H_2O (torr)	T (K)	N_2O_5 (ppb)	$10^{21} \times k_7$ (cm^3 $molecule^{-1}$ sec^{-1})[c]	$k_5[X]$ (sec^{-1})[d]
Loop Head	4/4/79	23	<6	0.4	-	279	<0.03	-	$>7.4 \times 10^{-4}$
(Ireland)	4/5/79	~43	<14	0.15	-	280	<0.02	-	$>2.3 \times 10^{-4}$
(Platt and	4/6/79	~40	<3	<0.15	-	280±1	<0.004	-	-
Perner 1980)	4/8/79	31	<8	2.5	-	277	<0.3	-	$>4.4 \times 10^{-3}$
	4/9/79	~30	<3	2.2	-	277	<0.1	-	$>1 \times 10^{-2}$
	4/12/79	~18	<2	0.4	-	-	-	-	-
	4/13/79	~30	<0.5	~0.1	-	280	<0.0005	-	$>3.0 \times 10^{-3}$
Riverside	8/4/79	107	>156	23	14.3	303	>1.5	<3.1	$>1.4 \times 10^{-2}$
(CA)	8/7/79	37	<17	70	14.3	303	<0.5	>10	>0.14
(Platt et	8/8/79	43	<8	45	15.4	303	<0.2	>23	>0.22
al. 1980a)	8/20/79	51	<6	42	13.8	293	<0.4	>8.5	>0.25
	8/24/79	41	<30	76	13.7	300	<1.4	>4.1	$>8.7 \times 10^{-2}$
	9/11/79	88	158	37	14.7	302	2.8	2.1	1.8×10^{-2}
	9/12/79	153	288	55	17.6	303	6.8	2.0	2.6×10^{-2}
	9/13/79	94	296	78	18.5	304	8.7	1.3	2.3×10^{-2}
	9/14/79	58	228	73	15.2	303	7.1	1.1	1.7×10^{-2}
	9/18/79	196	355	82	13.1	302	14	2.4	4.0×10^{-2}
Claremont	8/28/79	3	<7	62	13.8	293	<0.7	>0.43	$>1.9 \times 10^{-2}$
(CA)	8/30/79	48	18	51	14.4	294	1.2	3.0	9.8×10^{-2}
(Platt et al. 1980a)									

(continued)

Table V-1 (continued) - 2

Location and Investigators	Date (night of)	Concentration[a] O_3 (ppb)	NO_3[b] (ppt)	NO_2 (ppb)	H_2O (torr)	T (K)	N_2O_5 (ppb)	$10^{21} \times k_7$ (cm^3 $molecule^{-1}$ sec^{-1})[c]	$k_5[X]$ (sec^{-1})[d]
(Platt et	8/31/79	12	<7	89	18.8	295	<0.7	1.7	>0.11
al. 1980a)	9/1/79	62	36	67	20.6	297	2.2	2.2	8.9×10^{-2}
(cont'd)	9/2/79	50	33	48	24.5	299	1.1	2.2	5.9×10^{-2}
Colorado	8/5/79	~30	70	8	-	~285	2.6	-	2.0×10^{-3}
(Noxon et	8/28/79	~30	40	5	-	~285	0.9	-	2.1×10^{-3}
al. 1980)		~30	<15	~1.5	-	~285	<0.1	-	$>1.7 \times 10^{-3}$
	8/29/79	~30	<3.5	0.75	-	~285	<0.01	-	$>3.7 \times 10^{-3}$
	9/17/79	~30	<9.5	1.8	-	~285	<0.08	-	$>3.2 \times 10^{-3}$
	9/18/79	~30	<4	1.0	-	~285	<0.02	-	$>4.3 \times 10^{-3}$
		~30	~14	3.2	-	~285	0.2	-	3.9×10^{-3}
	9/21/79	~30	6.5	1.7	-	~285	0.05	-	4.5×10^{-3}
	10/3/79	~30	50	4.8	-	~285	1.1	-	1.6×10^{-3}
		~30	31	3.6	-	~285	0.5	-	2.0×10^{-3}
		~30	21	2.0	-	~285	0.2	-	1.6×10^{-3}
	10/4/79	~30	17	2.1	-	~285	0.2	-	2.1×10^{-3}
		~30	13	1.3	-	~285	0.08	-	1.7×10^{-3}
	10/6/79	~30	17	1.8	-	~285	0.1	-	1.8×10^{-3}
		~30	8	0.9	-	~285	0.03	-	1.9×10^{-3}
	10/10/79	~30	8	1.5	-	~285	0.05	-	3.2×10^{-3}
	10/17/79	~30	<5	<0.5	-	~285	<0.01	-	-
	10/17/79	-	<3.2	3.5-7	-	-		-	-
		~30	<3	<0.3	-	-		-	-

(continued)

Table V-1 (continued) - 3

Location and Investigators	Date (night of)	Concentration[a] O_3 (ppb)	NO_3[b] (ppt)	NO_2 (ppb)	H_2O (torr)	T (K)	N_2O_5 (ppb)	$10^{21} \times k_7$ (cm^3 $molecule^{-1}$ sec^{-1})[c]	$k_5[X]$ (sec^{-1})[d]
Julich	5/14/80	30	9	10-13	-	-		-	-
(Germany)		-	11	-	-	-		-	-
(Platt et	7/23/80	30	78	25	-	-		-	-
al. 1981,	7/24/80	≤15	16	20	-	-		-	-
1982)		-	19	-	-	-		-	-
		-	12	25	-	-		-	-
		-	8	-	-	-		-	-
	8/15/80	30	23	16	-	-		-	-
	8/21/80	35	39	11	-			-	-
Deuselbach	4/11/80	≤4	<6	~17	-	-		-	-
(Germany)	4/12/80	-	~40	~3	4.5	280	~1.1	-	-
(Platt et	4/13/80	~50	~170	~2	4.6	283	~2.1	0.17	3.2×10^{-4}
al. 1981,	4/14/80	~60	~190	~5	4.6	283	~5.7	0.18	8.5×10^{-4}
1982)	4/15/80	~60	~160	~5	5.1	285	~3.7	0.27	1.1×10^{-3}
	4/16/80	~60	~280	~13	5.7	~284	~19	0.12	1.5×10^{-3}
	4/17/80	-	~90	~6	5.2	282	~3.8	-	-
Whitewater	10/27/81	~30	92	12	7.9	292	1.9	0.49	3.7×10^{-3}
(CA)	10/28/81	~30	<2	17	10.1	291	<0.07	>15	$>1.7 \times 10^{-1}$
(Platt et	10/30/81	~30	55	<0.9	3.4	289	<0.1	1.2	$<3.4 \times 10^{-4}$
al. 1984)	10/31/81	~30	17	<0.9	2.3	288	<0.05	4.7	$<1.2 \times 10^{-3}$

(continued)

Table V-1 (continued) - 4

Location and Investigators	Date (night of)	Concentration[a] O_3 (ppb)	NO_3[b] (ppt)	NO_2 (ppb)	H_2O (torr)	T (K)	N_2O_5 (ppb)	$10^{21} \times k_7$ (cm^3 $molecule^{-1}$ sec^{-1})[c]	$k_5[X]$ (sec^{-1})[d]
	11/2/81	~30	4	<0.9	3.8	292	<0.006	23	$<4.6 \times 10^{-3}$
	11/5/81	~30	124	7	6.8	290	2.0	0.30	3.3×10^{-3}
	11/10/81	~30	134	1.5	5.4	291	0.4	0.42	2.7×10^{-4}
	11/11/81	~30	94	1.3	4.6	290	0.3	0.59	4.4×10^{-4}
	11/16/81	~30	168	1.4	5.7	296	0.2	0.70	3.7×10^{-4}
	11/23/81	~30	185	1.6	5.0	288	0.9	0.20	5.9×10^{-4}
	12/4/81	~30	64	3.2	4.8	286	0.8	0.43	1.0×10^{-3}
	12/8/81	~30	115	7.5	4.0	288	2.6	0.40	1.3×10^{-3}
	12/10/81	~30	66	1.3	5.1	290	0.2	0.76	4.2×10^{-4}
	12/11/81	~30	170	3.2	3.5	290	1.3	0.43	5.7×10^{-4}
Phelan (CA) (Platt et al. 1984)	4/2/82	~30	16	1.9	6.7	286	0.1	1.2	2.2×10^{-3}
	4/3/82	~30	10	9.2	6.9	285	0.4	1.6	3.9×10^{-2}
	4/4/82	~30	9	1.0	6.4	286	0.04	2.3	2.5×10^{-3}
	4/5/82	~30	8	2.4	6.8	290	0.04	4.7	7.8×10^{-3}
	4/6/82	~30	5	1.8	5.1	284	0.05	3.7	7.5×10^{-3}
	4/7/82	~30	25	1.2	5.7	284	0.2	0.65	3.3×10^{-3}
	4/8/82	~30	51	1.4	6.1	292	0.1	1.1	9.9×10^{-4}
	4/9/82	~30	53	4.3	9.8	289	0.6	0.42	1.9×10^{-3}
	4/10/82	~30	8	1.4	12.2	291	0.02	0.31	4.0×10^{-3}
	4/11/82	~30	11	3.9	9.2	286	0.2	1.3	6.9×10^{-3}
	4/12/82	~30	23	2.1	6.7	283	0.3	0.51	1.9×10^{-3}
	4/13/82	~30	27	2.5	6.4	281	0.5	0.32	4.2×10^{-3}

(continued)

Table V-1 (continued) - 5

Location and Investigators	Date (night of)	Concentration[a] O_3 (ppb)	NO_3[b] (ppt)	NO_2 (ppb)	H_2O (torr)	T (K)	N_2O_5 (ppb)	$10^{21} \times k_7$ (cm^3 $molecule^{-1}$ sec^{-1})[c]	$k_5[X]$ (sec^{-1})[d]
Death	4/24/82	~30	45	<0.3	4.3	301	<0.007	7.5	$<2.7 \times 10^{-4}$
Valley	4/25/82	~30	35	<0.3	3.8	303	<0.005	15	$<2.8 \times 10^{-4}$
(CA)	4/26/82	~30	30	<0.3	3.9	305	<0.003	23	$<3.8 \times 10^{-4}$
(Platt et	4/27/82	~30	33	<0.3	4.5	306	<0.003	21	$<9.6 \times 10^{-4}$
al. 1984)	5/3/82	~30	19	<0.3	9.3	302	<0.003	9.6	$<4.6 \times 10^{-4}$
Edwards	5/12/82	~30	40	1.2	7.2	297	0.04	2.7	1.5×10^{-3}
AFB	5/18/82	~30	93	1.8	6.7	298	0.1	1.5	7.1×10^{-4}
(CA)	5/19/82	~30	68	1.1	8.8	298	0.06	1.5	5.1×10^{-4}
(Platt et	5/20/82	~30	42	1.9	9.1	299	0.06	2.8	1.3×10^{-3}
al. 1984)	5/21/82	~30	88	1.3	8.5	301	0.06	1.9	4.6×10^{-4}
	5/22/82	~30	82	1.0	6.8	299	0.06	1.9	3.1×10^{-4}
	5/23/82	~30	84	0.9	9.8	304	0.03	2.8	3.1×10^{-4}
	5/24/82	~30	99	0.9	7.8	305	0.03	3.4	2.7×10^{-4}
	5/28/82	~30	25	2.0	11.9	297	0.05	2.6	1.9×10^{-3}
Mid-Pacific (Noxon 1983)	11/2-12/81	~40	0.25	0.03±0.01	-	~285	0.00003	-	2.7×10^{-3}

(continued)

Table V-1 (continued) - 6

Location and Investigators	Date (night of)	Concentration[a] O_3 (ppb)	NO_3[b] (ppt)	NO_2 (ppb)	H_2O (torr)	T (K)	N_2O_5 (ppb)	$10^{21} \times k_7$ (cm^3 $molecule^{-1}$ sec^{-1})[c]	$k_5[X]$ (sec^{-1})[d]
Riverside	9/15/82	90	77	19	18.3	302	0.7	3.6	1.9×10^{-2}
(CA)	9/16/82	106	88	23	18.9	302	1.0	3.6	2.4×10^{-2}
(Pitts et al. 1984b and Section VI)									
Riverside	9/13/84	18	114	38	15.8	297	4.0	0.26	4.7×10^{-3}
(CA)	9/14/84	<5	98	35	14.0	295	4.1	<0.07	$<1.3 \times 10^{-3}$
(This work	9/15/84	33	71	7	15.4	302	0.2	1.7	2.8×10^{-3}
see Section	9/16/84	-	49	19	-	-	-	-	-
IX.B)	9/17/84	110	342	31	19.5	303	4.5	1.1	8.9×10^{-3}
	9/18/84	79	431	35	17.4	301	8.3	0.51	5.5×10^{-3}
	9/19/84	27	145	18	16.3	298	2.1	0.35	2.7×10^{-3}
	9/20/84	<5	85	30	14.5	296	2.7	<0.09	$<1.3 \times 10^{-3}$
	9/21/84	23	50	<5	14.4	293	<0.4	0.44	$<1.6 \times 10^{-3}$
	9/22/84	15	16	21	14.8	294	0.5	1.0	1.4×10^{-2}

[a]The O_3, NO_2, and H_2O concentrations and temperatures are those at a time close to that at which the NO_3 radical concentration was observed.
[b]Maximum NO_3 radical concentrations observed.
[c]Estimated from equation (X) [see text].
[d]Estimated from equation (VIII) [see text]. The NO_3 radical lifetimes τ due to NO_3 radical or N_2O_5 loss processes are given by $\tau = (k_5[X])^{-1}$.

concentrations exceeded the detection limits appropriate for long pathlength Fourier transform infrared spectroscopy. Thus for a pathlength of ~1 km, which has been routinely attained by Tuazon et al. (1978, 1980, 1981), the detection limit for detection of N_2O_5 is estimated to be ~4 ppb using the 1246 cm^{-1} absorption band. Thus it now appears that the detection and quantitative measurements of N_2O_5 is indeed feasible on certain nights in relatively polluted urban atmospheres. At the concentrations as given in Table V-1, N_2O_5 now joins other "trace" pollutant species such as HONO, HCOOH, etc., as being present a high proportion of the time in polluted urban atmospheres at concentrations >1 ppb.

While recent computer modeling studies of the behavior of NO_3 radicals, N_2O_5, O_3 and NO_2 have been carried out (Jones and Seinfeld 1983, Stockwell and Calvert 1983, Russell et al. 1984), these modeling studies have concentrated on only a single nighttime event for which a not totally adequate associated data set was available. While these modeling studies have provided much valuable data concerning NO_3 radical reaction pathways and nitric acid formation routes and rates, these studies could not provide any further evidence concerning the homogeneous rate constant for the hydrolysis of N_2O_5. Thus the magnitude of this rate constant is important for nitric acid formation at night in the gas phase and hence for long range acid deposition modeling programs. We have used the approach of employing the complete data set available to derive upper limit estimates for each evening for this rate constant, and from these to estimate an upper limit rate constant. This approach, which is complementary to those used in the computer modeling tasks carried out to date (Jones and Seinfeld 1983, Stockwell and Calvert 1983, Russell et al. 1984) is discussed below, and indeed provides important new information. Furthermore, we have used the N_2O_5 concentrations derived in Table V-1 from the ambient NO_3 radical and NO_2 measurements together with our laboratory data concerning the rates of nitration of a series of adsorbed PAH by gaseous N_2O_5 to estimate the nitration yields of pyrene during a single night. These two aspects of N_2O_5 chemistry are discussed below.

C. The Magnitude of N_2O_5 and/or NO_3 Radical Loss Processes

These ambient measurements of NO_3 radical concentrations allow the magnitude of the N_2O_5 and/or NO_3 radical loss processes to be estimated, provided that the necessary associated data (temperature, water vapor concentrations, etc.) are available.

The available literature reports several types of NO_3 radical time-concentration profiles. In the Los Angeles air basin NO_3 radical levels have been observed to rise rapidly after sunset, peak at ~2000-2100 hr, and then decay rapidly to below the detection limits by around midnight (Platt et al. 1980a, 1982, and Section VI of this report) (see Figure V-1a). However, in non-urban atmospheres (Platt et al. 1981, 1984), after an initial rapid rise the NO_3 radical concentrations often remained essentially constant throughout the night until sunrise, when they decreased rapidly due to photolysis (Figures V-1b and V-2).

During many of these nighttime NO_3 radical time-concentration profile measurements, the NO_2, O_3 and H_2O concentrations, as well as the temperature, remained essentially constant. Hence, in these cases the effects of loss processes for the NO_3 radical and N_2O_5 on the expected NO_3 radical time-concentration profiles can be readily evaluated. Assuming that the reactions

$$NO_3 + X \rightarrow \text{products} \qquad (5)$$

and/or

$$N_2O_5 + Y \rightarrow \text{products} \qquad (6)$$

[where reaction (6) may include reaction with water vapor] are those removing NO_3 radicals, then from reactions (1)-(3) and (5) or (6), and for constant NO_2 and O_3 concentrations and temperature:

(a) For the reaction of the NO_3 radical with an as yet unspecified reactant at a constant concentration [reaction (6)]

$$[NO_3]_t = \frac{k_1[NO_2][O_3]}{k_5[X]} \left\{1 - e^{-k_5[X]t}\right\} \qquad (I)$$

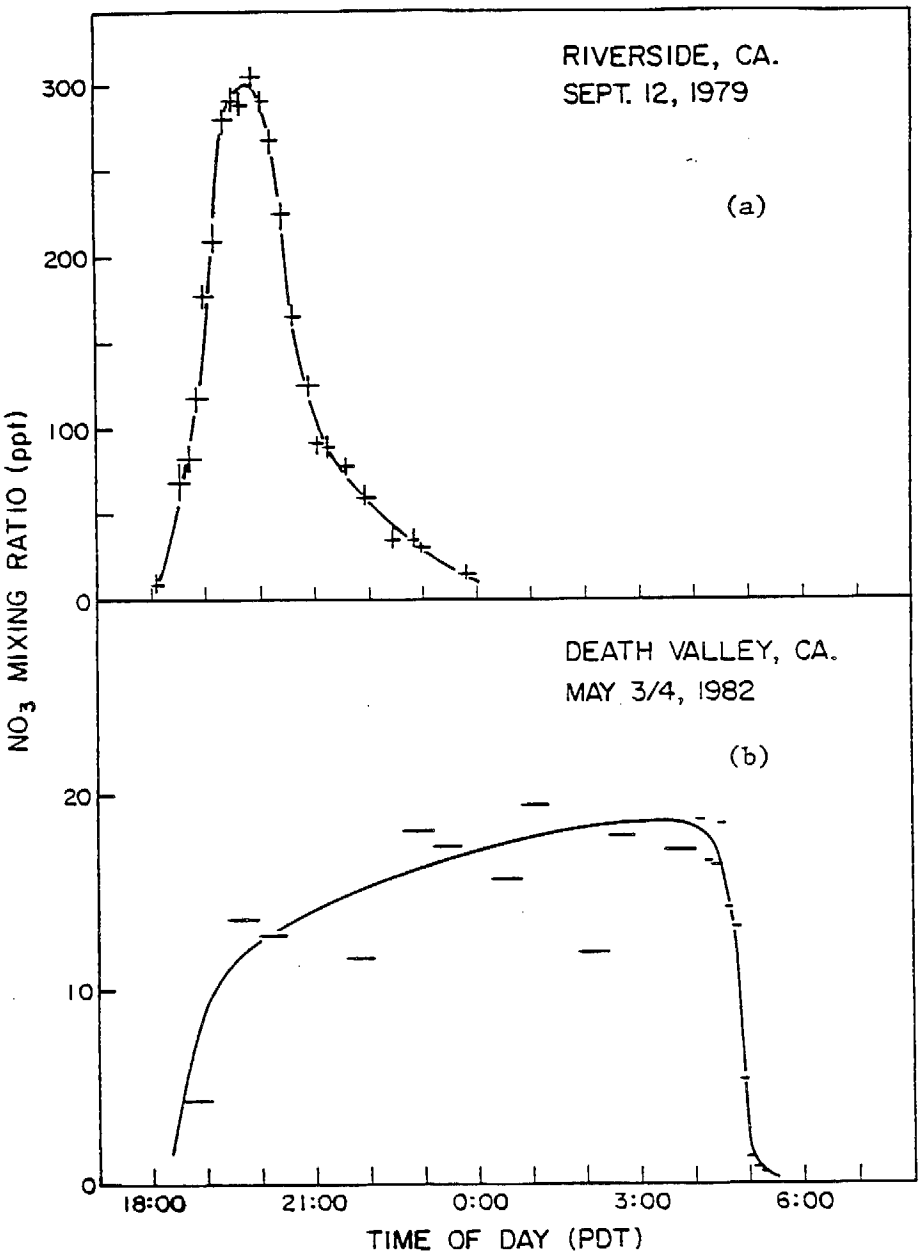

Figure V-1. Time-concentration profiles observed for NO_3 radicals by DOAS spectroscopy at (a) Riverside, CA during evening of September 12, 1979 (Platt et al. 1980a) and (b) Death Valley, CA on night of May 3-4, 1982 (Platt et al. 1984). The experimental data are denoted by the crosses (Figure V-1a) and horizontal bars (Figure V-1b).

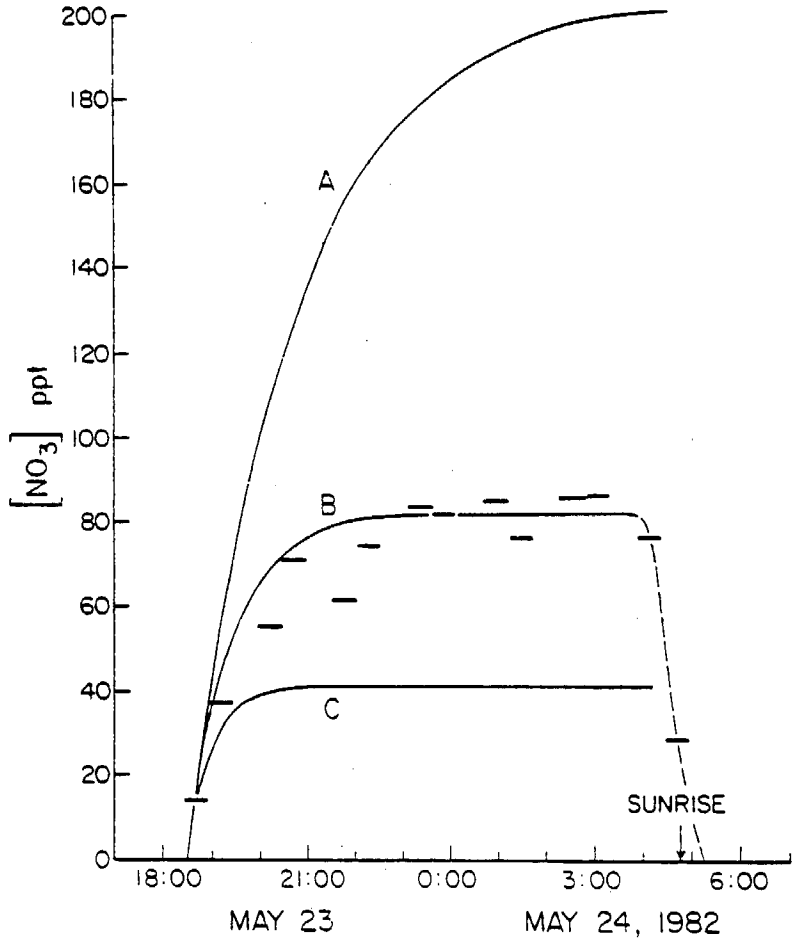

Figure V-2. Experimental data (solid horizontal bars) for NO_3 radicals at Edwards AFB on night of May 23-24, 1982 (Platt et al. 1984), together with calculated profiles from equation (V) for various values of k_7 (the rate constant for reaction of N_2O_5 with water vapor) or $k_5[X]$ (the NO_3 radical decay rate): A, $k_7 = 1.1 \times 10^{-21}$ cm^3 molecule^{-1} sec^{-1} or $k_5[X] = 1.2 \times 10^{-4}$ sec^{-1}; B, $k_7 = 2.8 \times 10^{-21}$ cm^3 molecule^{-1} sec^{-1} or $k_5[X] = 3.0 \times 10^{-4}$ sec^{-1}; C, $k_7 = 5.6 \times 10^{-21}$ cm^3 molecule^{-1} sec^{-1} or $k_5[X] = 6.1 \times 10^{-4}$ sec^{-1}. The observed photodissociation of NO_3 radicals around sunrise is shown by the dashed line.

(b) For the reaction of N_2O_5 radicals with an as yet unspecified reactant at constant concentration [reaction (6)], and making the reasonable assumption that equilibrium between NO_2 and NO_3 and N_2O_5 is attained, then

$$[NO_3]_t = \frac{k_1 [O_3]}{k_6 K_{2,3}[Y]} \left\{ 1 - e^{-k_6 K_{2,3}[NO_2][Y]t} \right\} \qquad (II)$$

were $k_6 = k_7$ and $Y = H_2O$ if the removal process for N_2O_5 is via reaction (7).

$$N_2O_5 + H_2O \rightarrow 2HNO_3 \qquad (7)$$

Both equations (II) and (IV) are of the form

$$[NO_3]_t = \frac{a}{b}(1-e^{-bt}) \qquad (III)$$

and it cannot be assessed from a single night's NO_3 radical time-concentration profile whether the NO_3 radical or N_2O_5 is the reacting species. A typical set of profiles generated by equations (III) are as shown in Figure V-2; they exhibit a rapid rise in the NO_3 radical concentration to an asymtotic value. Such profiles are in agreement with the experimental data for relatively unpolluted atmospheres (for example, in the case of Figure V-2 for Edwards Air Force Base on May 23/24, 1982). Though not explicit in equation (III), a rapid decay at sunrise occurs due to the photolysis of NO_3, as discussed above.

The NO_3 radical time-concentration profiles which deviate from this behavior for conditions of constant NO_2, O_3, and H_2O concentrations and temperature [see, for example, Figures 4, 7 and 8 of Platt et al. (1981) and Figure 3 of Platt et al. (1984)] must result from the effects of air parcel transport and/or changing patterns of emissions of reactant species [see, for example, the chemical modeling studies of Stockwell and Calvert (1983), Jones and Seinfeld (1983) and Russell et al. (1984)].

The experimental data for the NO_3 radical nighttime atmospheric concentrations presented in Table V-1 can only be analyzed in an approximate manner since associated data such as ambient NO and organic concentrations and meteorological conditions (as well as in many cases the

temperature and O_3 and water vapor concentrations) needed to carry out detailed chemical modeling studies are, with the exception of our September 1983 study (see Section VI), not available [see, for example, Stockwell and Calvert (1983) and Jones and Seinfeld (1983)], although Russell et al. (1984) have carried out a comprehensive modeling study of the dynamics of HNO_3 production in using the Los Angeles air basin and the data reported by Platt et al. (1980a) for the evening of September 12, 1979, in Riverside.

We use the approach of considering only the simplistic reaction system consisting of reactions (1)-(3) and (5) [or (7)] and (6) [where reactions (5) and (6) may include heterogeneous losses of NO_3 radicals or N_2O_5, as discussed by Heikes and Thompson (1983)], together with reaction (8).

$$NO_2 + NO_3 \rightarrow NO + NO_2 + O_2 \qquad (8)$$

where $k_8 = 2.5 \times 10^{-14} e^{-1230/T}$ cm^3 molecule^{-1} sec^{-1}

$= 4.0 \times 10^{-16}$ cm^3 molecule^{-1} sec^{-1} at 298 K

(Atkinson and Lloyd 1984)

From this reaction scheme, then at steady state when reactions (2) and (3) are at equilibrium, values of k_5 and k_6 can be estimated. Two limiting cases can then be considered: either that $k_6 = 0$ and that the only loss process of NO_3 radicals (and hence of N_2O_5) is via reaction (5), or that $k_5 = 0$ and that the only loss process of N_2O_5 (and hence of NO_3 radicals) is via reaction (6) [or reaction (7)].

For the first case, where $k_6 = 0$, then at steady state

$$[NO_3]_{ss} = \frac{k_1[NO_2][O_3]}{k_8[NO_{22}] + k_5[X]} \qquad (IV)$$

The quantity $k_8[NO_2]$ is $\sim 1 \times 10^{-5}$ sec^{-1} for 1 ppb of NO_2 at 298 K, and is much less than the observed NO_3 radical decay rates (Noxon et al. 1980, Platt et al. 1980a, 1984 and Table V-1). Hence to a good approximation

equation (IV) simplifies to

$$[NO_3]_{ss} = \frac{k_1[NO_2][O_3]}{k_5[X]} \qquad (V)$$

If $k_5 = 0$ and reaction of N_2O_5 is responsible for depleting the NO_3 radicals then a similar analysis can be carried out leading to [again neglecting reaction (8)]:

$$[NO_3]_{ss} = \frac{k_1[O_3]}{k_6 K_{2,3}[Y]} \qquad (VI)$$

The only postulated atmospherically significant homogeneous reaction of N_2O_5 is with water vapor [reaction (7)], and assuming that reaction (7) is indeed responsible for the observed losses of N_2O_5 and NO_3 radicals allows equation (VI) to be replaced by equation (VII)

$$[NO_3]_{ss} = \frac{k_1[O_3]}{k_5 K_{2,3}[H_2O]} \qquad (VII)$$

We have used equations (IV) and (VII) to derive the values of $k_5[X]$ (i.e., the NO_3 radical decay rate) and the rate constant k_7 given in Table V-1 from the observed NO_3 radical, O_3 and H_2O concentrations and temperature (where available).

These values of $k_5[X]$ and k_7 will in general be upper limits since the assumption that steady-state has been attained is not true in all cases, and of course intermediate situations where both reactions (5) and (6) [or (7)] contribute to the NO_3 radical and N_2O_5 loss processes can also occur. It can be seen from Table V-1 that the derived values of k_7 range from $<7 \times 10^{-23}$ to $>2 \times 10^{-20}$ cm^3 molecule^{-1} sec^{-1}.

However, a further complication in using these data to derive rate constant estimates for k_7 arises from the disturbing influence of point source emissions of, for instance, NO_x in these studies. Thus in general, over continental areas, NO_2 and NO_3 radical concentrations have been monitored by DOAS over column lengths of 0.6 to 17 kms, while O_3 has often been measured by ultraviolet absorption or chemiluminescence instruments at a single point source (Platt et al. 1980a, 1984, Pitts et al. 1984b and

our present 1984 study). Thus local point source emissions of NO_x can lead to significant inhomogenieties in the concentrations of, for example, O_3, NO_2, NO_3 radicals and N_2O_5. Indeed in our most recent study in September 1984, discrepancies of factors of $\gtrsim 2$ were observed in the NO_2 concentration data as measured by DOAS over a 2 km pathlength and as measured by a chemiluminescence instrument at the collecting site (Figure V-3). While such inhomogeneities are probably of little consequence for the estimation of average N_2O_5 concentrations over the column lengths used (since these use the DOAS NO_3 radical and NO_2 concentrations), they can lead to major errors in estimating upper limit values of k_7, because a combination of DOAS and conventional point source continuous monitor data are used.

Hence, we believe that data sets obtained in polluted urban areas should not be used for this purpose, unless the O_3, NO_2 and NO_3 radical concentrations were all monitored sumultaneously in the same air mass. Thus we elect to use the rate constant estimates k_7 from the studies of Noxon et al. (1980) in Colorado, Platt et al. (1981, 1982) for Deuselbach, Germany, and Platt et al. (1984) for a series of semi-arid/desert sites. These are all studies carried out in relatively clean atmospheres with reasonably constant O_3 and NO_2 concentrations during the nights studied. The lower of these values of k_7 appear to correlate with lower temperature, and a plot of these estimates of k_7 against temperature is shown in Figure V-4. Since the values of k_7 are upper limits, a lower bound of the rate constants should be evident, and this appears to be the case, with a value of k_7 of $\sim 1 \times 10^{-22}$ cm^3 $molecule^{-1}$ sec^{-1} at 284 K, increasing to $\sim 1 \times 10^{-21}$ and $\sim 3 \times 10^{-21}$ cm^3 $molecule^{-1}$ sec^{-1} at 298 K and at 304 K, respectively.

This upper limit value of k_7 derived at 298 K of $\sim 1 \times 10^{-21}$ cm^3 $molecule^{-1}$ sec^{-1} is in remarkably good agreement with that of 1.3×10^{-21} cm^3 $molecule^{-1}$ estimated by Tuazon et al. (1983) at 298 K from environmental chamber experiments and which, although rigorously an upper limit, was regarded as probably being the rate constant for the homogeneous reaction of N_2O_5 with water vapor. The present data obtained from ambient atmospheric measurements thus suggest that this rate constant estimate of Tuazon et al. (1983) may indeed have been that for the homogeneous reaction of N_2O_5 with water vapor.

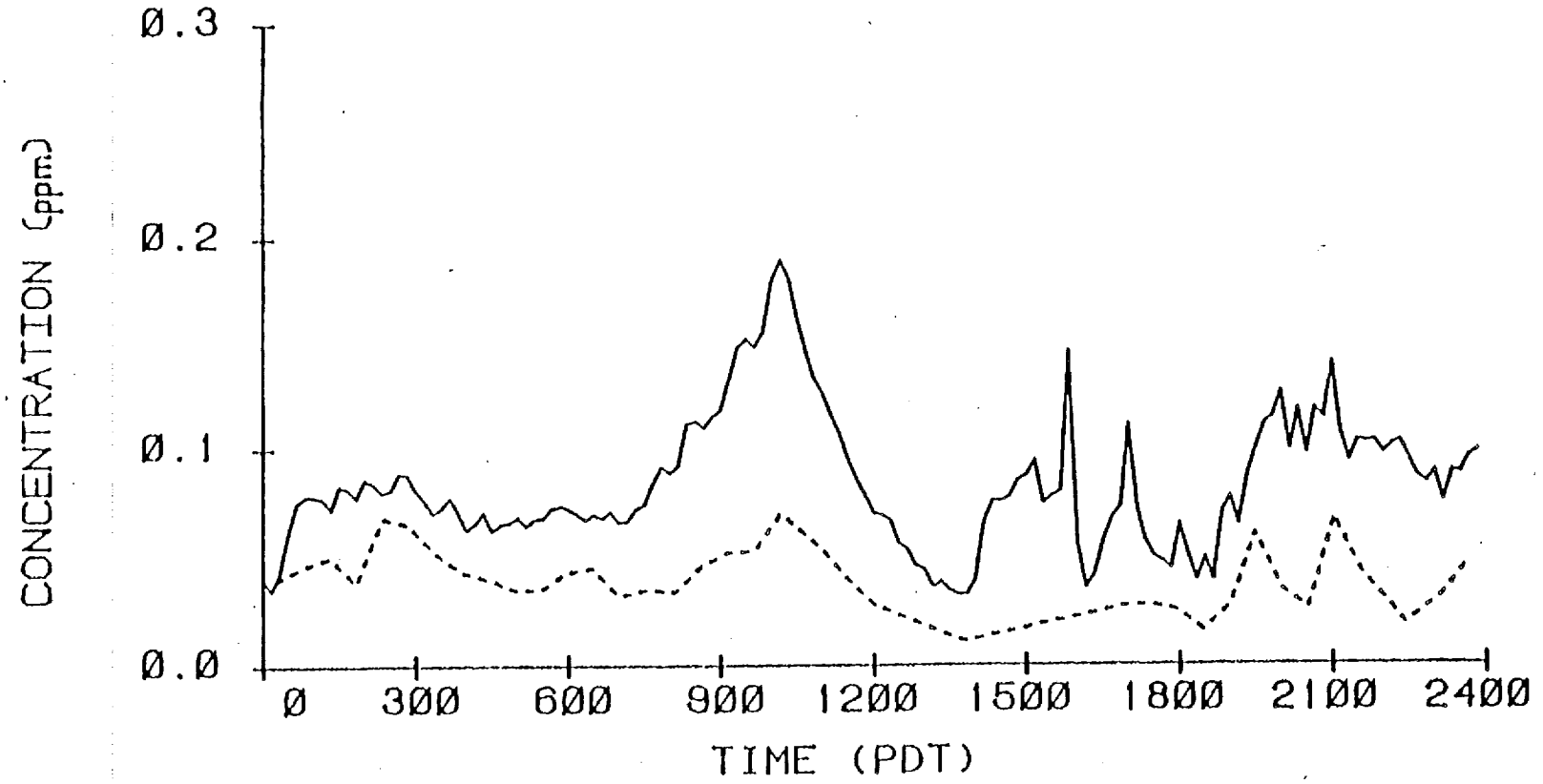

Figure V-3. NO_2 time-concentration profiles measured by DOAS (---) and by a chemiluminescence analyzer, uncorrected for interferences, (——) on September 18, 1984.

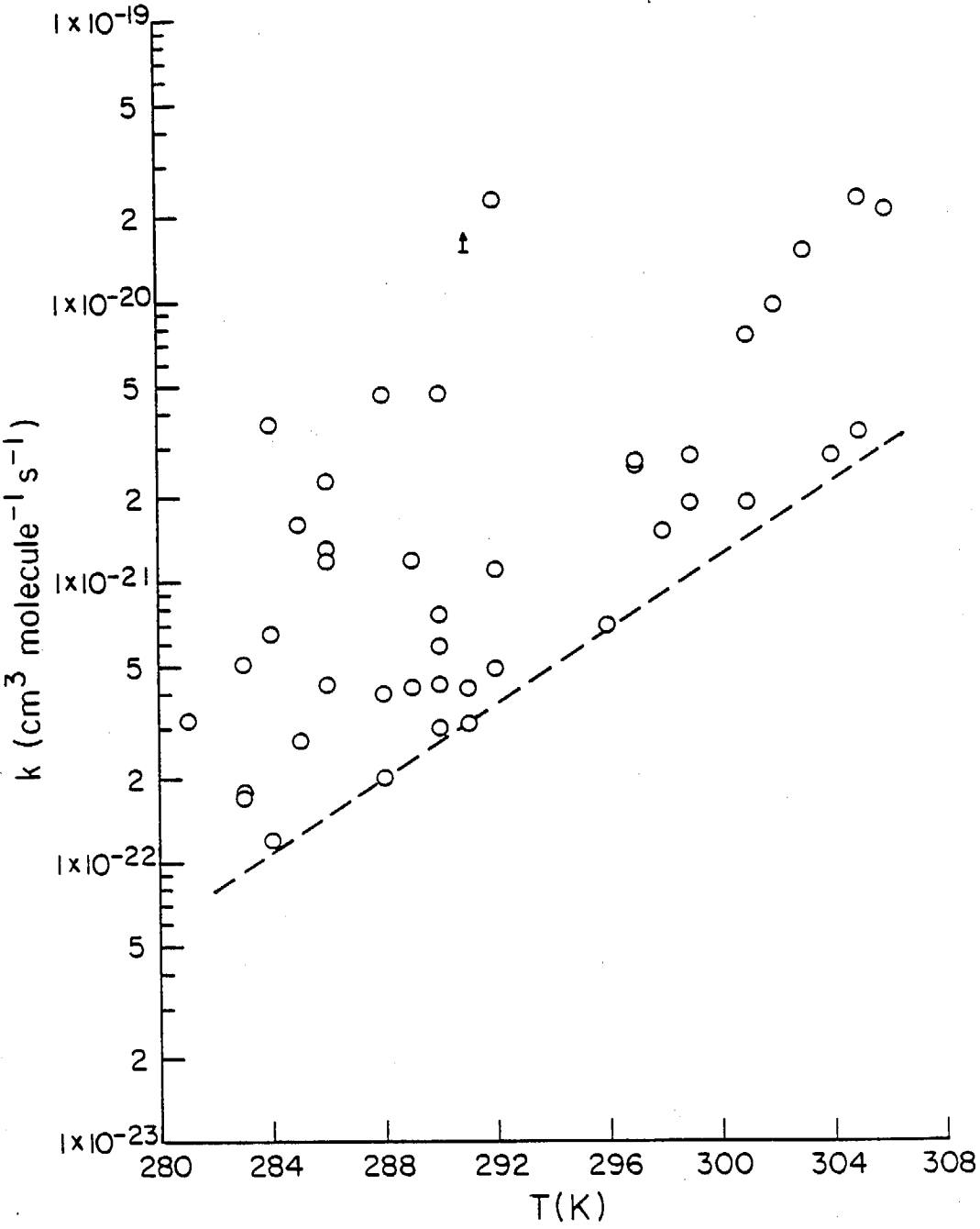

Figure V-4. Plot of the rate constant k_7 against temperature.

For such a rate constant, the importance of this reaction of N_2O_5 with water vapor as a loss process for N_2O_5 (and hence for NO_x) and as a formation route to HNO_3, a key species involved in acid deposition, is as discussed previously (Tuazon et al. 1983, Calvert and Stockwell 1983, Russell et al. 1984) and further reiteration here is not warranted. However, for a rate constant k_7 of this magnitude, it is clear (Tuazon et al. 1983, Calvert and Stockwell 1983, Russell et al. 1984) that this reaction of N_2O_5 with water vapor is an important nighttime formation route to nitric acid formation, a key species involved in acid deposition.

D. Reaction of N_2O_5 with PAH as a Source of Nitroarenes

A further reaction involving N_2O_5 may be of critical importance due to the formation of highly mutagenic nitro- and dinitroarenes from the parent PAH. Thus, recently, we have shown that N_2O_5 reacts in the gas phase with naphthalene with a rate constant of $\sim(2\text{-}3) \times 10^{-17}$ cm^3 $molecule^{-1}$ sec^{-1} (Pitts et al. 1984c) and with fluoranthene and pyrene adsorbed on glass fiber filters (Pitts et al. 1984a,d). Based upon the 1-nitropyrene time-concentration profiles observed during the exposures of adsorbed pyrene to gaseous N_2O_5 (Figure V-5) an ~3% min^{-1} nitration rate of pyrene in the presence of ~1.5 ppm of N_2O_5 can be derived from the initial slope. The estimation up to ~15 ppb of N_2O_5 in nighttime hours, with an average concentration of ~10 ppb over a 4-hr period for the night of September 18, 1979 in Riverside, then allows a very approximate estimate of an ~2% hr^{-1} nitration rate of pyrene under these conditions and a ~5% nitration of pyrene during the entire night assuming that our nitration rates observed in the laboratory at ppm concentrations of N_2O_5 can be extrapolated to the N_2O_5 concentrations appropriate for ambient conditions.

Obviously, from Table V-1 the maximum levels of N_2O_5 are often an order of magnitude or more lower than for this night, and the nitration rates will decrease proportionally. However, such a transformation of selected PAH to their nitroderivatives could contribute to the direct acting mutagenicities observed in ambient air (see, for example, Section IV above). Clearly, further experimental work is necessary to determine if this process is indeed of significance.

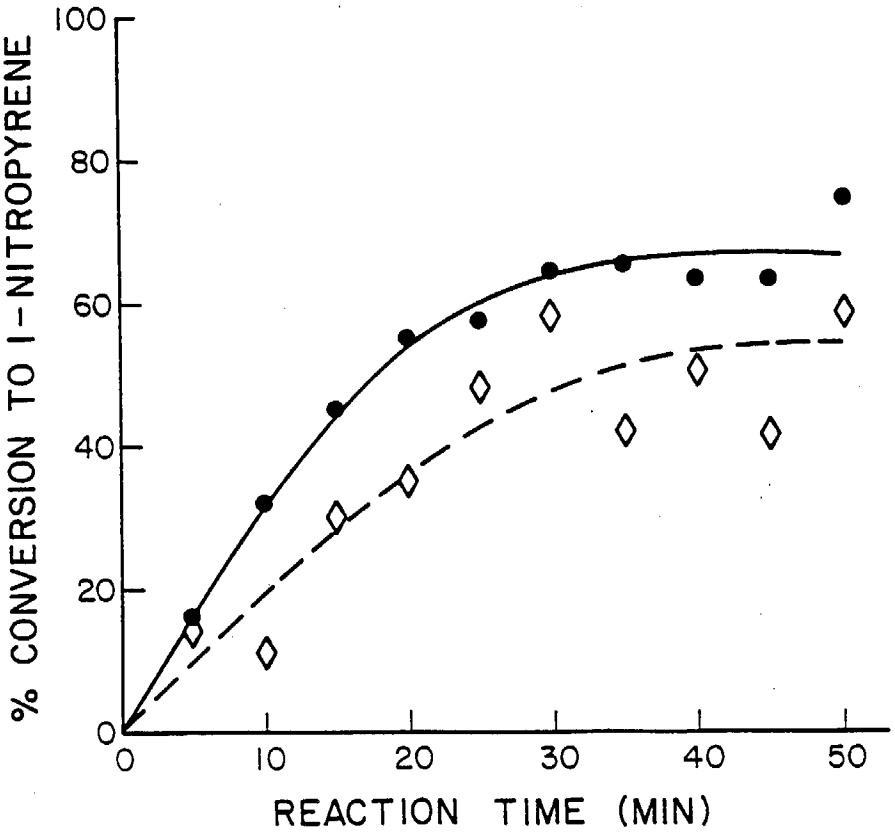

Figure V-5. Percent of 1-nitropyrene formed from passive exposures of pyrene in the dark to various gaseous nitrogenous species at initial concentrations as follows: ◊ - Exposure to N_2O_5 (1.5 ppm), NO_2 (5 ppm), HNO_3 (~0.1 ppm) and the NO_3 radical (~0.0005 ppm); ● - Exposure to N_2O_5 (1.5 ppm), NO_2 (~0.3 ppm), HNO_3 (~0.1 ppm) and the NO_3 radical (~0.01 ppm).

E. Conclusions

In the above section, we have estimated the N_2O_5 levels in nighttime atmospheres from the observed NO_2 and NO_3 radical concentration data, and show that they can reach 15-20 ppb on certain nights, levels which should be readily observed and measured using long pathlength Fourier transform infrared absorption spectroscopy. Furthermore, we have estimated from these data upper limit rate constants for the reaction of N_2O_5 with water vapor, and these data suggest that at 298 K this rate constant is $\lesssim 1 \times 10^{-21}$ cm^3 $molecule^{-1}$ sec^{-1}, in good agreement with a recent laboratory measurement. Further laboratory work is however needed concerning this reaction together with ambient atmospheric measurements of low levels of NO and/or reactive organics at night. Finally, we have extrapolated our measured nitration rates of pyrene by N_2O_5 from laboratory conditions to the ambient atmosphere, and predict that nitration rates of up to ~2% hr^{-1} (5% during a single night) can be attained, which could explain, at least in part, the observed direct acting mutagenicities.